

Rapports PSS N° 12

Production Soudano-Sahélienne (PSS)
Exploitation optimale des éléments nutritifs en élevage

Projet de coopération scientifique

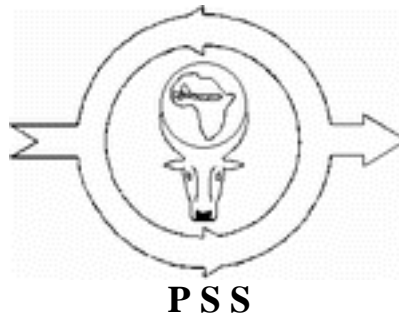
RECAFS: a model for resource competition and cycling in agroforestry systems

Model Description and User Manuel

J.G. Conijn ¹⁾

¹⁾ AB-DLO, B.P. 14, 6700 AA Wageningen, les Pays-Bas

IER, Bamako
AB-DLO, Wageningen, Haren
DAN-UAW, Wageningen



Rapports PSS N° 12

Wageningen, 1995

Table of Contents

- [Abstract](#)
 - [1. Introduction](#)
- [I. Model description](#)
 - [2. General outline of the model](#)
 - [2.1. Spatial arrangement and time resolution](#)
 - [2.2. Light competition](#)
 - [2.3. Soil water dynamics](#)
 - [2.4. Nitrogen dynamics](#)
 - [2.5. Carbon dynamics](#)
 - [2.6. Data input](#)

- [3. Description of the model](#)
 - [3.1. Geometry of the agroforestry system](#)
 - [3.1.1. Aboveground](#)
 - [3.1.2. Belowground](#)
 - [3.1.3. Parameterization](#)
 - [3.2. Distribution of radiation](#)
 - [3.2.1. Introduction](#)
 - [3.2.2. Absorption of photosynthetically active radiation \(PAR\)](#)
 - [3.2.2.1. Absorption and reflection by the tree population](#)
 - [3.2.2.2. PAR transmission pattern at groundlevel](#)
 - [3.2.2.3. Absorption of PAR by the herbaceous vegetation](#)
 - [3.2.3. Parameterization](#)
 - [3.3. Potential transpiration and soil evaporation](#)
 - [3.3.1. Potential transpiration](#)
 - [3.3.1.1. Tree population](#)
 - [3.3.1.2. Herbaceous vegetation](#)
 - [3.3.2. Potential soil evaporation](#)
 - [3.3.3. Rain interception, tree stem flow and throughfall](#)
 - [3.3.4. Parameterization](#)
 - [3.4. Root length distribution and water uptake](#)
 - [3.4.1. Root length distribution](#)
 - [3.4.1.1. Introduction](#)
 - [3.4.1.2. Tree population](#)
 - [3.4.1.2. Herbaceous vegetation](#)
 - [3.4.2. Water uptake](#)
 - [3.4.2.1. Tree population](#)
 - [3.4.2.2. Herbaceous vegetation](#)
 - [3.4.2.3. Competition for water](#)
 - [3.4.3. Parameterization](#)
 - [3.5. Biomass production](#)
 - [3.5.1. Tree population](#)
 - [3.5.2. Herbaceous vegetation](#)
 - [3.5.3. Parameterization](#)
 - [3.6. Growth and death of plant parts](#)
 - [3.6.1. Tree population](#)
 - [3.6.1.1. Phenology](#)
 - [3.6.1.2. Growth of plant components](#)
 - [3.6.1.3. Death of plant components](#)

- [3.6.1.4. Leaf and wood area dynamics](#)
 - [3.6.1.5. Reserve dynamics](#)
 - [3.6.2. Herbaceous vegetation](#)
 - [3.6.2.1. Development](#)
 - [3.6.2.2. Growth of plant components](#)
 - [3.6.2.3. Death of plant components](#)
 - [3.6.2.4. Leaf area dynamics](#)
 - [3.6.3. Parameterization](#)
 - [3.7. Soil water balance](#)
 - [3.7.1. Introduction](#)
 - [3.7.2. SAHEL water balance](#)
 - [3.7.3. Run-on / runoff calculation](#)
 - [3.7.4. Parameterization](#)
 - [3.8. Nitrogen demand, uptake and partitioning](#)
 - [3.8.1. Nitrogen demand](#)
 - [3.8.2. Nitrogen uptake](#)
 - [3.8.3. Competition for nitrogen](#)
 - [3.8.4. Nitrogen partitioning](#)
 - [3.8.5. Tree nitrogen reserve dynamics](#)
 - [3.8.6. Parameterization](#)
 - [3.9. Soil nitrogen balance](#)
 - [3.9.1. Nitrogen mineralization](#)
 - [3.9.2. Carbon and nitrogen inputs](#)
 - [3.9.2.1. Herbaceous vegetation](#)
 - [3.9.2.2. Tree population](#)
 - [3.9.3. Vertical nitrogen redistribution](#)
 - [3.9.4. Parameterization](#)
 - [3.10 List of symbols](#)
- [II. User manuel](#)
 - [4. Model input requirements](#)
 - [4.1. Introduction](#)
 - [4.2. CONTROL.DAT](#)
 - [4.3. RERUNS.DAT](#)
 - [4.4. TIMER.DAT](#)
 - [4.5. MLI61.973](#)
 - [4.6. TREE.DAT](#)
 - [4.6.1. Biomass](#)
 - [4.6.2. Water](#)

- [4.6.3. Nitrogen](#)
- [4.7. GRASS.DAT](#)
 - [4.7.1. Biomass](#)
 - [4.7.2. Water](#)
 - [4.7.3. Nitrogen](#)
- [4.8. LISAG.DAT](#)
- [5. Model run checks](#)
 - [5.1. Introduction](#)
 - [5.2. Balance checks](#)
 - [5.3. Range checks](#)
 - [5.4. Warnings](#)
- [References](#)
- [Appendix A: Program listing](#)
- [Appendix B: List of acronyms](#)
- [Appendix C: Input data](#)

Rappports du projet Production Soudano-Sahélienne (PSS)

Numéro 12

« The research for this publication was financed by the Netherlands' Minister for Development Co-operation. Citation is encouraged. Short excerpts may be translated and/or reproduced without prior permission, on the condition that the source is indicated. For translation and/or reproduction in whole the Section DST/SO of the aforementioned Minister should be notified in advance (P.O. Box 20061, 2500 EB The Hague). Responsibility for the contents and for the opinions expressed rests solely with the authors; publication does not constitute an endorsement by the Netherlands' Minister for Development Co-operation ».

Preface

The agroforestry model RECAFS was developed in the framework of the PSS project (Production Soudano-Sahélienne) at the Department of Agrosystems Research of the DLO-Research Institute for Agrobiolgy and Soil Fertility (AB-DLO).

A number of people contributed to this study. I thank Henk Breman and Herman van Keulen for their supervision and their comments on a draft of this report. Jan Goudriaan and Marcos Silveira Bernandes also contributed by commenting the draft. I am grateful to Peter Uithol for his assistance and for making the figures.

I also thank Santiago Bonachela Castaño for his support and the many discussions we had on crop modelling.

Abstract

RECAFS simulates absorption of light, water and nitrogen by an annual grass species and a tree species in a mixed stand and the dry matter production of both species as a function of the absorbed resources. It also calculates the dynamics of carbon and nitrogen in the soil organic matter. The tree population, as described in the model, consists of a number of trees planted in a rectangular planting pattern. The area per tree is subdivided into a number of subareas and growth and development of an annual grass species is simulated in each subarea separately. Light interception by the trees and remaining light availability at groundlevel for each subarea is computed and the production of both species is calculated by using a direct relation between light interception and dry matter production. Potential soil evaporation and potential herb transpiration per subarea are calculated with the Penman-Monteith equation. For simulating potential tree transpiration, the water use efficiency approach is used. Actual water uptake is modelled as a function of soil water status and root length distribution of both species. A simple soil water balance (storage overflow concept) with a number of horizontal compartments is included separately for each subarea. Lateral soil water movement is not incorporated. Uptake of nitrogen is related to its availability in the soil, root length distribution and the demand for nitrogen of living plant biomass. Net nitrogen mineralization is calculated in dependence of organic matter decomposition rate and carbon-nitrogen ratios in the soil organic matter. Growth of plant parts is simulated by partitioning of total biomass production of each species. Death of plant parts is also modelled, thus providing carbon and nitrogen input to the soil organic matter.

1. Introduction

The agroforestry model RECAFS was developed as part of the PSS project (Production Soudano-Sahélienne). The overall objective of the PSS project is to develop strategies for a more sustainable development of rural areas in the Sahel-Sudan zone of West Africa with special attention to animal husbandry systems (Anonymous, 1992). In the late seventies it was established that nutrients rather than water are the main limiting factor for forage production in a large part of the Sahel region ([Penning de Vries & Djitéye, 1982](#)). Furthermore, analysis of the nutrient balance at regional scale revealed that external nutrients are needed for further development of the region (van Keulen & Breman, 1990). Therefore part of the PSS research concentrates on the improvement of the nutrient use efficiency of external nutrients in the fodder production. Various fodder production systems are being investigated, including a leguminous crop, a perennial grass sward and a mixed culture of grass and trees.

The general hypothesis of the project with respect to agroforestry is that in the long-term an agroforestry system can sustain higher fodder production through reduced losses of limiting resources, associated with higher levels of soil organic matter. However, trees also compete with the grass species for limiting resources and can therefore have a negative effect on fodder production. The overall balance between the positive aspects, such as the higher soil organic matter level, and the negative aspects, like competition for limiting resources, depends on site characteristics (rainfall, soil type and fertility level) and the characteristics of the species comprising the agroforestry system. The key questions now are to

determine under which site conditions agroforestry may increase the nutrient recovery and whether this can be improved by a better choice of the species.

Field research was conducted in Niono in Mali (5.58 W; 14.16 N), where detailed data were collected on the effect of trees on their biophysical environment (e.g. [Soumaré *et al.*, 1994](#) and Radersma, 1994)). Development of an agroforestry model has been undertaken to reduce the costs of experimentation by increasing our understanding of the field measurements so that existing experimental results can be used for extrapolation to other conditions. Three modelling objectives were formulated corresponding to different aspects of the interaction between trees and grass in an agroforestry system. Short-term effects of the competition for limiting resources can be investigated by analysing herbage growth under and outside the tree crown as a function of resource level and the characteristics of both species (1st objective). Conflicting evidence is found in literature: Kessler (1992) and Kater *et al.* (1992) report reduced productivity under the tree, but Belsky *et al.* (1989) an increased productivity. Long-term effects should be analysed to determine the conditions for which the general hypothesis (see above) would hold. Simulation of the effects of a tree population on long-term availability of water and nutrients in the agro-ecosystem is the 2nd objective. The 3rd objective refers to the situation where trees, in addition to their protective role by maintaining or even increasing the amount of organic matter in the soil, also have a productive role in the system by producing fodder or other valuable products. The model should therefore also be able to calculate the production possibilities of a mixed culture of trees and grass with varying tree densities. This can be used as input for an economic analysis to find optimal tree-grass combinations.

I. Model description

2. General outline of the model

2.1. Spatial arrangement and time resolution

The tree population density is a model parameter and can be selected from a range between 1 tree per ha and the tree population density of a forest with a closed canopy. The trees are assumed to be equal-sized and homogeneously distributed in a rectangular planting pattern. The area per tree is subdivided into a maximum of three subareas, (i) that under the tree crown, (ii) that outside the tree crown, but still rooted by the tree and (iii) the remaining area per tree. The model simulates growth and development of an annual grass species in each subarea separately and that of a deciduous tree population.

The time resolution of RECAFS is one day.

2.2. Light competition

Daily light interception of a solitary tree and the remaining light level for the herbaceous vegetation

around the tree are calculated as a function of tree and site characteristics. It is assumed that the herbaceous vegetation does not affect the light availability for the trees. Light levels are computed for each subarea separately. Light absorption by the herbaceous vegetation is proportional to the remaining light availability in each subarea and is calculated as a negative exponential function of the leaf area index of the grass species.

2.3. Soil water dynamics

For each subarea the soil profile is subdivided into a number of horizontal compartments. Daily rainfall forms the input of water for the ecosystem. Upward flow through capillary rise or lateral flow from one subarea to another is not modelled. In case of run-on or run-off the infiltration of water is increased or decreased. Water that enters a soil compartment from the top is used to fill this compartment up to a maximum water content. The remainder will drain into the next compartment. Potential transpiration of a species equals its water demand for unlimited growth with respect to water. With respect to the grass species it is calculated with the Penman-Monteith equation as a function of absorbed radiation and microclimate characteristics. These microclimate characteristics can be affected by the trees as a function of shade level in each subarea. The water demand of the tree species is correlated directly to its biomass production by using the water use efficiency approach. Evaporation of water from the soil is modelled as a function of the amount of radiation at groundlevel and the microclimate characteristics, again by the Penman-Monteith equation, and the square root of time, where time is expressed as the number of days since last rain. Actual transpiration equals the sum of water uptake from each soil compartment containing roots. Water uptake per soil compartment is modelled as a function of the root length distribution, a characteristic transpiration rate and reduced soil water content, defined as a function of actual soil water content and soil water contents at field capacity and wilting point. If total water uptake from a soil compartment by both species exceeds the available amount of water for plant uptake, the available water is distributed among both species according to their relative strength in extracting water from that compartment.

2.4. Nitrogen dynamics

Natural nitrogen deposition related to rainfall and fertilizer nitrogen are the inputs of nitrogen for the ecosystem. The soil nitrogen balance is related to the soil water balance: if water flows from one soil compartment to the next nitrogen will be transported as well. Uptake of nitrogen from the soil by each species is modelled as a function of mass flow and diffusion of nitrogen towards the root systems. Mass flow is simply calculated as the product of water uptake and nitrogen concentration in each soil compartment, whereas diffusion is modelled as a function of root length and water content in each soil compartment. Total nitrogen uptake of a species from all soil compartments is limited by its nitrogen demand or by a maximum nitrogen uptake rate as function of total root length. Nitrogen demand equals the amount of nitrogen needed to reach maximum nitrogen concentrations in all plant parts. If nitrogen uptake by both species exceeds available nitrogen in a soil compartment, the available amount is distributed among both species according to their relative uptake strengths with respect to nitrogen in that compartment. Biomass losses from the grass vegetation and the tree population form the input of

nitrogen for the soil organic matter. Net mineralization of nitrogen from the organic matter in the soil is calculated as a function of its decomposition rate, microbial growth efficiency and the difference between actual and critical nitrogen contents in the soil organic matter. Immobilization occurs if the critical nitrogen content exceeds the actual nitrogen content.

2.5. Carbon dynamics

Biomass production of both species is modelled as a function of daily absorbed radiation, the ratio between water uptake and water demand and a reduction factor for suboptimal leaf nitrogen concentration. For the tree species a linear function between absorbed radiation and potential production is applied and for the grass species a non-linear function with a decreasing light use efficiency at increasing radiation levels. The partitioning of the produced biomass is modelled as a function of the development stage and can be affected by water and nitrogen stress for both species and by shade level in case of the grass species. Carbon input for the soil organic matter originates from biomass losses of both species which are related to development, but can also be induced by water stress.

Total organic matter in the soil is subdivided into 4 classes which mainly differ in their decomposition rate. Fresh litter originating from the vegetation is added directly to the 4 soil organic matter classes by using partitioning coefficients which differ between various litter types. Decomposition of organic matter is modelled as a first order process for each organic matter pool and for each subarea. Decomposition rate is also affected by soil water content.

2.6. Data input

Many input data are used by RECAFS concerning daily weather variables, physical properties of the soil, characteristics of soil organic matter and physiomorphological attributes of both species in the agroforestry system. Especially with respect to the tree species and the organic matter dynamics, parameterization could not be completed due to lack of quantitative data and therefore proper validation of the model was not yet possible.

3. Description of the model

3.1. Geometry of the agroforestry system

3.1.1. Aboveground

Starting point for the model calculations is an unit area of 1 ha with a tree population and an annual grass vegetation. The tree population consists of a number of trees, that are equal-sized and homogeneously distributed in a rectangular planting pattern (Fig. 3.1).

Figure 3.1. A field of 1 ha with 9 tree-grass units and 3 subareas per tree-grass unit.

Tree population density, which is fixed during a simulation run, defines the number of tree-grass units, i. e. the smallest subunit of the field for which all calculations are performed in an identical way. The area of a tree-grass unit or the area per tree equals the inverse of the tree population density. Various radiation distributions and water or nutrient uptake patterns can be simulated by increasing tree population density from a sparsely scattered tree population towards a dense forest.

The effect of a tree on the surrounding herbaceous vegetation varies with the distance from the tree base. To account for this variability the area of a tree-grass unit is subdivided into a number of subareas (Fig. 3.2).

[Figure 3.2.](#) A tree-grass unit with 3 subareas and 4 soil compartments in each subarea.

The number of subareas per tree can be one, two or three depending on tree population density and tree size. At low tree densities and small tree sizes three subareas are distinguished. The first subarea equals the vertical projection of the tree crown, i.e. the crown cover. It is assumed that the crown cover can be described by a circle. The tree crown cover is simulated as a function of tree stem biomass. Subarea 2 is rooted by the trees, but not covered by tree crowns. The boundary between the second and third subarea is thus given by the average lateral tree root extension in the top soil compartment, that is assumed equal in all directions. The average lateral tree root extension in the top soil is linearly related to the crown radius. The third subarea, which is not exploited by the tree roots, equals the remaining area of the area per tree. At higher tree densities the area per tree decreases or in case of trees with a larger lateral root extension, the size of subarea 2 increases. Both can result in a situation where subarea 3 ceases to exist, because the top soil compartment of the whole field is rooted by the tree population. The outer boundary of subarea 2 is then no longer given by the lateral tree root extension, but determined by the size of the area per tree. In the field situation tree roots can invade neighbouring tree-grass units at higher tree densities, but for computational reasons it is assumed that all roots of a tree are restricted to its own tree-grass unit. If the product of tree population density and individual crown cover equals 1 ha, even subarea 2 disappears. This situation represents a forest with a closed canopy, where all plants of the herbaceous species grow under the tree crowns. Contrary to the tree population density, crown cover and lateral tree root extension may change during a simulation run as a result of increasing tree size.

The model calculates per subarea average resource depletion rates due to the presence of the trees and simulates growth and development of the herbaceous vegetation separately for each subarea. Between the subareas the development of the herbaceous vegetation may differ, but within each subarea an homogeneous development is assumed. Any interaction between the herbaceous vegetation of different subareas, such as shading or water competition, is not considered.

3.1.2. Belowground

For each subarea a number of soil compartments have been distinguished to calculate vertical movement of water and nutrients in the soil and uptake of and competition for these soil resources. Lateral

movement of water or nutrients in the soil from one subarea to another has not been modelled. The only transport of soil resources in lateral direction is caused by uptake by trees if they have roots outside their own crown cover area.

3.1.3. Parameterization

Variable	Value	Unit	Source
C_c	0, 0 50, 15 100, 30 200, 60 400, 100 1000, 200	$m^2 (\text{plant})^{-1}$	H. Breman (pers. comm.)
$X_{c,0}$	13	m	(a)

C_c individual tree crown cover (2nd column) as function of stem biomass (1st column);

$X_{c,0}$ initial value of lateral root extension in the first soil compartment containing tree roots.

(a) Value estimated

3.2. Distribution of radiation

3.2.1. Introduction

For calculating the radiation distribution between trees and the herbaceous species two horizontal layers are distinguished: a grass layer and a tree layer. The grass layer does not affect the light availability of the tree layer, by assuming that the tree crowns are always situated above the grass sward. On the other hand, the presence of the trees decreases the radiation level available for the herbaceous vegetation.

3.2.2. Absorption of photosynthetically active radiation (PAR)

3.2.2.1. Absorption and reflection by the tree population

Firstly, absorption of an individual tree in a closed tree canopy is calculated (Eqn. 3.1). It is assumed that the closed tree canopy forms a monolayer of identical trees with homogeneously distributed leaf and wood area with a tree population density equal to the inverse of the crown cover. Part of the radiation is reflected.

$$A_c = \frac{I_p * (1 - r_p) * (1 - e^{-(L * K_L + W * K_W)})}{N_c} \quad \text{[Equation 3.1]}$$

A_c absorption of PAR by an individual tree in a closed tree canopy ($J \text{ (plant)}^{-1} \text{ d}^{-1}$)

N_c tree population density of a closed tree canopy (tree ha^{-1})

I_p daily photosynthetically active radiation ($J \text{ ha}^{-1} \text{ d}^{-1}$)

r_p reflection coefficient for I_p (-)

L leaf area index of a tree ($\text{m}^2 \text{ m}^{-2}$)

W wood area index of a tree ($\text{m}^2 \text{ m}^{-2}$)

K_L extinction coefficient of leaves for I_p ($\text{m}^2 \text{ m}^{-2}$)

K_W extinction coefficient of branches for I_p ($\text{m}^2 \text{ m}^{-2}$)

Secondly, the absorption of PAR by a solitary tree is calculated as a function of the absorption by an individual tree of equal dimensions in a closed tree canopy (Eqn. 3.2).

$$A_s = q_{sc} * A_c \quad \text{[Equation 3.2]}$$

A_s absorption of PAR by a solitary tree ($J \text{ (plant)}^{-1} \text{ d}^{-1}$)

q_{sc} ratio between absorbed PAR of a solitary tree and an individual tree in a closed tree canopy (-)

The ratio q_{sc} is determined with the model TREESHA (Knevel, 1993), which calculates daily light interception and resulting shade pattern at ground level of a solitary tree, as a function of latitude, atmospheric transmission, crown dimensions, leaf area, wood area and extinction coefficients. In the model TREESHA the envelope of the tree crown is described by a symmetrical ellipsoid. This description allows simulation of many different crown shapes, such as spheres ($a = c$), erect ($a < c$) and prostrate ($a > c$) ellipsoids (Fig. 3.3). The influence of the stem from ground level to the lower boundary of the tree crown on the radiation interception by the tree, is not included.

[Figure 3.3. Possible tree crown ellipsoids.](#)

An average correlation between the absorption of a solitary tree and that of an individual forest tree is found by performing several simulations with TREESHA during the growing season, using fixed crown dimensions and extinction coefficients, but with varying leaf and wood area and with actual weather data.

Absorption of PAR by the tree population is given in Fig. 3.4 as a function of tree population density. For estimating the tree population density at which mutual shading starts, the model TREESHA has also been used. TREESHA calculates the light intensity at ground level as a function of the distance from the tree base. The sum of the crown cover radius and the distance at which the light intensity at the level of the lower crown boundary approximately equals global PAR gives the diameter of the minimum area per tree required to avoid competition for light. The inverse of this minimum area per tree represents the threshold tree population density for intertree shading.

Figure 3.4. Relation between tree population density and daily absorbed PAR of a tree population.

For $N \leq N_s$: $I_a = N * A_s$

For $N_s < N < N_c$: non-linear interpolation between $N_s * A_s$ and $N_c * A_c$

For $N = N_c$: $I_a = N_c * A_c$

I_a daily absorbed PAR by a tree population ($J ha^{-1} d^{-1}$)

N actual tree population density (tree ha^{-1})

N_s threshold tree population density for intertree shading (tree ha^{-1})

The amount of PAR, reflected by the tree population, is calculated by weighing the reflection of a closed tree canopy with the ratio between absorbed PAR by the actual tree population and absorbed PAR by a closed tree canopy (Eqn. 3.3).

$$I_r = I_p * r_p * \frac{I_a}{N_c * A_c} \quad \text{[Equation 3.3]}$$

I_r daily reflected PAR by a tree population ($J ha^{-1} d^{-1}$)

The amount of PAR, absorbed by the tree leaves, is used for the calculation of dry matter production of the tree population and is estimated from the contribution of the foliage in absorbing radiation (Eqn. 3.4). This procedure has also been applied in calculating the distribution of absorbed radiation among two competing species (Spitters, 1989; Conijn, 1989; Kropff & Van Laar, 1993).

$$I_{a,L} = \frac{L * K_L}{L * K_L + W * K_W} \quad \text{[Equation 3.4]}$$

$I_{a,L}$ daily absorbed PAR by the foliage of a tree population ($J ha^{-1} d^{-1}$)

3.2.2.2. PAR transmission pattern at groundlevel

The model TREESHA is used to determine cumulative fractional shade as a function of the distance from the tree base relative to the crown cover radius (Fig. 3.5). This relation is based upon calculated light transmission values at ground level, given in a two-dimensional array, resulting from the interception of PAR by a solitary tree. Differences in shading intensities in North-South and East-West directions, due to the interception of direct radiation, are averaged. For use in RECAFS the shade distribution function is approximated by line segments between some specified points.

Figure 3.5. Relation between the relative distance from the tree with respect to crown cover radius, x_r , and the cumulative shade fraction, F_{sh} .

For each subarea of a tree-grass unit an average amount of transmitted PAR, available for the herbaceous vegetation, is calculated. If the tree population density equals one, the cumulative fractional shade function, obtained from TREESHA, is used to calculate the fraction intercepted radiation with respect to each subarea. At higher tree densities the cumulative fractional shade function of TREESHA is no longer valid, because trees affect the light availability in neighbouring tree-grass units. The fraction of intercepted radiation is then calculated for each subarea as an interpolation between the shade function of a solitary tree and the shade caused by a forest with a homogeneous closed canopy. The light availability for the herbaceous vegetation is found by subtracting the amount of intercepted PAR relevant for each subarea from the daily available PAR (Eqn. 3.5).

$$I_t(n) = I_p - f_{sh}(n) * (I_a + I_r) * \frac{10000}{A(n)} \quad \text{[Equation 3.5]}$$

$I_t(n)$ daily transmitted PAR towards the herbaceous vegetation ($J \text{ ha}^{-1} \text{ d}^{-1}$)

$f_{sh}(n)$ fraction of the intercepted radiation by the tree population with respect to each subarea (-)

$A(n)$ total area of a subarea ($\text{m}^2 \text{ ha}^{-1}$)

n subarea indication number

3.2.2.3. Absorption of PAR by the herbaceous vegetation

Light absorption by the herbaceous vegetation is calculated with a negative exponential function of the leaf area index (Eqn. 3.6). For a monoculture of the herbaceous species transmitted PAR ($I_t(n)$) equals daily incoming PAR (I_p).

$$I_a(n) = I_t(n) * (1 - r_p) * (1 - e^{-(L(n) * K_L)}) \quad \text{[Equation 3.6]}$$

$I_a(n)$ daily absorbed PAR by the herbaceous vegetation ($J ha^{-1} d^{-1}$)

$L(n)$ leaf area index of the herbaceous vegetation ($m^2 m^{-2}$)

3.2.3. Parameterization

Variable	Value	Unit	Source
<i>General</i>			
q_{ps}	47	-	Begue <i>et al.</i> (1991)
r_p	0.08	-	Lövenstein <i>et al.</i> (1992)
<i>Tree population</i>			
K_L	0.7	$m^2 m^{-2}$	(a)
K_W	0.7	$m^2 m^{-2}$	(a)
q_{sc}	1.7	-	Knevel (1993) ^b
N_s	15	tree ha^{-1}	Knevel (1993) ^b
F_{sh}	0, 0.0 1, 0.25 4, 0.8 7, 1.0	-	Knevel (1993, page 46) ^b
<i>Herbaceous vegetation</i>			
K_L	0.6	$m^2 m^{-2}$	(a)

q_{ps} ratio between PAR (I_p) and daily short-wave radiation;

F_{sh} 1st column gives the relative distance from the tree base and 2nd column equals the cumulative shade fraction (see also [Fig. 3.5](#)).

a. Value estimated

b. Based on characteristics of Karité, *Vitellaria paradoxa*

3.3. Potential transpiration and soil evaporation

3.3.1. Potential transpiration

3.3.1.1. Tree population

For calculating potential transpiration of the tree population the water use efficiency approach is used (Eqn. 3.7). It is assumed that the tree species can regulate stomatal aperture depending on the rate of CO₂ - fixation (Goudriaan & Van Keulen, 1979, [Penning de Vries & Djitéye, 1982](#), van Keulen & Wolf, 1986). This implies that if biomass production is limited, e.g. by nutrient shortage, the demand for water decreases proportionally.

$$T_p = \frac{P_p}{E_w} * R d_B \quad \text{[Equation 3.7]}$$

T_p potential transpiration rate of the tree population (mm d⁻¹)

P_p potential rate of dry matter production, as function of absorbed radiation (kg ha⁻¹ d⁻¹)

E_w water use efficiency for dry matter production (kg ha⁻¹ mm⁻¹)

Rd_B reduction factor for potential biomass production, e.g. caused by nutrient stress (-)

An individual tree in a forest has a lower water demand per unit biomass produced than a solitary tree, because solitary trees are much more exposed to the drying power of the air. In the model, the water use efficiency of solitary trees, $E_{w,s}$, is used at low tree densities, whereas at higher tree densities a linear interpolation is applied between $E_{w,s}$ and the water use efficiency of a closed tree canopy, $E_{w,c}$. Thus, effects of reduced wind speed and vapour pressure deficit of the air surrounding the trees at higher tree densities are not explicitly incorporated. For both water use efficiencies an average seasonal value is used. If there are no leaves, e.g. for a deciduous tree during the dry season, potential transpiration equals zero.

3.3.1.2. Herbaceous vegetation

For the herbaceous vegetation, the Penman-Monteith combination equation is used to calculate the potential transpiration rate (van Laar *et al.*, 1992). Input data from a standard weather file can not be used directly for this calculation, because they are measured in the absence of a tree population. For each subarea separately the climate conditions, necessary for the equation and relevant for the herbaceous vegetation, are estimated by calculating the following parameters as a function of shading intensity caused by the presence of the tree population: (1) daily short-wave radiation transmitted through the tree canopies, (2) atmospheric transmission, (3) daily minimum and maximum temperature, (4) early morning vapour pressure of the air and (5) mean wind speed.

1) The transmitted daily short-wave radiation for the herb layer in each subarea is calculated from daily global radiation by subtracting intercepted radiation, that is calculated by multiplying the intercepted

short-wave radiation by a closed tree canopy with the ratio of intercepted PAR in a subarea and intercepted PAR by a closed tree canopy (Eqn. 3.8).

$$I_s(n) = I_0 - (I_{a,0} + I_{r,0}) * q_i(n) \text{ [Equation 3.8a]}$$

$$I_{a,0} = I_0 * (1 - r_c) * (1 - e^{-q_K * (L_T * K_L + W * K_w)}) \text{ [Equation 3.8b]}$$

$$I_{r,0} = I_0 * r_c \text{ [Equation 3.8c]}$$

$$r_c = r_{0,v} * (1 - e^{-q_K * (L_T * K_L + W * K_w)}) \text{ [Equation 3.8d]}$$

$$q_i(n) = \frac{I_p - I_t(n)}{N_c * A_c + I_p * r_p} \text{ [Equation 3.8e]}$$

$I_s(n)$ daily transmitted short-wave radiation towards the herbaceous vegetation ($J m^{-2} d^{-1}$)

I_0 daily short-wave radiation ($J m^{-2} d^{-1}$)

$I_{a,0}$ absorbed short-wave radiation by a closed tree canopy ($J m^{-2} d^{-1}$)

$I_{r,0}$ reflected short-wave radiation by a closed tree canopy ($J m^{-2} d^{-1}$)

$q_i(n)$ ratio of intercepted PAR in a subarea and intercepted PAR by a closed tree canopy (-)

L_T total dead and living leaf area index of the trees ($m^2 m^{-2}$)

K_L extinction coefficient of leaves for I_p ($m^2 m^{-2}$)

W wood area index of a tree ($m^2 m^{-2}$)

K_W extinction coefficient of branches for I_p ($m^2 m^{-2}$)

q_K ratio between extinction coefficient for short-wave radiation and photosynthetically active radiation

(-)

$r_{0,v}$ reflection coefficient for I_0 at 100% absorption (albedo) (-)

r_c reflection coefficient for I_0 of a forest (-)

I_p daily photosynthetically active radiation ($J ha^{-1} d^{-1}$)

$I_t(n)$ daily transmitted PAR ($J ha^{-1} d^{-1}$)

A_c absorption of PAR by an individual tree in a closed tree canopy ($J (plant)^{-1} d^{-1}$)

N_c tree population density of a closed tree canopy ($tree ha^{-1}$)

r_p reflection coefficient for I_p (-)

- 2) Atmospheric transmission is now calculated as the ratio of transmitted short-wave radiation and daily extraterrestrial radiation, which is a function of latitude and day of year.
- 3) Minimum and maximum air temperatures may decrease due to the presence of the trees. This effect is simulated by a positive linear correlation between the decrease in both temperatures and the fraction intercepted PAR by the tree population, $q_i(n)$, multiplied with the fraction absorbed short-wave radiation. The product of both fractions has a value between 0 and 1. If it equals zero, which corresponds with no shading, the temperatures remain unchanged. On the other hand if the interception of radiation equals 100 % in a subarea, temperatures are decreased maximally, compared to the open field situation.
- 4) Vapour pressure of the air may increase due to the presence of the trees. This effect is modelled in a similar way as the change in temperatures.
- 5) Wind speed may decrease due to the presence of the trees. This effect is simulated in the same way as the temperature change.

The maximum change of these 3 microclimate characteristics is an input to the model and is expressed as a fraction of the measured values in the open field situation. Its value, set by the user, can vary between 0 and 1.

The radiation term (T_r) and the drying power term (T_d) are calculated from the climate characteristics of each subarea. Both are used to determine potential transpiration of the herbaceous vegetation per subarea with the Penman-Monteith combination equation (van Laar *et al.* , 1992).

$$T_p(n) = ((1 - e^{-q_k * L(n) * K_L}) * T_r(n) + T_d(n) * \text{MIN}(2.5; L(n))) * R_d_B \quad \text{[Equation 3.9a]}$$

$$T_r(n) = \frac{\Delta * R_N(n)}{\Delta + \gamma} \quad \text{[Equation 3.9b]}$$

$$T_d(n) = \frac{\gamma * E_A(n)}{\Delta + \gamma} \quad \text{[Equation 3.9c]}$$

$T_p(n)$ potential transpiration rate of the herbaceous vegetation, (mm d^{-1})

$T_r(n)$ radiation term of potential transpiration (mm d^{-1})

$T_d(n)$ drying power term of potential transpiration (mm d^{-1})

$L(n)$ leaf area index of the herbaceous vegetation ($\text{m}^2 \text{m}^{-2}$)

Rd_B reduction factor for potential biomass production, caused e.g. by nutrient stress, per subarea (assuming constant water use efficiency) (-)

$R_N(n)$ net absorbed radiation term (mm d^{-1})

$E_A(n)$ evaporative demand of the atmosphere (mm d^{-1})

[Delta] derivative of saturated vapour pressure curve with respect to temperature (mbar K^{-1})

[gamma] psychrometric constant (mbar K^{-1})

As for trees, it is assumed that the herbaceous species also regulates its stomata resulting in a lower water demand if biomass production is limited by stress factors other than soil water supply.

3.3.2. Potential soil evaporation

Potential soil evaporation is estimated for each subarea separately as a function of the radiation and drying power terms, as calculated above, and the fraction transmitted short-wave radiation at ground level (van Laar *et al.*, 1992).

$$E_p(n) = (T_r(n) + T_d(n)) * e^{-\gamma K * L_T(n) * K_L} \quad [\text{Equation 3.10}]$$

$E_p(n)$ potential soil evaporation rate (mm d^{-1})

$L_T(n)$ total dead and living leaf area index of the herbaceous vegetation ($\text{m}^2 \text{m}^{-2}$)

3.3.3. Rain interception, tree stem flow and throughfall

Interception of rain by aboveground plant structures influences the amount of water available for infiltration and potential transpiration, because part of the energy absorbed by leaves is dissipated through evaporation of intercepted rain. In passing through the tree crowns rain is distributed into direct throughfall (1), interception (2), indirect throughfall (3) and tree stem flow (4) (Pressland, 1973; Slatyer, 1965; de Jongh, 1992).

1) Direct throughfall is described as fraction, defined as a negative linear function of total leaf and wood area, of daily rainfall (Eqn. 3.11).

$$P_{dt} = P_r * \left(1 - \frac{L_T * K_L + W * K_W}{D_T}\right) \quad [\text{Equation 3.11}]$$

P_{dt} rate of direct throughfall (mm d⁻¹)

P_r daily rainfall (mm d⁻¹)

D_T direct throughfall threshold value (-)

The difference between daily rainfall and direct throughfall is distributed amongst interception, indirect throughfall and tree stem flow.

2) Interception of rain by the tree canopies involves a fraction of this remaining part of the precipitation. The fraction intercepted by the tree canopies is negatively correlated to shower intensity. It is assumed that shower intensity is positively correlated to daily rainfall, resulting in complete interception at days with low rainfall and a low value for the interception fraction at days with high rainfall. The fraction intercepted is derived by linear interpolation for days with rainfall between those two threshold values (Fig. 3.6).

Figure 3.6. Relation between daily precipitation and the fraction intercepted rain by the tree canopies.

f_i fraction intercepted rain, applied to precipitation minus direct throughfall (-);

$f_{i,m}$ minimum fraction intercepted rain (-);

P_1, P_2 precipitation threshold values for calculating f_i (mm d⁻¹).

Potential transpiration of the trees is decreased with 50 % of the amount of intercepted rain (Singh & Sceicz, 1979).

3) The remaining water is allocated to tree stem flow and indirect throughfall by using a constant ratio between the two. Total throughfall which infiltrates homogeneously over the ground area of the tree crown cover, equals the sum of direct and indirect throughfall.

4) Tree stem flow is assumed to infiltrate near the trunk of each tree and may therefore percolate into deeper soil compartments compared to total throughfall.

Interception of rain by the herbaceous vegetation is described as a linear function of total leaf area index (van Laar *et al.*, 1992). No stem flow nor direct or indirect throughfall is distinguished here, so that total throughfall equals the non-intercepted part of the precipitation. Again, as for the trees, potential transpiration is corrected by subtracting half of the intercepted rain.

3.3.4. Parameterization

Variable	Value	Unit	Source
----------	-------	------	--------

General

$r_{0,v}$	0.25	-	Penman (1956)
$r_{0,s}$	0.15	-	Penman (1956)
q_K	0.75	-	van Diepen <i>et al.</i> (1988)
f_{Pr}	0.5	-	Singh & Sceicz (1979)

Tree population

$E_{w,s}$	10	kg ha ⁻¹ mm ⁻¹	Lövenstein <i>et al.</i> (1991)
$E_{w,c}$	30	kg ha ⁻¹ mm ⁻¹	Lövenstein <i>et al.</i> (1991)
C_{tm}	0.5	-	(a)
C_{vp}	0.5	-	(a)
C_{wn}	0.5	-	(a)
D_T	2.0	-	(a)
$f_{i,m}$	0.1	-	(a)
P_1	2	mm d ⁻¹	(a)
P_2	20	mm d ⁻¹	(a)
f_{st}	0.4	-	Leyton (1987) ^b

Herbaceous vegetation

C_{Pr}	0.4	mm d ⁻¹	van Laar <i>et al.</i> (1992)
----------	-----	--------------------	-------------------------------

$r_{0,s}$ reflection coefficient for I_0 of a soil surface (albedo);

f_{Pr} fraction intercepted rain subtracted from potential transpiration;

C_{tm} maximum relative decrease in minimum and maximum air temperatures due to the presence of the trees;

C_{vp} maximum relative increase in early morning vapour pressure of the air due to the presence of the trees;

C_{wn} maximum relative decrease in average wind speed due to the presence of the trees

f_{st} fraction of tree stem flow, applied to precipitation minus direct throughfall and interception;

C_{Pr} rainfall interception capacity per leaf layer of the herbaceous vegetation.

a. Value estimated b. Value calibrated with cumulative stemflow equal to 5 - 15 % of cumulative rainfall on an annual basis

3.4. Root length distribution and water uptake

3.4.1. Root length distribution

3.4.1.1. Introduction

Root length distribution in the soil is used to calculate water uptake per soil compartment and per subarea for both species. In each soil compartment the root length of trees and of the herbaceous species is calculated, assuming homogeneous distribution of these roots per compartment. Because the average lateral tree root extension in the top soil forms the boundary between subareas 2 and 3, tree roots are absent in subarea 3. The amount of tree roots in subareas 1 and 2 depends on the total amount of roots per tree and the root distribution in the vertical and radial direction. In the model the roots of the herbaceous species are only distributed in vertical direction, for each subarea separately, assuming homogeneous distribution in the lateral direction. Differences in calculated herbaceous root length per soil compartment between subareas are due to differences in rooted depth or total root length of this species. The development of rooted depth and total root length of the herbaceous species is not identical for all subareas, because the intensity of the competitive interaction with the trees depends on the distance to the tree.

3.4.1.2. Tree population

For modelling the distribution of tree roots per soil compartment in each subarea two functions are applied. Firstly, a negative exponential function is used to calculate root length per soil compartment for all subareas combined (Eqn. 3.12).

$$D_z = 1 - e^{-p_v * z} \quad \text{[Equation 3.12a]}$$

$$z = \frac{Z - Z_c}{Z_r} \quad \text{[Equation 3.12b]}$$

D_z total cumulative relative root length (-)

z relative soil depth (-)

p_v vertical root distribution parameter (-)

Z soil depth (m)

Z_r rooted depth of a tree at the tree base (m)

Z_c soil depth at which the first tree roots are found (m)

A constant tree rooted depth is assumed in the model and can be varied as part of a sensitivity analysis. Contrary to the roots of the herbaceous species, tree roots may be absent in the upper soil compartments, depending on species characteristics or management practice, like ploughing. The parameter Z_c has been incorporated to simulate this effect. If Z_c is located at a boundary between two soil compartments, water available in the soil above Z_c can only be taken up by the herbaceous species. Total root length per tree is found as a function of root mass and a constant specific root length parameter for all situations.

Secondly, the lateral extension of tree roots at different depths is modelled to determine the amount of tree roots per subarea in each soil compartment. Lateral root extension of a solitary tree in the first soil compartment containing tree roots, X_c , is described as a linear function of crown cover radius. For subsequent soil compartments the lateral root extension is calculated as a function of X_c and the root length density of that soil compartment relative to the root length density of the first soil compartment containing tree roots (Eqn. 3.13).

$$X(l) = X_c * \frac{D_r(l)}{D_{r,c}}$$

[Equation 3.13]

$X(l)$ lateral tree root extension per soil compartment (m)

X_c lateral root extension of the first soil compartment containing tree roots (m)

$D_r(l)$ root length density per soil compartment ($m\ m^{-3}$)

$D_{r,c}$ root length density in the first soil compartment containing tree roots ($m\ m^{-3}$)

l soil compartment indication number (-)

The decrease in lateral root extension with soil depth is also exponentially, because root length density per soil compartment is calculated according to Eqn. 3.12. It is assumed that the lateral tree root extension in any soil compartment does not extend beyond the radius of the tree-grass unit. At a high tree population densities lateral root extension in the upper soil compartments is thus given by this radius instead of by the lateral root extension of a solitary tree.

Finally, total root length per soil compartment for all subareas, computed with Eqn. 3.12 and with total tree root length, is distributed in radial direction among the different subareas by using a negative

exponential equation (Eqn. 3.14).

$$D_x = 1 - e^{-p_h * x(l)} \quad \text{[Equation 3.14a]}$$

$$x(l) = \frac{R_s(n)}{X(l)} \quad \text{[Equation 3.14b]}$$

D_x cumulative relative root length per soil compartment (-)

$x(l)$ relative lateral tree root extension (-)

p_h lateral root distribution parameter (-)

$R_s(n)$ radius of a subarea with respect to the tree base (m)

3.4.1.2. Herbaceous vegetation

The vertical root distribution of the herbaceous vegetation has been described with a negative exponential function (Eqn. 3.15).

$$D_z = 1 - e^{-p_v * z} \quad \text{[Equation 3.15a]}$$

$$z = \frac{Z}{Z_r(n)} \quad \text{[Equation 3.15b]}$$

$Z_r(n)$ rooted depth of the herbaceous species (m)

The vertical root distribution parameter p_v was derived from root length measurements as a function of soil depth ([Penning de Vries & Djitéye, 1982](#); see Fig. 3.7).

Figure 3.7. The relation between the total cumulative relative root length and relative soil depth: data and fitted curve.

The vertical root distribution function of Eqn. 3.15 is used in the model for all subareas and at all stages of growth of the herbaceous species. Total root length index is estimated by multiplying total root mass with a constant specific root length. The development of the rooted depth is simulated in a very simple way: a constant vertical root extension rate is assumed, unless the growth in root mass equals zero or unless the water content in the soil compartment containing the root tip is equal to or below wilting point (van Laar *et al.*, 1992). After reaching the maximum root depth, which may be set either as a species or

as a soil characteristic, the rooted depth remains constant. No decrease in rooted depth, e.g. during the senescence phase, is simulated.

Roots of the herbaceous vegetation are assumed to be present from the top soil onwards.

3.4.2. Water uptake

3.4.2.1. Tree population

Water extraction per soil compartment in each subarea is simulated by means of the following equations:

$$U_{w,T}(n,l) = T_p * \frac{R_L(n,l)}{\sum \sum R_L(n,l)} * \text{MIN}(1; Rd_w) * \frac{10000}{A(n)} \quad [\text{Equation 3.16a}]$$

$$Rd_w = \left(1 + \frac{T_c}{T_m}\right) * Wc_r \quad [\text{Equation 3.16b}]$$

$$Wc_r = \frac{Wc_a - Wc_w}{Wc_f - Wc_w} \quad [\text{Equation 3.16c}]$$

$U_{w,T}(n,l)$ water uptake rate per soil compartment in each subarea by the tree population (mm d^{-1})

T_p potential transpiration rate of the tree population (mm d^{-1})

$R_L(n,l)$ root length per soil compartment in each subarea (m)

[Sigma] [Sigma] ... summation over all subareas and all soil compartments

Rd_w water uptake reduction factor (-)

$A(n)$ total area of a subarea ($\text{m}^2 \text{ha}^{-1}$)

T_c characteristic transpiration rate (mm d^{-1})

T_m potential transpiration rate of a closed vegetation (mm d^{-1})

Wc_r reduced water content per soil compartment in each subarea (-)

Wc_a actual water content ($\text{cm}^3 \text{cm}^{-3}$)

Wc_w water content at wilting point ($\text{cm}^3 \text{cm}^{-3}$)

Wc_f water content at field capacity ($\text{cm}^3 \text{cm}^{-3}$)

Potential transpiration T_p sets the upper limit to total water extraction from the whole soil profile.

Extraction of water from each soil compartment and subarea is proportional to the relative root length of a compartment and to a water uptake reduction factor. In addition, a weighing factor is applied to account for differences in the areas of the subareas from which water can be taken up. The reduction factor Rd_w is a function of a species characteristic sensitivity parameter T_c , potential transpiration of a closed vegetation T_m and the reduced water content in the soil compartment (Denmead & Shaw, 1962; van Laar *et al.*, 1992). The characteristic transpiration equals the actual transpiration of a closed vegetation at a reduced water content of 0.5, without causing reduction in the water uptake. The ratio of T_c and T_m determines the ability of a species to extract water from the soil at low soil water availabilities. The characteristic transpiration is an input for the model, whereas the maximum transpiration is computed dynamically. By the incorporation of T_m in Eqn. 3.16b daily meteorological conditions also influence the water uptake ability of a species. Water uptake may also be limited by the transport capacity of the tree roots. The transport capacity is found by multiplying root length index with a maximum water uptake rate per unit root length, $U_{w,x}$ ($\text{kg H}_2\text{O m}^{-1} \text{d}^{-1}$).

If water uptake from a compartment is below the demand either because of low soil moisture conditions or of insufficient transport capacity, roots from other compartments may take up an additional amount of water. This will continue until the roots of all compartments are limited or until the demand is satisfied. In this way roots from moist compartments may compensate reduced water uptake from dryer compartments, resulting in a deviation from the original distribution of water extraction according to the relative root lengths of Eqn. 3.16a.

3.4.2.2. Herbaceous vegetation

An equation similar to that for the tree population is used for the calculation of water extraction by the herbaceous vegetation from each soil compartment as a function of potential transpiration, soil moisture conditions, relative root length, root transport capacity, characteristic and maximum transpiration (Eqn. 3.17). Water uptake by the herbaceous vegetation is calculated for each subarea separately.

$$U_{w,H}(n,l) = T_p(n) * \frac{R_L(n,l)}{\sum R_L(n,l)} * \text{MIN}(1; Rd_w)$$

[Equation

3.17]

$U_{w,H}(n,l)$ water uptake rate per soil compartment in each subarea by the herbaceous vegetation (mm d^{-1})

$T_p(n)$ potential transpiration rate of the herbaceous vegetation (mm d^{-1})

[Sigma] summation over all soil compartments per subarea

Again, an iteration loop is used to allow for compensation if water uptake from some compartments is limited, either by low soil moisture conditions or by insufficient transport capacity, while water can still be taken up from other soil compartments.

3.4.2.3. Competition for water

Competition for water between trees and the herbaceous species is modelled in a simplified way. First water extraction per soil compartment and per subarea is calculated without any interference of the other species during the time step of integration of one day. Insufficient soil moisture conditions may limit water uptake of a species, depending on its sensitivity to low water availability. The characteristic transpiration is used as a measure for this sensitivity.

If the total water extraction by trees and the grass species from a soil compartment in a subarea exceeds total water availability, i.e. the amount of water stored in this compartment above wilting point, water uptake of both species from this compartment is corrected. Available water for plant uptake in this compartment is distributed among both species in proportion to their water uptake rates, as calculated before, to account for differences in competitive strength of the species (Eqn. 3.18).

$$U_{w,H}(n,l) = \frac{A_w(n,l)}{\Delta t} * \frac{U_{w,H}(n,l)}{U_{w,H}(n,l) + U_{w,T}(n,l)} \quad [\text{Equation 3.18a}]$$

$$U_{w,T}(n,l) = \frac{A_w(n,l)}{\Delta t} * \frac{U_{w,T}(n,l)}{U_{w,H}(n,l) + U_{w,T}(n,l)} \quad [\text{Equation 3.18b}]$$

$A_w(n,l)$ amount of water stored above wilting point, per soil compartment and per subarea (mm)

Compensatory water uptake from other soil compartments associated with limitation of water uptake due to competitive interactions is not modelled within the time step of integration. Eqn. 3.18 deals with the competition for water at a daily time scale. Competition for water also takes place at seasonal scale, if species differ in their water uptake rate at non-limiting water supply. Eventually, soil water availability may drop to limiting conditions as a result of the water extraction by both species, but at that time the species with the higher uptake rate will have used most of the initially available soil water.

3.4.3. Parameterization

Variable	Value	Unit	Source
----------	-------	------	--------

Tree population

Z_c	0.05	m	(a)
Z_m	4.0	m	Soumaré <i>et al.</i> (1994) ^b
p_v	6.9	-	(c)
p_h	3.5	-	(a)
S_r	0.5	$m\ g^{-1}$	(d)
T_c	4	$mm\ d^{-1}$	(a)
$U_{w,x}$	0.5	$kg\ m^{-1}\ d^{-1}$	(d)

Herbaceous vegetation

Z_0	0.075	m	van Keulen <i>et al.</i> (1986)
Z_m	2.0	m	Penning de Vries & Djitèye (1982)
p_v	6.9	-	Penning de Vries & Djitèye (1982) ^e
S_r	200	$m\ g^{-1}$	Jansen (1984)
R_{el}	0.04	m	van Keulen <i>et al.</i> (1986)
T_c	7	$mm\ d^{-1}$	(a)
$U_{w,x}$	$1.25 \cdot 10^{-3}$	$kg\ m^{-1}\ d^{-1}$	Jansen & Gosseye (1986) ^f

 Z_m maximum root depth S_r specific root length Z_0 initial rooted depth of the herbaceous species R_{el} rooted depth elongation rate

a. Value estimated

b. Based on measurements on *Acacia seyal*

c. Value identical to that of the herbaceous vegetation

d. Value estimated by setting the product of U_m and S_r of the tree species equal to that of the herbaceous speciese. Based on root length measurements of *Schoenefeldia gracilis*. The parameter p_v has been obtained by non-linear regression (see also [Fig. 3.7](#)).f. Calculated from a maximum transpiration capacity of $50\ mm\ d^{-1}$ for a full-grown vegetation with a root mass of approx. $2000\ kg\ ha^{-1}$. See also Azam-Ali *et al.* (1984).

3.5. Biomass production

3.5.1. Tree population

Actual biomass production of the tree population is calculated as a linear function of the photosynthetically active radiation (PAR), absorbed by the foliage of the trees. Under conditions of ample soil water supply the amount of dry matter produced per unit absorbed PAR, i.e. the light use efficiency, is related to tree size and nutrient concentrations in the foliage of the tree. A negative correlation between the light use efficiency and total standing wood and root biomass, as an estimate for tree size, is used to account for higher respiratory needs of larger trees. The effect of nutrient concentration on light use efficiency is given in Fig. 3.8 and Eqn. 3.19.

Figure 3.8. The relation between leaf nitrogen concentration and the reduction factor for dry matter production (see text for explanation).

Rd_B reduction factor for potential biomass production, caused by nitrogen deficiency (-)

$C_{N,l}$ actual leaf nitrogen concentration ($g\ g^{-1}$)

$C_{Nm,l}$ minimum leaf nitrogen concentration ($g\ g^{-1}$)

$C_{No,l}$ optimum leaf nitrogen concentration ($g\ g^{-1}$)

Two characteristic nitrogen concentrations are used in Fig. 3.8: a concentration below which the light use efficiency and therefore production equals zero ($C_{Nm,l}$) and a concentration above which the light use efficiency attains its maximum value, $E_{I,m}$ as a function of tree size. A linear interpolation is applied to estimate the light use efficiency between these two concentrations.

It is assumed that under conditions of suboptimal water supply actual production is proportional to the ratio between actual and potential transpiration (Eqn. 3.20).

$$P_p = I_{a,L} * E_{I,m} \text{ [Equation 3.19]}$$

$$P_a = P_p * Rd_B * \frac{T_a}{T_p} \text{ [Equation 3.20]}$$

$$= T_a * E_w$$

P_p potential rate of dry matter production, as function of absorbed radiation ($kg\ ha^{-1}\ d^{-1}$)

$I_{a,L}$ daily absorbed PAR by the foliage of a tree population ($J ha^{-1} d^{-1}$)

$E_{I,m}$ maximum light use efficiency as function of total wood and root biomass ($kg J^{-1}$)

P_a actual rate of dry matter production ($kg ha^{-1} d^{-1}$)

T_a actual transpiration rate of the tree population ($mm d^{-1}$)

T_p potential transpiration rate of the tree population ($mm d^{-1}$)

(Eqn. 3.7)

E_w water use efficiency for dry matter production ($kg ha^{-1} mm^{-1}$)

3.5.2. Herbaceous vegetation

Biomass production of the herbaceous vegetation is also calculated using the light use efficiency approach. But, contrary to the linear correlation in case of the tree species, biomass production of the herbaceous species is calculated as a non-linear function of absorbed PAR, because light use efficiency also depends on the radiation level, which may vary substantially among subareas due to shading. The non-linear function between biomass production and absorbed PAR, which includes the effect of shading, is described with a Monod function under the assumption that the light use efficiency expressed as $P / (I_m * f_a)$ is constant for situations with various leaf area indices of the grass species (Eqn. 3.21 and [Fig. 3.9a](#)).

$$P = \frac{P_m * I_m}{P_m / E_0 + I_m} * f_a \quad \text{[Equation 3.21a]}$$

$$I_m = I_p * (1 - r_p) \quad \text{[Equation 3.21b]}$$

$$f_a = 1 - e^{-K_L * L(n)} \quad \text{[Equation 3.21c]}$$

P net rate of herbaceous biomass increase ($kg ha^{-1} d^{-1}$)

I_m amount of PAR, available for absorption (equal to absorbed PAR, if $f_a = 1$) ($J ha^{-1} d^{-1}$)

f_a fraction absorbed PAR (-)

P_m theoretical rate of maximum production ($kg ha^{-1} d^{-1}$)

E_0 initial light use efficiency ($kg J^{-1}$)

I_p daily photosynthetically active radiation ($J ha^{-1} d^{-1}$)

r_p reflection coefficient for I_p (-)

$L(n)$ leaf area index of the herbaceous vegetation ($m^2 m^{-2}$)

K_L extinction coefficient of leaves for I_p ($m^2 m^{-2}$)

Figure 3.9a. Relation between daily total PAR, available for absorption, and ratio of net biomass production P and fraction absorbed PAR, f_a . Simulated data and fitted curves; see text for explanation.

The data in Fig. 3.9 have been derived from calculations with a model based on the assimilation and respiration calculations of SUCROS1 (van Laar *et al.*, 1992) using parameters for millet, *Pennisetum typhoides*, as input (Erenstein, 1990). Net biomass increase and the amount of absorbed PAR were simulated for each day with daily weather input of 1977, for Niono in Mali. To simulate various shading intensities, i.e. various values for I_m , different weather data files were created by multiplying measured daily short-wave radiation with several reduction factors. These new data files were used as input for the model. Because SUCROS1 assumes a decline in maximum assimilation rate ('AMAX') during reproductive development, only results from the vegetative stage have been plotted in Fig. 3.9. Curve 1 in Fig. 3.9 represents the potential production situation, whereas curves 2 and 3 refer to calculations with a lower maximum assimilation rate. Also the maintenance requirements were reduced in these calculations so that both curves represent a situation with limiting nutrient concentrations. It is assumed that the initial light use efficiency E_0 was equal for all production situations.

The results of this model show that the daily light use efficiency is approximately constant at constant irradiation within a range of 0 to 5 for the leaf area index, as has been assumed. All three curves illustrate that the production decreases as a function of shading intensity (Fig. 3.9a), but that the light use efficiency, i.e. $P / (I_m * f_a)$, is positively correlated to the shade level (Eqn. 3.21d and Fig. 3.9b).

$$E_I = \frac{P_m}{P_m / E_0 + I_m} \quad \text{[Equation 3.21d]}$$

E_I daily light use efficiency with ample soil water supply ($kg J^{-1}$)

Figure 3.9b. Relation between daily total PAR, available for absorption, and daily light use efficiency. Simulated data and fitted curves; see text for explanation.

With respect to biomass production, a decrease in available PAR due to shading is partly compensated by an increase in light use efficiency. The compensation of E_I due to shading is stronger if nutrients are limiting. The negative effect of shading on biomass production of the herbaceous species is thus less severe in a nutrient-deficient environment (compare curves 1 and 3 in Fig. 3.9a).

For the potential production situation the theoretical production maximum P_m can be found by

substituting the average light use efficiency of a vegetation grown under optimal field conditions, $E_{I,a}$, and the average radiation level during its vegetative growth, $I_{m,a}$, into Eqn. 3.21d. The slope of the regression line, describing the relation between cumulative production and cumulative absorption of PAR, gives the average light use efficiency for a growth period. The use of an average radiation level is only permitted if there is no clear trend in daily radiation levels in the course of the vegetative period. In such a situation a weighted average should be used. During the reproductive phase or if nutrients are limiting, a different light use efficiency is used for substitution into Eqn. 3.21d to determine the theoretical production maximum, which correlates with these less productive situations. The relation between light use efficiency under nutrient limited growth conditions and the nutrient concentration in the leaves is described in a similar way as for the tree species (Fig. 3.8). Rd_B now equals the ratio of the light use efficiency under nutrient limited conditions and that under optimal growth conditions, $E_{I,a}$. A reduction due to ageing is also incorporated to account for decreasing maximum assimilation rate and thus decreasing light use efficiency during the reproductive phase (Fig. 3.10).

Figure 3.10. Relation between development stage (DVS) and the reduction factor for light use efficiency.

Rd_2 reduction factor for potential biomass production due to ageing at DVS = 2 of the herbaceous species (-).

The minimum of the light use efficiencies, as determined by nutrient status and senescence, is used as the average light use efficiency instead of $E_{I,a}$ to calculate the theoretical production maximum with Eqn. 3.21d in combination with the average light intensity $I_{m,a}$. Daily light use efficiency E_I is now determined by substituting daily actual radiation, I_m , as influenced by shading and weather variability, into Eqn. 3.21d, using the theoretical production maximum, calculated before as a function of nutrient level and senescence. Biomass production with ample soil water supply is estimated by multiplying E_I with total absorbed radiation, $I_a(n)$.

Under conditions of suboptimal water supply, it is assumed that the actual production is proportional to the ratio of actual and potential transpiration.

The ratio of daily light use efficiency E_I and average light use efficiency under optimal growth conditions $E_{I,a}$, equals the correction factor used for calculating potential transpiration (Eqn. 3.9).

3.5.3. Parameterization

Variable	Value	Unit	Source
----------	-------	------	--------

Tree population

$E_{I,m}$	0, 3.0 400, 2.0 800, 1.5 2400, 1.0	$g MJ^{-1}$	(a)
<i>Herbaceous vegetation</i>			
E_0	5.0	$g MJ^{-1}$	(b)
$E_{I,a}$	3.5	$g MJ^{-1}$	(b)
$I_{m,a}$	$23 * 10^6$	$J m^{-2} d^{-1}$	(b)
Rd_2	0.5	-	(van Laar <i>et al.</i> , 1992)

$E_{I,m}$ light use efficiency (2nd column) as function of total wood and root biomass (1st column)

a. Values estimated;

b. Results of a non-linear regression analysis with the Monod function ([Fig. 3.9a](#) and [3.9b](#)). Crop parameters from Erenstein (1990) in combination with weather data from 1977 in Niono (Mali).

3.6. Growth and death of plant parts

3.6.1. Tree population

3.6.1.1. Phenology

Phenology of the trees is described in a simple way, based on leaf dynamics. Four stages are distinguished in the phenology of a deciduous tree (Table 3.1). Different phenological stages are used because in the model processes such as production, transpiration and nutrient uptake are correlated to these stages through the presence or absence of leaves. Leaf dynamics of an evergreen tree species should be modelled more continuously throughout the year, but this is not yet included. With minor modifications the model can be adapted to simulate evergreen trees.

Table 3.1. Number of phenological stages and descriptions in terms of leaf and reserve dynamics

stage	description
0	leafless period

- 1 leaf flush period, including reserve utilization
 - 2 major growth period and reserve storage
 - 3 leaf fall period
-

Four transition dates at which the tree in the model switches from one phenological stage to the next, are determined as a function of season and species characteristics. Two different ways can be selected to simulate the beginning of the leaf flush period, which marks the end of the leafless period. The leaf flush can start either at a fixed date or three days after daily rainfall has exceeded a threshold value. In the leaf flush period reserves are mobilized to accelerate leaf growth. The end of this period is marked by meeting either of three conditions: (i) the reserves are exhausted, (ii) leaves have completed their flush by reaching their maximum biomass or (iii) the maximum number of days for the leaf flush has been exceeded. Leaf death only occurs during the leaf fall period, unless caused by water stress. Hence, the beginning of the leaf fall period can either be triggered by water shortage, if leaf death due to prolonged water stress exceeds a critical value, or by a calendar time, determined by the phenology of the tree. At the end of the leaf fall period the leaf biomass of the tree equals zero and the length of this period depends on the degree of water stress or equals the exogenously supplied maximum duration for this period. Leaves are assumed to be photosynthetically active as long as they remain attached to the tree.

3.6.1.2. Growth of plant components

For the tree species five plant components are distinguished: leaves, flowers or fruits, branches, stems and roots. Total biomass that can be allocated to these organs consists of current production, biomass relocated from dying leaves and reserves. The latter are exclusively used for acceleration of early leaf development (3.6.1.5), whereas the other two sources are distributed among all plant components by applying partitioning factors during the three periods in which leaves are present. However, during leaf fall period the partitioning to leaves and fruits is halted and the biomass available for allocation is distributed among the roots, branches and stems, only. The partitioning factors are defined as a function of stem biomass to take into account changes in partitioning at increasing age of the tree. Stem biomass is thus used as an indicator for the physiological age of the tree. Biomass partitioning between above- and belowground parts of the tree can be modified by the availability of growth resources. The shoot partitioning factor derived from stem biomass, is used under potential production conditions. If water or nutrient supply limit biomass production of the tree, lower shoot and thus higher root partitioning factors are used. The relative decrease in the shoot partitioning factor is derived from the ratio of actual and potential production on a daily basis (van Laar *et al.*, 1992; Fig. 3.12a). After the biomass has been allocated to roots and shoots, total shoot growth is partitioned among leaves, branches, stems and flowers or fruits.

3.6.1.3. Death of plant components

During the leaf fall period, a deciduous tree gradually loses all of its leaves. If no severe water stress has occurred during the growth phase before leaf shedding, the model computes a decrease in leaf

biomass only during this period. A simple function relating relative death rate of leaves to time is used during this period. On the other hand if severe water stress has occurred during one of the leaf bearing periods, an accelerated leaf death is simulated. To keep track of severe water stress and its effect on leaf biomass an intermediate variable, i.e. accumulated days of water stress for leaves, is introduced in the model. The rate of change of this variable depends on the transpiration ratio and a threshold value, that represents the sensitivity of the tree leaves to water stress (Fig. 3.11)

Figure 3.11. The relation between the transpiration ratio and the change in the accumulated amount of water stress days for leaves.

R_{ws} rate of change in accumulated water stress days (d^{-1});

T_h transpiration ratio threshold value (-);

T_a actual transpiration rate of the tree population ($mm\ d^{-1}$);

T_p potential transpiration rate of the tree population ($mm\ d^{-1}$).

The accumulated water stress days for leaves increases if soil water supply is inadequate, but decreases again if enough soil water is available for transpiration. In this way the effect of a period of water stress may be mitigated again if it is followed by a period of ample soil water supply. The minimum value of the accumulated number of water stress days is zero.

To model the effect of water stress on leaf biomass dynamics, a correlation between the accumulated water stress days for leaves and the accelerated relative death rate of leaves is used. Only a prolonged period of water stress leads to leaf death and eventually to total leaf shedding, if the water supply does not recover in time. The sum of the relative death rate as determined by tree phenology and the relative death rate due to water stress gives the actual relative death rate of the leaves. The relative death rate of fruits is set equal to the relative death rate of the leaves.

The daily rates of reduction in biomass of roots and branches are estimated by using relative death rates based on annual values (Eqn. 3.22). It is assumed that the daily relative death rates are constant throughout the year.

$$r_{i,d} = \frac{-\ln(1 - r_{i,y})}{365} \quad [\text{Equation 3.22}]$$

$r_{i,d}$ mean daily relative death rate of tree roots and branches (d^{-1})

$r_{i,y}$ annual relative death rate of tree roots or branches (yr^{-1})

i plant component indication number

In the model the death rate of the stems is zero. However, stem biomass can decrease during the leaf flush period as a result of the utilization of reserves that are partly stored in the stems. Whole tree death

is not modelled yet, but could be related to tree size if the total decrease in biomass of the perennial structures of roots, branches and stems significantly exceeds total production on an annual basis.

The processes of growth and death of plant components are integrated in time with a time step of one day to determine the amount of living and dead biomass of each plant component. At the start of the simulation initial values of all plant components of an individual tree and the tree population density, should be given.

3.6.1.4. Leaf and wood area dynamics

Leaf area per tree is calculated as the product of leaf biomass per tree and a constant specific leaf area. The ratio of leaf area per tree and the vertical projection of the tree crown, i.e. crown cover, gives the leaf area index in the model for the tree species (Eqn. 3.23). Wood area index is determined in a similar way as a function of branch biomass per tree, a specific branch area and tree crown cover.

$$L = \frac{W_{lv} * S_L}{C_c * N} * 1000$$

[Equation 3.23]

L leaf area index of a tree (m² m⁻²)

W_{lv} leaf biomass (kg ha⁻¹)

N actual tree population density (tree ha⁻¹)

S_L specific leaf area (ha kg⁻¹)

C_c individual tree crown cover (m² (plant)⁻¹)

3.6.1.5. Reserve dynamics

Reserve carbohydrates provide an additional source for the growth of leaves during early development of a deciduous tree after its leafless period. By utilization of the reserves the formation of leaves is accelerated compared to the situation where only current production of biomass is available. In the model reserve utilization is treated in a simple way. Leaves are assumed to follow an exponential growth curve during the reserve utilization period. The effect of water or nutrient stress on leaf growth is included. The relative growth rate of leaves is proportional to a maximum relative growth rate and to the ratio of actual and potential biomass production. The demand for reserves equals the difference between leaf growth based upon the exponential growth curve and growth realized by the partitioning of current biomass production. This difference is multiplied with an efficiency factor to take into account the losses due to conversion of reserves into leaf biomass. If the available reserves exceed the demand for exponential growth, leaf growth will follow its exponential curve. If the reserves are nearly depleted, leaf growth equals the sum of biomass growth originating from current production and the available reserves, corrected for the efficiency (Eqn. 3.24). In this case the reserve level becomes zero and the leaf flush stops, because during the reserve mobilization period biomass production is not used for

replenishment of the reserves.

$$W_{dm} = (G_{e_{lv}} - G_{c_{lv}}) * Q_A \text{ [Equation 3.24a]}$$

$$\text{if } W_{dm} \leq (W_{rs} / [\Delta]t)$$

$$G_{lv} = G_{e_{lv}} \text{ [Equation 3.24b]}$$

$$\text{if } W_{dm} > (W_{rs} / [\Delta]t)$$

$$G_{lv} = G_{c_{lv}} + W_{rs} / (Q_A * [\Delta]t) \text{ [Equation 3.24c]}$$

W_{dm} demand for reserves for leaf growth ($\text{kg ha}^{-1} \text{ d}^{-1}$)

W_{rs} total amount of reserves (kg ha^{-1})

$G_{e_{lv}}$ exponential leaf growth rate ($\text{kg ha}^{-1} \text{ d}^{-1}$)

$G_{c_{lv}}$ leaf growth rate realized from current biomass production ($\text{kg ha}^{-1} \text{ d}^{-1}$)

G_{lv} actual leaf biomass growth rate ($\text{kg ha}^{-1} \text{ d}^{-1}$)

Q_A assimilate requirement in dry matter production (kg kg^{-1})

$[\Delta]t$ time interval of integration (d)

It is assumed that the reserves, used only by the leaves in this model, are stored in the stems and branches of the tree and that the partitioning of reserves among these plant components is proportional to their biomass ratios. Following the reserve utilization period, part of the biomass allocated to the branches and the stems are reserves to restore the reserve level. The rate of increase in reserves is described as a negative linear function of the reserve level (Eqn. 3.25).

$$G_{rs} = (G_{st} + G_{br}) * \frac{C_{r,m} - C_{r,a}}{C_{r,m}} \text{ [Equation 3.25]}$$

G_{rs} rate of increase in reserves ($\text{kg ha}^{-1} \text{ d}^{-1}$)

G_{st} growth rate of stem biomass ($\text{kg ha}^{-1} \text{ d}^{-1}$)

G_{br} growth rate of branch biomass ($\text{kg ha}^{-1} \text{ d}^{-1}$)

$C_{r,m}$ maximum reserve concentration (g g^{-1})

$C_{r,a}$ current reserve concentration (g g^{-1})

If the tree has reached its maximum reserve level reserves are no longer accumulated from current biomass production ($G_{rs} = 0$), whereas if the reserves are fully exhausted the complete share of stem and branch growth is stored as reserves. The maximum daily increase in reserves is thus limited by the sum of branch and stem growth. In the model biomass of the branches and the stems includes their reserves. Total aboveground biomass in the leafless period is then simply given by their sum.

3.6.2. Herbaceous vegetation

3.6.2.1. Development

The development stage of the herbaceous vegetation (acronym: DVS) is used in the model to govern biomass partitioning factors and death rates. It increases from 0 at emergence to 1 at flowering and 2 at maturity. During vegetative development ($0 < DVS < 1$) and during reproductive development ($1 < DVS < 2$) the rate of change in DVS is calculated by using a reference development rate, different for both periods, and various factors, which decrease or increase the reference development rate. The reference development rates are constant in the model, whereas the factors are computed dynamically. In general, development rate is positively correlated to temperature, which is taken into account in the model by a temperature factor. Stress, whether due to water or nutrient shortage, is also known to affect development rate, especially during early vegetative growth. An estimate for the stress level with respect to dry matter production is given by the ratio of actual and potential production. A negative relation between this ratio and the stress factor for calculating the development rate is incorporated in the model, but is only used during vegetative growth. Latitude and daylength also affect development rate. The values of the latitude factor increases with increasing latitude, whereas the daylength factor decreases with increasing daylength (de Ridder, 1979; Jansen, 1984; Erenstein, 1990). These two factors are only used during the vegetative phase. The various factors affecting development have been applied in a multiplicative way (Eqn. 3.26).

$$R_{vd} = R_{vd,0} * f_{t,v} * f_s * f_l * f_d \text{ [Equation 3.26a]}$$

$$R_{gd} = R_{gd,0} * f_{t,g} \text{ [Equation 3.26b]}$$

R_{vd} development rate during the vegetative phase of the herbaceous species (d^{-1})

$R_{vd,0}$ reference development rate during the vegetative phase of the herbaceous species (d^{-1})

$f_{t,v}$ effect of average daily temperature on development rate during the vegetative phase of the herbaceous species (-)

f_s effect of stress on development rate during the vegetative phase of the herbaceous species (-)

f_l effect of latitude on development rate during the vegetative phase of the herbaceous species (-)

f_d effect of daylength on development rate during the vegetative phase of the herbaceous species (-)

R_{gd} development rate during the reproductive phase of the herbaceous species (d^{-1})

$R_{gd,0}$ reference development rate during the reproductive phase of the herbaceous species (d^{-1})

$f_{t,g}$ effect of average daily temperature on development rate during the reproductive phase of the herbaceous species (-)

3.6.2.2. Growth of plant components

The starting day of the growth calculations for the herbaceous species can either be given by the user or depends on soil water status. If the amount of water, stored above wilting point, in the top soil compartments exceeds a threshold value, germination and emergence are assumed to begin. These two processes are not actually modelled, because the calculations start with values for the state variables of the herbaceous species that correspond to a situation occurring a few days after a successful emergence.

The dry matter partitioning factors of roots and shoots of the herbaceous species are calculated on a daily basis as a function of development stage. They are modified if shortage in belowground resources occurs and in case of shading. A lower production ratio, i.e. the ratio of actual and potential production under the prevailing light conditions of each subarea, results in a lower shoot and thus higher root partitioning factor. On the other hand, the shoot partitioning factor is increased if trees decrease the radiation level for the herbaceous vegetation. The shading intensity is given by the ratio of intercepted PAR by the trees, averaged per subarea, and the available PAR in an herbaceous monocrop. The effects, due to below- and aboveground stress, have simply been multiplied to arrive at the net change in the root-shoot partitioning factors, as determined by development stage (Fig. 3.12 and Eqn. 3.27). They are only applied during the vegetative phase.

$$p_{sh} = p_{sh,0} * f_p * f_{shd} \text{ [Equation 3.27a]}$$

$$p_{rt} = 1 - p_{sh} \text{ [Equation 3.27b]}$$

p_{sh} actual shoot biomass partitioning factor (-)

p_{rt} root biomass partitioning factor (-)

$p_{sh,0}$ shoot biomass partitioning factor as function of development stage of the herbaceous species (-)

Growth of roots and shoots is given by the product of the partitioning factors and the total amount of biomass available for allocation. The biomass partitioning factors for the aboveground structures, i.e. leaves, stems and reproductive organs, are computed as a function of development stage and are used to distribute shoot biomass growth among the aerial parts of the plant.

Figure 3.12. *The relation between the production ratio and the relative reduction in shoot biomass partitioning factor (a) and the relation between the light availability ratio and the relative increase in shoot biomass partitioning factor (b).*

f_p effect of production stress due to belowground resources on the shoot biomass partitioning factor (-)

f_{shd} effect of shading on the shoot biomass partitioning factor (-)

P_a actual rate of dry matter production ($\text{kg ha}^{-1} \text{d}^{-1}$)

P_p potential rate of dry matter production, as function of absorbed radiation ($\text{kg ha}^{-1} \text{d}^{-1}$)

I_p daily photosynthetically active radiation ($\text{J ha}^{-1} \text{d}^{-1}$)

$I_t(n)$ daily transmitted PAR towards the herbaceous vegetation ($\text{J ha}^{-1} \text{d}^{-1}$)

During vegetative phase the total amount of biomass that can be allocated to the various plant parts equals current dry matter production. During the reproductive phase also reserves stored in the stem during the vegetative phase, become available. The reserve mobilization rate, which is added to the current biomass production before calculating the biomass partitioning, is computed as the product of the reproductive development rate, a fixed fraction of reserves in the stem and stem biomass during the entire reproductive phase (van Laar *et al.*, 1992; Eqn. 3.28).

$$R_{w,st} = W_{st} * f_{r,st} * R_{gd} \text{ [Equation 3.28]}$$

$R_{w,st}$ stem reserve mobilization rate during the reproductive phase ($\text{kg ha}^{-1} \text{d}^{-1}$)

W_{st} stem biomass (kg ha^{-1})

$f_{r,st}$ fraction of reserves in the stem (-)

Also leaf senescence may contribute to the pool of assimilates available for allocation towards the various plant parts (Kropff & Van Laar, 1993). A fraction of the decrease rate of leaf biomass can be withdrawn and reallocated towards growing tissues.

3.6.2.3. Death of plant components

The relative death rate of the leaves is either governed by a function of development stage or by a function of leaf area index. In this way the effect of severe shading on the senescence of leaves positioned low in the canopy has been simulated. The critical leaf area index is estimated with Eqn. 3.29, which also contains the effect of additional shading by the trees on the herbaceous vegetation.

$$L_c(n) = \frac{-\ln(f_c * (I_p / I_t(n)))}{K_L} \text{ [Equation 3.29]}$$

$L_c(n)$ critical leaf area index per subarea with respect to leaf death ($m^2 m^{-2}$)

f_c critical fraction of PAR with respect to leaf death (-)

I_p daily photosynthetically active radiation ($J ha^{-1} d^{-1}$)

$I_t(n)$ daily transmitted PAR towards the herbaceous vegetation ($J ha^{-1} d^{-1}$)

K_L extinction coefficient of leaves for I_p ($m^2 m^{-2}$)

The leaves located under a top layer with a leaf area index equal to $L_c(n)$ receive only a fraction f_c of the available PAR. It is assumed that this low radiation level causes additional leaf death if the death rate corresponding with the low radiation level exceeds the leaf death that has been calculated as function of development stage (van Laar *et al.*, 1992; Eqn. 3.30).

$$r_{L,s}(n) = r_{Lc} * \frac{L(n) - L_c(n)}{L_c(n)} \quad [\text{Equation 3.30a}]$$

$$r_L(n) = \text{MIN}(r_{L,d}; r_{L,s}(n)) \quad [\text{Equation 3.30b}]$$

$r_{L,s}(n)$ relative rate of leaf death per subarea as function of radiation level (d^{-1})

r_{Lc} reference relative rate of leaf death as function of radiation level (d^{-1})

leaf area index of the herbaceous vegetation ($m^2 m^{-2}$)

$r_{L,d}$ relative rate of leaf death as function of development stage (d^{-1})

$r_L(n)$ relative death rate of leaf biomass (d^{-1})

A prolonged drought period may also induce leaf death which is added to the leaf death due to development stage or low radiation level. Equations identical to those for the tree population are used, but with parameters characteristic for the herbaceous species. The additional leaf death is thus described as a function of the transpiration ratio, a critical transpiration ratio and the sensitivity of the herbaceous vegetation for water stress accumulation. This may lead to total plant death under prolonged water stress. A new vegetation can establish again if soil water content above wilting point of the top soil compartments exceeds the threshold value. The initial values of the state variables of this new vegetation are identical to those used for the original vegetation. Several germination flushes can be mimicked in this way.

Death of plant roots is correlated to leaf death to maintain a balance between both plant components. A delay in the timing of root death relative to leaf death is incorporated. Relative root death equals relative leaf death as soon as the leaf area index has dropped below a threshold value defined as a fraction of the

maximum leaf area index during the growing season.

3.6.2.4. Leaf area dynamics

Except during early vegetative development, leaf area index is described as a function of leaf biomass dynamics and specific leaf area (Eqn. 3.31).

$$G_L = G_{IV}(n) * S_L \text{ [Equation 3.31a]}$$

$$D_L = r_L(n) * L(n) \text{ [Equation 3.31b]}$$

G_L rate of increase in leaf area index ($m^2 m^{-2} d^{-1}$)

D_L rate of decrease in leaf area index ($m^2 m^{-2} d^{-1}$)

During early vegetative development leaf area index follows an exponential curve in time. As soon as leaf area index has reached a threshold value, simulation of leaf area development switches to Eqn. 3.31a (Kropff & Van Laar, 1993; van Laar *et al.*, 1992). To incorporate effects of temperature on leaf area development, time in the exponential growth curve is expressed in degree days ($^{deg}C d$) with a base temperature of $0^{deg}C$. The relative leaf area growth rate ($m^2 m^{-2} (^{deg}C d)^{-1}$) also depends on the supply of water and nutrients and is therefore linearly related to the ratio of actual and potential production for each subarea.

3.6.3. Parameterization

Variable	Value	Unit	Source
<i>Tree population^a</i>			
t_1	150	-	(b)
t_{12}	60	d	(b)
t_3	240	-	(b)
P_{t1}	20	mm d^{-1}	(c)
$r_{L,d}$	0, 0.001	d^{-1}	(c)
	30, 0.005		
	60, 0.01		
	90, 1.0		

$W_{lv,x}$	0, 0 50, 7 100, 14 200, 28 500, 56	kg (plant) ⁻¹	Breman & Kessler (1995)
$P_{sh,0}$	0, 0.40 1000, 0.40	-	Breman & Kessler (1995)
P_{st}	0, 0.48 1000, 0.48	-	
P_{br}	0, 0.32 1000, 0.32	-	
P_{lv}	0, 0.10 1000, 0.10	-	
f_p	0, 0.5 0.5, 1.0 1.0, 1.0/td>	-	van Laar <i>et al.</i> (1992)
$W_{st,0}$	200 kg	(plant) ⁻¹	Breman & Kessler (1995)
$W_{br,0}$	135	kg (plant) ⁻¹	
$W_{rt,0}$	220	kg (plant) ⁻¹	
$W_{rs,0}$	33.5	kg (plant) ⁻¹	(d)
T_h	0.01	-	(b)
$r_{L,ws}$	0, 0 5, 0 10, 0.01 20, 0.1 30, 1.0	d ⁻¹	(b)
$r_{br,y}$	0.02	yr ⁻¹	(e)/
$r_{rt,y}$	0.20	yr ⁻¹	(e)
S_L	0.001	ha kg ⁻¹	Penning de Vries & Djitèye (1982)

S_W	0, 0.00005 100, 0.000025 400, 0.00000125	ha kg ⁻¹	(f)
Q_A	1.4	g g ⁻¹	(b)
r_{glv}	0.15	d ⁻¹	(b)
$C_{r,m}$	0.15	g g ⁻¹	(b)
<i>Herbaceous vegetation</i>			
t_1	180	-	Penning de Vries & Djitèye (1982)
t_{ei}	5	d	(b)
n_{sl}	3	-	(b)
W_t	15	mm	(b)
$R_{vd,0}$	0.035	-	Jansen (1984) ^g
$R_{gd,0}$	0.033	-	Jansen (1984) ^g
$f_{t,v}$	0, 0 26, 1.0 44, 1.2 50, 1.2	-	Jansen (1984) ^g
f_l	12, 0.75 14, 1.0 16, 1.5	-	de Ridder (1984)
f_d	0, 1.0 12.5, 1.0 13.5, 0.43 24.0, 0.43	-	Jansen (1984) ^g
f_s	0, 1.3 0.5, 1.1 1.0, 1.0	-	(b)
$W_{st,0}$	$5 * 10^{-7}$	kg (plant) ⁻¹	van Keulen <i>et al.</i> (1986) ^h
$W_{lv,0}$	$5 * 10^{-7}$	kg (plant) ⁻¹	

$W_{rt,0}$	$5 * 10^{-7}$	kg (plant) ⁻¹	
L_0	$2.5 * 10^{-9}$	ha (plant) ⁻¹	(b)
$P_{sh,0}$	0,0, 0.6	-	Penning de Vries & Djitèye (1982)
	1.0, 0.9		
	1.25, 1.0		
	3.0, 1.0		
P_{lv}	0,0, 0.67	-	
	1.0, 0.39		
	1.25, 0.20		
	1.50, 0.0		
	3.0, 1.0		
P_{st}	0,0, 0.33	-	
	1.0, 0.61		
	1.25, 0.5		
	1.50, 0.5		
	1.75, 0.0		
	3.0, 0.0		
f_p	0, 0.5	-	van Laar <i>et al.</i> (1992)
	0.5, 1.0		
	1.0, 1.0		
f_{shd}	0, 1.0	-	(b)
	0.5, 1.2		
	1.0, 1.5		
$f_{r,st}$	0.15	g g ⁻¹	(b)
$f_{r,lv}$	0.0	g g ⁻¹	(b)
f_c	0.05	-	van Diepen <i>et al.</i> (1988)
$r_{L,d}$	0, 0.0	d ⁻¹	van Keulen (1975)
	0.89, 0.0		
	0.90, 0.005		
	1.8, 0.005		
	2.0, 0.10		

	2.1, 1.0		
$r_{L,ws}$	0, 0.0	d^{-1}	(b)
	2.0, 0.0		
	5.0, 0.05		
	7.5, 0.1		
	10, 1.0		
T_h	0.01	$mm\ d^{-1}$	(b)
r_{Lc}	0.05	d^{-1}	(b)
S_L	0.002	$ha\ kg^{-1}$	(b)
r_{LAI}	0.008	$g\ g^{-1}\ (^{\circ}Cd)^{-1}$	(b) ⁱ
L_e	0.75	$m^2\ m^{-2}$	van Laar <i>et al.</i> (1992)

t_1 number of first possible day of growth calculations of the herbaceous species or number of first day of tree leaf flush;

t_{12} maximum period of reserve mobilization for tree leaf growth;

t_3 number of latest possible day of beginning of leaf fall period;

P_{t1} rainfall threshold value for starting tree leaf flush;

$r_{L,d}$ relative leaf death rate (2nd column) as function of development stage (herbaceous species) or as function of time (tree species);

$W_{lv,x}$ maximum tree leaf biomass (2nd column) as function of branch biomass;

p_i biomass partitioning factors (2nd column);

$p_{sh,0}$ shoot biomass partitioning factor (2nd column) as function of stem biomass (tree species) or as function of DVS (herbaceous species);

$W_{i,0}$ biomass per plant component at initialization;

$r_{L,ws}$ relative rate of leaf death (2nd column) as function of accumulated days for water stress

$r_{br,y}$ annual relative death rate of tree branches;

$r_{rt,y}$ annual relative death rate of tree roots;

S_W specific wood area (2nd column) as function of branch biomass;

r_{glv} maximum relative tree leaf growth rate during leaf flush;

t_{ei} number of days between emergence and initialization of the herbaceous species;

n_{sl} number of soil compartments for determining emergence of the herbaceous species;

W_t water availability threshold value for determining emergence;

$f_{t,v}$ 1st column: average air temperature and 2nd column: effect on DVR;

f_l 1st column: latitude and 2nd column: effect on DVR;

f_d 1st column: day length and 2nd column: effect on DVR;

f_s 1st column: stress and 2nd column: effect on DVR;

L_0 herbaceous leaf area index at initialization;

$f_{r,lv}$ fraction of reserves in the leaves that can be translocated;

r_{LAI} maximum relative rate of increase in leaf area index of the herbaceous species;

L_e threshold LAI for exponential leaf area growth of the herbaceous species;

- a. For most input data characteristics of trees occurring in the North-Sudan zone of West-Africa have been chosen as example.
- b. Value estimated.
- c. Based on unpublished results of *Acacia seyal* and *Sclerocarya birrea* near Niono (Mali).
- d. Value estimated at 10 % of stem and branch biomass.
- e. Pers. comm. H. Breman.
- f. Value estimated with wood area index approximately equal to $0.5 \text{ m}^2 \text{ m}^{-2}$.
- g. Based on de Ridder (1979).
- h. Total biomass in combination with a plant population density of 1000 m^{-2} equals 15 kg ha^{-1} .
- I. Comparable to the value used for spring wheat (0.009; van Laar *et al.*, 1992).

3.7. Soil water balance

3.7.1. Introduction

The soil water balance used in RECAFS is called SAHEL (Soils in semi-Arid Habitats that Easily Leach) and has been extensively described in other publications (van Keulen, 1975; Stroosnijder & Koné, 1982; Penning de Vries *et al.*, 1989). Therefore, only a brief description is given here. Horizontal water movement from one subarea to another is not taken into account.

3.7.2. SAHEL water balance

In each subarea the soil profile is subdivided into a number of horizontal compartments. Total soil depth, which is equal for all subareas, is given by the sum of the compartment thicknesses. The water content in each soil compartment is assumed to be homogeneously distributed in all directions. By integrating actual transpiration (1), soil evaporation (2), infiltration (3) and percolation, the water content of each soil compartment is found on a daily basis.

1) Water loss from the soil due to water uptake by plants has been described in 3.4 for each compartment and is subtracted from the available amount of water in a compartment. The remaining soil water content is used for determining the water loss per compartment due to actual soil evaporation.

2) Potential soil evaporation rate has been described in 3.3 and equals the maximum amount of water that can evaporate through the soil surface. Actual soil evaporation also depends on the daily rainfall pattern and the availability of water in the soil above air dry. The amount of water at air dry is the minimum amount of water present in the soil and can not be used for transpiration or evaporation. On days with a significant infiltration of water into the soil, total actual evaporation rate from all compartments equals the potential soil evaporation, but is limited by the availability of water (Eqn. 3.32a). Another calculation is used for days without significant infiltration (Eqn. 3.32b and Fig. 3.13).

If $F_w(n,1) > 0.5 \text{ mm d}^{-1}$

$$E_s(n) = \text{MIN}(E_p(n), \frac{A_a(n,1)}{\Delta t} + F_w(n,1)) \quad [\text{Equation 3.32a}]$$

If $F_w(n,1) < 0.5 \text{ mm d}^{-1}$

$$E_s(n) = \text{MIN}(E_p(n) , 0.6 * E_p(n) * ([\text{radical}](t_r + 1) - [\text{radical}]t_r) + F_w(n,1)) \quad [\text{Equation 3.32b}]$$

$E_p(n)$ potential soil evaporation rate (mm d^{-1})

$E_s(n)$ actual soil evaporation rate (mm d^{-1})

$F_w(n,1)$ water infiltration of the 1st soil compartment (mm d^{-1})

$A_a(n,1)$ amount of water stored above air dry of the 1st soil compartment,
per subarea (mm)

t_r number of days without significant infiltration counted from the

last day with significant infiltration (d)

n subarea indication number

Figure 3.13. Graphical presentation of Eqn. 3.32b, assuming that

(i) $E_s(n) = E_p(n)$ at $t_r = 0$ with $F_w(n,1) > 0.5$,

(ii) $F_w(n,1) = 0$ at the following days ($t_r > 0$) and

(iii) a constant $E_p(n)$ during 10 days.

Total actual soil evaporation of a subarea, $E_s(n)$, is distributed among the soil compartments by applying

a distribution factor for each compartment. These factors are calculated as a positive linear function of the amount of water stored above air dry and as a negative exponential function of the average depth of the centre of each compartment. The product of $E_s(n)$ and the distribution factor of a soil compartment gives the water loss per compartment due to soil evaporation. The soil water content remaining after water has evaporated from the soil is used in the calculation of the influx and efflux of water per compartment due to infiltration.

3) In calculating the downward movement of water which infiltrates, the simple 'storage-overflow' concept is used. Each soil compartment is characterized by a maximum water storage capacity, i.e. the water content at field capacity. Current storage capacity is dynamically computed as the difference between water content at field capacity and current water content after water extraction due to evapotranspiration. For each compartment influx and efflux of water is calculated. The efflux of a soil compartment equals the influx into the next compartment in downward direction. Water can only enter the next compartment if the influx into the preceding compartment exceeds its current storage capacity. Upward flow of water only takes place in case of plant water uptake or soil evaporation. Water flowing through the lower boundary of the whole soil profile is assumed to be lost through deep percolation.

Tree stem flow infiltration is calculated in a similar way as the infiltration of total throughfall except for the estimation of water storage capacity. Water storage capacity used for the homogeneous infiltration of total throughfall is decreased by multiplication with a factor between 0 and 1 for each compartment to simulate the concentrated infiltration of tree stem flow. This factor represents the ratio of the area where tree stem flow infiltrates and crown cover, where total throughfall infiltrates. In case of equal tree stem flow and total throughfall, water from tree stem flow will in general infiltrate deeper than that of throughfall.

3.7.3. Run-on / runoff calculation

The amount of water infiltrating, $F_w(n,1)$, depends on daily precipitation, rainfall interception and run-on/runoff patterns. For calculating run-on/runoff a very simple approach has been chosen. Field observations should be used to distinguish between runoff, where infiltration is lower than precipitation, and run-on where infiltration exceeds precipitation. This selection has been incorporated in the model by a switch that has a constant value. Runoff is modelled by calculating a maximum infiltration rate as a function of the leaf area index of the herbaceous vegetation (Fig. 3.14). Daily total throughfall as calculated in 3.3 infiltrates the soil up to this maximum and the surplus is lost by run off.

Figure 3.14. The relation between herbaceous leaf area index and the maximum infiltration rate.

$L(n)$ leaf area index of the herbaceous vegetation ($m^2 m^{-2}$)

L_r leaf area index threshold value with respect to runoff ($m^2 m^{-2}$)

$Q_m(n)$ actual maximum infiltration rate per subarea ($mm d^{-1}$)

Q_b maximum infiltration rate of bare soil ($mm d^{-1}$)

Q_v maximum infiltration rate of a soil with an herbaceous leaf area index of L_r or higher (mm d^{-1})

Run-on is calculated by defining a maximum infiltration rate, Q_s , which applies to the surrounding fields from which the run-on is received. The amount of water added to the total throughfall equals the product of the ratio of the areas of the surrounding fields and the field that receives run-on, and that part of the daily rainfall, which exceeds the maximum infiltration rate of the surrounding fields.

3.7.4. Parameterization

Variable	Value	Unit	Source
<i>General</i>			
p_e	20	m	van Keulen (1975)
t_r	100	d	(a)
L_r	5	$\text{m}^2 \text{m}^{-2}$	(b)
Q_s	20	mm d^{-1}	(b)
q_a	2	-	(b)
Z_1	0.05, 0.05 0.20, 0.20 0.5, 0.5, 0.5 2.0, 2.0, 2.0	m	
<i>Sandy / loamy soil</i>			
W_{c_d}	0.017 ^c 0.021 ^d	$\text{cm}^3 \text{cm}^{-3}$	Pirt (1983) ^e
W_{c_w}	0.052 ^c 0.064 ^d	$\text{cm}^3 \text{cm}^{-3}$	
W_{c_f}	0.126 ^c 0.211 ^d	$\text{cm}^3 \text{cm}^{-3}$	
Q_b	30	mm d^{-1}	(b)
Q_v	50	mm d^{-1}	(b)
W_{c_a}	0.017 ^c	$\text{cm}^3 \text{cm}^{-3}$	(f)

0.021

0.021, 0.064, 0.064

0.10, 0.14, 0.17

p_e evaporation proportionality factor;

q_a ratio of area of surrounding fields and field that receives run-on;

Z_l thickness per soil compartment;

Wc_d water content at air dry;

Wc_f water content at field capacity;

Wc_w water content at wilting point;

Wc_a actual water content in a soil compartment.

- The length of the dry season until the end of the year near Niono in Mali equals approximately 100 days.
- Based on the range in run-on / runoff as published in [Breman & De Ridder \(1991\)](#).
- Value for soil layers up to a depth of 0.30 m.
- Value for soil layers beyond 0.30 m.
- Values for 'LISA-g' soil (Table 3.3.1).
- Values estimated.

3.8. Nitrogen demand, uptake and partitioning

3.8.1. Nitrogen demand

For determining the maximum nitrogen uptake rate from the soil by the tree population and the herbaceous vegetation, the demand for nitrogen is calculated for each species separately. The demand for nitrogen is defined as the amount of nitrogen needed to achieve maximum nitrogen concentrations in all plant components. It is assumed that at ample soil nitrogen supply the demand for nitrogen can be satisfied within the time interval of integration. Total nitrogen demand consists of two parts: nitrogen needed for existing biomass and nitrogen needed for current growth of biomass (Eqn. 3.33).

$$D_N = [\text{Sigma}] D_{Ne,i} + [\text{Sigma}] D_{Ng,i} \text{ [Equation 3.33a]}$$

$$D_{Ne,i} = \frac{(W_i - D_{W,i} * dt) * (C_{Nx,i} - C_{N,i})}{\Delta t} \text{ [Equation 3.33b]}$$

$$D_{Ng,i} = G_{W,i} * C_{Nx,i} \text{ [Equation 3.33c]}$$

D_N total nitrogen demand ($\text{kg ha}^{-1} \text{d}^{-1}$)

$D_{Ne,i}$ nitrogen demand of existing biomass per plant component ($\text{kg ha}^{-1} \text{d}^{-1}$)

$D_{Ng,i}$ nitrogen demand of current growth per plant component ($\text{kg ha}^{-1} \text{d}^{-1}$)

W_i biomass per plant component (kg ha^{-1})

$D_{W,i}$ biomass decrease rate per plant component ($\text{kg ha}^{-1} \text{d}^{-1}$)

$G_{W,i}$ biomass growth rate per plant component ($\text{kg ha}^{-1} \text{d}^{-1}$)

$C_{N,i}$ actual nitrogen concentration per plant component (g g^{-1})

$C_{Nx,i}$ maximum nitrogen concentration per plant component (g g^{-1})

$[\Delta]t$ time interval of integration (d)

$[\Sigma]$ summation over all plant components

i plant component indication number

Nitrogen demand of existing tree biomass is based on the biomass produced in the current year. Biomass produced in preceding years is excluded in this calculation to avoid excessively high demands in case of high standing wood biomass and low actual nitrogen concentrations.

Maximum nitrogen concentrations for each plant component can be measured in the field after supplying an unlimited amount of nitrogen to the soil. These concentrations are correlated to actual phosphorus concentrations of each plant component in the lower range of phosphorus concentrations (Fig. 3.15). In this way it is mimicked that at severe phosphorus shortage the uptake of nitrogen and its tissue concentration decrease ([Penning de Vries & Djitéye, 1982](#)).

Phosphorus dynamics are not modelled in this version of RECAFS, i.e. field observations on phosphorus concentrations are required as input for the model. For the herbaceous vegetation, the maximum nitrogen concentrations at high phosphorus concentrations, $C_{Nxx,i}$, and the phosphorus concentrations are defined as a function of development stage. They decrease in the course of the development of the herbaceous species because of changes in the composition of the plant due to ageing ([Penning de Vries & Djitéye, 1982](#)). For the tree population, constant values are used for both concentrations.

[Figure 3.15](#). Relation between actual phosphorus concentration and maximum nitrogen concentration.

$C_{Nxx,i}$ maximum nitrogen concentration at high phosphorus concentrations (g g^{-1})

$C_{P,i}$ actual phosphorus concentration per plant component (g g^{-1})

Total nitrogen demand can be met by uptake from the soil and by withdrawal of nitrogen from plant tissues. The amount of nitrogen needed from the soil, is set equal to the difference between the nitrogen demand, D_N , and the amount of nitrogen translocated, W_N . The rate of translocation of nitrogen is

related to the death rate of each plant component and its actual nitrogen concentration, whereas the remainder, i.e. the amount of nitrogen not reallocated, is lost and becomes part of the organic nitrogen pool in the soil (Eqn. 3.34).

$$W_N = [\Sigma] W_{N,i} \text{ [Equation 3.34a]}$$

$$W_{N,i} = D_{W,i} * C_{N,i} * f_{w,i} \text{ [Equation 3.34b]}$$

$$L_{N,i} = D_{W,i} * C_{N,i} * (1 - f_{w,i}) \text{ [Equation 3.34c]}$$

W_N total nitrogen translocation rate ($\text{kg ha}^{-1} \text{ d}^{-1}$)

$W_{N,i}$ nitrogen translocation rate per plant component ($\text{kg ha}^{-1} \text{ d}^{-1}$)

$L_{N,i}$ nitrogen loss rate per plant component ($\text{kg ha}^{-1} \text{ d}^{-1}$)

$f_{w,i}$ nitrogen translocation fraction per plant component (-)

[Σ] summation over all plant components

3.8.2. Nitrogen uptake

The actual uptake rate depends on the two processes by which nitrogen is transported to the root system. One is called mass flow, where water uptake is responsible for the nitrogen supply to the root surface. Nitrogen uptake due to mass flow is calculated as the water uptake rate times the mineral soil nitrogen concentration.

$$U_{N,mf}(l) = U_w(l) * C_{Nm}(l) \text{ [Equation 3.35a]}$$

$U_{N,mf}(l)$ nitrogen uptake rate by mass flow ($\text{kg ha}^{-1} \text{ d}^{-1}$)

$U_w(l)$ water uptake rate by a species per soil compartment

($U_{w,T}(n,l)$ or $U_{w,H}(n,l)$) (mm d^{-1})

$C_{Nm}(l)$ mineral nitrogen concentration in the soil ($\text{kg ha}^{-1} \text{ mm}^{-1}$)

l soil compartment indication number (-)

At high mineral nitrogen concentrations in the soil the process of mass flow can supply most of the nitrogen needed by the plant. In many situations however, where either the transpiration rate or the soil nitrogen concentration is low, the transport of nitrogen towards the root system through mass flow is not adequate. Diffusion of nitrogen towards the roots may then supply an additional amount of nitrogen to the root surface which can be taken up. The rate of nitrogen diffusion through the soil is not modelled at the process level, but described as a function of maximum uptake capacity and water content per soil

compartment (Eqn. 3.35b). The effect of Eqn. 3.35b is that most nitrogen supplied by diffusion will be taken up from the soil compartments which contain most of the roots in combination with a high water content.

$$U_{N,df}(l) = Z_l * D_r(l) * U_{N,x} * 10 * Rd_U \text{ [Equation 3.35b]}$$

$$Rd_U = 1, \text{ if } Wc_r \geq Wc_T$$

$$= Wc_r / Wc_T, \text{ if } Wc_r < Wc_T$$

$U_{N,df}(l)$ nitrogen uptake rate by diffusion ($\text{kg ha}^{-1} \text{ d}^{-1}$)

Z_l thickness per soil compartment (m)

$D_r(l)$ root length density per soil compartment (m m^{-3})

$U_{N,x}$ maximum rate of nitrogen uptake by diffusion per unit root length ($\text{g m}^{-1} \text{ d}^{-1}$)

Rd_U nitrogen uptake reduction factor (-)

Wc_r reduced water content per soil compartment in each subarea (Eqn. 3.16c) (-)

Wc_T water content threshold value for nitrogen uptake by diffusion (-)

The sum of the nitrogen uptake by mass flow and diffusion from all soil compartments gives total actual nitrogen uptake rate of each species. It is assumed that the actual nitrogen uptake from the soil can not exceed the nitrogen demand of a plant species while taking into account the internal nitrogen supply by withdrawal of nitrogen before abscission of plant components (Eqn. 3.36). The uptake by mass flow and by diffusion as calculated by Eqn. 3.35a and 3.35b is adjusted to meet this condition, if necessary.

$$[\text{Sigma}] U_{N,mf} + [\text{Sigma}] U_{N,df} \leq D_N - W_N \text{ [Equation 3.36]}$$

[Sigma] summation over all soil compartments per species.

3.8.3. Competition for nitrogen

At first the nitrogen uptake rates from each soil compartment are calculated independently per species. If total nitrogen uptake by both species exceeds the available amount of nitrogen in a soil compartment, another calculation method is used that distributes available nitrogen in that soil compartment among both species. A distinction is made between the nitrogen taken up through mass flow and the nitrogen supplied by diffusion. If total mass flow already exceeds available nitrogen in a soil compartment, then available nitrogen is distributed between both species proportional to their water uptake rates. The amount of nitrogen taken up by diffusion can also be responsible for exceeding the nitrogen availability.

In that case both species take up nitrogen by mass flow as calculated before (Eqn. 3.35a), but instead of using Eqn. 3.35b the residual nitrogen in the soil is now distributed among both species proportional to their root lengths in the soil compartment.

3.8.4. Nitrogen partitioning

The total amount of nitrogen available for allocation towards the plant components equals the actual soil nitrogen uptake rate plus the total amount of nitrogen reallocated from dying plant tissues. The nitrogen partitioning factors are computed dynamically as a function of the nitrogen demand of each organ. Nitrogen needed for growing tissues, is given priority over nitrogen needed for existing biomass. The available nitrogen is at first allocated towards the growing tissues until maximum nitrogen concentrations in this new biomass are attained and after that any surplus is partitioned between the existing biomass components. For the nitrogen partitioning towards growing plant components, the partitioning factor of each organ is given by the ratio of its demand, $D_{Ng,i}$, and the total demand of new growth $[\Sigma] D_{Ng,i}$. A similar calculation is performed for the nitrogen allocation towards existing biomass, where the ratio between $D_{Ne,i}$ and $[\Sigma] D_{Ne,i}$ is used to estimate the nitrogen partitioning factors. Total nitrogen uptake of each plant organ is now computed as the sum of the nitrogen uptake due to growth activity and the nitrogen uptake due to submaximal nitrogen concentrations in the existing biomass of this organ.

Total nitrogen decrease rate of each plant organ equals the sum of the nitrogen translocation rate, $W_{N,i}$, and the nitrogen loss rate $L_{N,i}$ (Eqn. 3.34).

3.8.5. Tree nitrogen reserve dynamics

During the leaf flush of the tree population, nitrogen can be mobilized from nitrogen reserves located in the stems and branches to support leaf growth. Maximum nitrogen reallocation to tree leaves equals the difference between total demand for leaf nitrogen and leaf nitrogen uptake as a result of the partitioning of current soil nitrogen uptake and nitrogen withdrawn from dying plant components. Actual nitrogen mobilization towards the tree leaves is calculated as the minimum of the available nitrogen reserves and the maximum reallocation. The available nitrogen reserves are estimated as a fraction of the actual nitrogen content in the stems and branches of the tree population with the limitation that part of the total wood nitrogen is stored in chemical compounds that can not be mobilized (Eqn. 3.37).

$$N_{rs,s} = \text{MIN} (f_{w,s} * N_{st}; N_{st} - (W_{st} * C_{Nm,s})) \text{ [Equation 3.37]}$$

$N_{rs,s}$ tree nitrogen reserves located in the stems (kg ha^{-1})

N_{st} stem nitrogen content (kg ha^{-1})

W_{st} stem biomass (kg ha^{-1})

$f_{w,s}$ stem nitrogen translocation fraction (-)

$C_{Nm,s}$ minimum nitrogen concentration in the stems (g g^{-1})

A similar equation is used for the nitrogen reserves in the branches of the trees.

3.8.6. Parameterization

Variable	Value	Unit	Source
<i>Tree population</i>			
$N_{st,0}$	1	kg (plant)^{-1}	Breman & Kessler (1995)
$N_{br,0}$	0.7	kg (plant)^{-1}	
$N_{rt,0}$	1.65	kg (plant)^{-1}	
$f_{w,l}$	0.6	-	(a)
$f_{w,b}$	0.2	-	(a)
$f_{w,s}$	0.2	-	(a)
$f_{w,r}$	0.2	-	(a)
$C_{Nxx,l}$	0.030	g g^{-1}	Breman & Kessler (1995)
$C_{Nxx,d}$	0.025	g g^{-1}	
$C_{Nxx,b}$	0.015	g g^{-1}	
$C_{Nxx,s}$	0.015	g g^{-1}	
$C_{Nxx,r}$	0.015	g g^{-1}	
$C_{Nm,l}$	0.01	g g^{-1}	Pers. comm. H. Breman
$C_{Nm,b}$	0.002	g g^{-1}	
$C_{Nm,s}$	0.002	g g^{-1}	
q_{PN}	0.04	g g^{-1}	Penning de Vries & Djitèye (1982) ^b
$U_{N,x}$	$5 * 10^{-4}$	$\text{g m}^{-1} \text{d}^{-1}$	(a)

Herbaceous vegetation

$N_{lv,0}$	$0.2 * 10^{-7}$	kg (plant) ⁻¹	(c)
$N_{st,0}$	$0.06 * 10^{-7}$	kg (plant) ⁻¹	(d)
$N_{rt,0}$	$0.06 * 10^{-7}$	kg (plant) ⁻¹	(d)
$f_{w,l}$	0.4	-	(a)
$f_{w,r}$	0.0	-	(a)
$C_{Nxx,l}$	0.0, 0.05 2.0, 0.025	g g ⁻¹	Penning de Vries & Djitèye (1982)
$C_{Nxx,d}$	0.0, 0.05 2.0, 0.05	g g ⁻¹	
$C_{Nxx,s}$	0.0, 0.015 2.0, 0.010	g g ⁻¹	
$C_{Nxx,r}$	0.0, 0.015 2.0, 0.010	g g ⁻¹	
$C_{Nm,l}$	0.0075	g g ⁻¹	Penning de Vries & Djitèye (1982)
q_{PN}	0.04	g g ⁻¹	Penning de Vries & Djitèye (1982)
$U_{N,x}$	$5 * 10^{-5}$	g m ⁻¹ d ⁻¹	(a)

$N_{i,0}$ initial nitrogen content per plant component;

$C_{Nm,i}$ minimum nitrogen concentration per plant component;

q_{PN} minimum nitrogen-phosphorus ratio;

$C_{Nxx,i}$ 1st column: development stage and 2nd column: maximum concentration (herbaceous vegetation).

a. Value estimated;

b. Value obtained from annual grass vegetation;

c. Value estimated as 4 % of standing biomass;

d. Value estimated as 1.2 % of standing biomass.

3.9. Soil nitrogen balance

3.9.1. Nitrogen mineralization

Due to the decomposition of organic matter in the soil, organic nitrogen may be transformed into a

mineral form and becomes available for plant uptake. To account for differences in organic matter with respect to decomposition and mineralization rates, total soil organic matter is subdivided into 4 pools. The rate of decomposition forms the main difference among these pools. The organic matter in C_1 and C_2 has a relatively high decomposition rate, whereas that in C_3 and C_4 decomposes relatively slowly. For each pool in each subarea decomposition and nitrogen mineralization are calculated using the following equations (cf. Berendse *et al.*, 1987; 1989).

$$D_{C_j}(n) = k_j * C_j(n) \text{ [Equation 3.38]}$$

$$M_{N,j}(n) = \frac{k_j}{1 - e_j} * (N_j(n) - C_j(n) * C_{Nc,j})$$

[Equation 3.39]

$C_j(n)$ amount of carbon in soil organic matter pool j (kg ha^{-1})

$N_j(n)$ amount of nitrogen in soil organic matter pool j (kg ha^{-1})

$D_{C_j}(n)$ organic matter decomposition rate ($\text{kg ha}^{-1} \text{ d}^{-1}$)

$M_{N,j}(n)$ nitrogen mineralization rate ($\text{kg ha}^{-1} \text{ d}^{-1}$)

k_j decomposition constant (d^{-1})

e_j microbial growth efficiency (g g^{-1})

$C_{Nc,j}$ critical nitrogen concentration in soil organic matter pool j (g g^{-1})

n subarea indication number

j soil organic matter pool indication number

If the critical nitrogen content of a soil organic matter pool exceeds the actual nitrogen content, immobilization of nitrogen occurs ($M_{N,j}(n) < 0$) which decreases in the short-term the availability of nitrogen for the plant roots. Microbial biomass is not simulated separately, but is included in each organic matter pool, which means that the organic matter decomposition rate, $D_{C_j}(n)$, equals the loss of carbon from the soil organic matter through respiration.

It is assumed that the distribution of soil organic matter with soil depth can be described by a negative exponential function, which is identical for all pools. A mineralization rate for each soil compartment is calculated by distributing the total mineralization, i.e. the sum of the mineralization rates of the 4 soil organic matter pools, among the soil compartments with this exponential function. The values calculated with the Eqn. 3.38 and 3.39 refer to potential rates where water availability and the amount of mineral

nitrogen in each soil compartment are not limiting the decomposition of organic matter. The effect of water content on decomposition and mineralization is incorporated by calculating a reduction factor at low soil water contents (Fig. 3.16).

Figure 3.16. The relation between soil water content and the reduction factor for organic matter decomposition and mineralization.

Rd_m reduction factor for soil organic matter decomposition due to low soil water content (-)

Wc_a actual water content in a soil compartment ($cm^3 cm^{-3}$)

Wc_1 threshold water content in a soil compartment for decomposition ($cm^3 cm^{-3}$)

Wc_2 critical water content in a soil compartment for decomposition ($cm^3 cm^{-3}$)

The decomposition and mineralization can also be affected if the amount of mineral nitrogen in the soil is inadequate to supply nitrogen for immobilization. The ratio between nitrogen availability and nitrogen demand for the decomposition process in a soil compartment, equals the reduction factor due to mineral nitrogen limitation. Both reduction factors, due to water and nitrogen, are multiplied with the potential decomposition and mineralization rates to determine the actual rates. It is assumed that the reduction affects the four organic matter pools in a similar way. The decomposition of each pool is thus equally sensitive to water or nitrogen limitations.

3.9.2. Carbon and nitrogen inputs

3.9.2.1. Herbaceous vegetation

The herbaceous vegetation produces non-woody litter in the form of roots, stems, leaves and seeds. The carbon content of this litter is estimated by multiplying the amount of dry matter of the dead plant components with 0.50. The nitrogen content depends on the actual nitrogen concentrations of the plant components and on the fraction withdrawn (3.8.1). Carbon and nitrogen input is added directly to the four soil organic matter pools by using one set of partitioning coefficients for all four non-woody litter types. No distinction is thus made between roots and shoots of the herbaceous species with respect to decomposition and mineralization.

The partitioning of carbon towards the two more slowly decomposable organic matter pools (C_3 and C_4) is calculated by using constant partitioning coefficients. The amount of carbon which remains is partitioned between the two faster decomposable organic matter pools (C_1 and C_2) by calculating partitioning coefficients which depend on the nitrogen concentration of the litter. At low nitrogen concentrations the carbon partitioning to C_1 equals zero, whereas at high nitrogen concentration the organic matter pools C_1 and C_2 both receive an equal share of the residual carbon.

The amount of nitrogen partitioned towards each pool is calculated in first instance by applying constant

carbon-nitrogen ratios for each pool (Verberne *et al.*, 1990). At low nitrogen concentrations however, there may not be enough nitrogen in the litter and the nitrogen concentration of the litter input for the three pools N_2 , N_3 and N_4 is decreased proportionally with a zero nitrogen supply for N_1 . At higher litter nitrogen concentrations the constant carbon-nitrogen ratios are only used for these three pools, whereas the remaining nitrogen is allocated to N_1 .

3.9.2.2. Tree population

The calculation of carbon and nitrogen input into the soil organic matter pools from the tree population is similar to that for the herbaceous vegetation, but differs in two aspects. For the tree litter a distinction is made between woody and non-woody organic matter. The non-woody litter types are the leaves, fruits and part of the roots of the trees. They are partitioned among the 4 organic matter pools by applying the same set of parameters and equations as used for the grass litter. The woody litter types are the branches and the other part of the roots of the trees and they are partitioned by applying different carbon partitioning coefficients for C_3 and C_4 , which are higher than those used for the non-woody material.

The second difference refers to the distribution of tree litter among the subareas. Tree root litter is simply distributed proportionally to the distribution of the tree root biomass, which means that in general most of the root litter is found under the tree crown and the remainder in subarea 2. With respect to aboveground litter, leaves, fruits and branches of the trees, a choice can be made at the beginning of each simulation run for a homogeneous distribution among all subareas or for a concentrated litterfall under the tree crown. This choice, which is incorporated in the model as a switch, affects all aboveground litter types of the trees identically.

3.9.3. Vertical nitrogen redistribution

Mineral nitrogen in the soil is transported downwards if water flows across a soil compartment boundary. The amount of nitrogen that enters the soil system from the top depends on the amount of rainfall, its nitrogen concentration, which comprises natural wet deposition and nitrogen fixation by algae ([Penning de Vries & Djitèye, 1982](#)) and the amount of nitrogen added through fertilization. It is assumed that the infiltration of nitrogen at the top is complete if water infiltrates the soil system, irrespective of the amount of water infiltrated. Furthermore, it is also assumed that nitrogen which flows through the lower boundary of the soil profile is lost permanently for the agroforestry system.

The nitrogen flows across each boundary between two soil compartments are correlated to the water flows (3.7.2) and the mineral nitrogen content of each soil compartment. At first the water influx into a soil compartment is converted into a virtual water column as function of the water content at field capacity (Eqn. 3.40a).

$$Z_w = \frac{F_w(n,1) * \Delta t}{W_{cf} * 1000} \quad \text{[Equation 3.40a]}$$

Z_w virtual water column (m)

$F_w(n,1)$ water infiltration into soil compartment 1 (mm d⁻¹)

W_{cf} water content at field capacity (cm³ cm⁻³)

Δt time interval of integration (d)

It is assumed that a layer of water with a thickness of Z_w moves into soil compartment 1 together with an amount of nitrogen (Fig. 3.17).

Figure 3.17. This picture gives an illustration of the calculation of nitrogen flows through the soil. For explanation see text.

In the example of Fig. 3.17 compartment 1 receives the total mineral nitrogen content of compartment 1-1 multiplied with a leaching efficiency. The leaching efficiency l_e , which can have values between 0 and 1, is a soil characteristic and a constant value is used throughout the whole soil profile. Because the thickness of the water column exceeds the compartment thickness of 1-1 ($Z_w > Z_{1-1}$), compartment 1 also receives nitrogen from compartment 1-2. The amount of water which comes from compartment 1-2 and flows into compartment 1 is estimated by using Eqn. 3.40a in the reverse direction (Eqn. 3.40b)

$$F_{w,2}(n,1) = \frac{(Z_w - Z_{1-1}) * W_{cf} * 1000}{\Delta t} \quad \text{[Equation 3.40b]}$$

$F_{w,2}(n,1)$ water infiltration into soil compartment 1 which comes from soil compartment 1-2 (mm d⁻¹)

The nitrogen flow associated with this water flow is calculated as the product of $F_{w,2}(n,1)$ and the average mineral nitrogen concentration at the boundary of the compartments 1-2 and 1-1. Total mineral nitrogen content of compartment 1-2 sets the maximum contribution of this compartment to the nitrogen input into compartment 1. Again, this nitrogen flow is multiplied with the leaching efficiency parameter of the soil. The sum of both nitrogen flows from compartment 1-1 and 1-2 equals total nitrogen input into soil compartment 1. This calculation method is applied to each compartment boundary. The net change in mineral nitrogen of a soil compartment due to soil water flows is now equal to the nitrogen influx into the soil compartment minus the nitrogen efflux into the next soil compartment in downward direction.

3.9.4. Parameterization

(a)

Variable	Value	Unit	Source
<i>General</i>			
$P_{nw,3}$	0.4	-	
$P_{nw,4}$	0.1	-	(a)
$P_{wd,3}$	0.6	-	(a)
$P_{wd,4}$	0.3	-	(a)
f_{wd}	0.1	-	(a)
$C_{N,Pr}$	0.0125	kg ha ⁻¹ mm ⁻¹	Penning de Vries & Djitèye (1982.)
Z_{OM}	2.0	m	(a)
POM	1.5	-	(a)
<i>Sandy / loamy soil</i>			
$N_{m,0}$	0	kg ha ⁻¹ m ⁻¹	(a)
$C_{1,0}$	0	kg ha ⁻¹	(a)
$C_{2,0}$	0	kg ha ⁻¹	(a)
$C_{3,0}$	2000	kg ha ⁻¹	(a)
$C_{4,0}$	38000	kg ha ⁻¹	(a)
$N_{1,0}$	0	kg ha ⁻¹	
$N_{2,0}$	0	kg ha ⁻¹	
$N_{3,0}$	200	kg ha ⁻¹	(b)
$N_{4,0}$	3800	kg ha ⁻¹	(b)
k_1	0.1	d ⁻¹	(a)
k_2	0.01	d ⁻¹	(a)
k_3	0.001	d ⁻¹	(a)
k_4	0.0001	d ⁻¹	(a)
e_1, e_2, e_3, e_4	0.3	-	(a)

$C_{nc,1}, C_{Nc,2}$	0.03	$g\ g^{-1}$	(a)
$C_{nc,3}, C_{Nc,4}$	0.02	$g\ g^{-1}$	(a)
Wc_1	0.064	$cm^3\ cm^{-3}$	(c)
Wc_2	0.126	$cm^3\ cm^{-3}$	(d)
l_e	0.9	-	(a)

$p_{nw,j}$ partitioning coefficient of non-woody litter to organic matter pool j;

$p_{wd,j}$ partitioning coefficient of woody litter to organic matter pool j;

f_{wd} fraction of woody tree root litter;

$C_{N,Pr}$ concentration of nitrogen in rain, including nitrogen fixation by algae;

Z_{OM} maximum depth of soil organic matter distribution;

p_{OM} soil organic matter distribution parameter;

$N_{m,0}$ initial amount of mineral nitrogen per unit soil thickness;

$N_{j,0}$ initial amount of nitrogen in soil organic matter pool j;

$C_{j,0}$ initial amount of carbon in soil organic matter pool j.

a. Value estimated;

b. Value estimated by using a C:N ratio of 10 ([Penning de Vries & Djitéye, 1982](#));

c. Value equal to water content at air dry;

d. Value equal to water content at field capacity.

3.10 List of symbols

$A(n)$ total area of a subarea $m^2\ ha^{-1}$

$A_a(n,l)$ amount of water stored above air dry, per soil compartment and per subarea mm

A_c absorption of PAR by an individual tree in a closed tree canopy $J\ (plant)^{-1}\ d^{-1}$

A_s absorption of PAR by a solitary tree $J\ (plant)^{-1}\ d^{-1}$

$A_w(n,l)$ amount of water stored above wilting point, per soil compartment and per subarea mm

a horizontal radius of the tree crown m

C_c individual tree crown cover as function of stem biomass $m^2\ (plant)^{-1}$

$C_j(n)$ amount of carbon in soil organic matter pool j $kg\ ha^{-1}$

- $C_{j,0}$ initial amount of carbon in soil organic matter pool j kg ha^{-1}
- $C_{N,i}$ actual nitrogen concentration per plant component g g^{-1}
- $C_{N,Pr}$ concentration of nitrogen in rain, including nitrogen fixation by algae $\text{kg ha}^{-1} \text{mm}^{-1}$
- $C_{Nc,j}$ critical nitrogen concentration in soil organic matter pool j g g^{-1}
- $C_{Nm(l)}$ mineral nitrogen concentration in the soil $\text{kg ha}^{-1} \text{mm}^{-1}$
- $C_{Nm,i}$ minimum nitrogen concentration per plant component g g^{-1}
- $C_{No,l}$ optimum leaf nitrogen concentration g g^{-1}
- $C_{Nx,i}$ maximum nitrogen concentration per plant component g g^{-1}
- $C_{Nxx,i}$ maximum nitrogen concentration at high phosphorus concentration
per plant component g g^{-1}
- $C_{P,i}$ actual phosphorus concentration per plant component g g^{-1}
- C_{Pr} rainfall interception capacity per leaf layer of the herbaceous vegetation mm d^{-1}
- $C_{r,a}$ current reserve concentration g g^{-1}
- $C_{r,m}$ maximum reserve concentration g g^{-1}
- C_{tm} maximum relative decrease in minimum and maximum air temperatures due to
the presence of the trees -
- C_{vp} maximum relative increase in early morning vapour pressure of the air due to
the presence of the trees -
- C_{wn} maximum relative decrease in average wind speed due to the presence of the trees -
- c vertical radius of the tree crown m
- D derivative of saturated vapour pressure curve with respect to temperature mbar K^{-1}
- Dt time interval of integration d
- $D_{C,j(n)}$ organic matter decomposition rate $\text{kg ha}^{-1} \text{d}^{-1}$
- D_L rate of decrease in leaf area index $\text{m}^2 \text{m}^{-2} \text{d}^{-1}$
- D_N total nitrogen demand $\text{kg ha}^{-1} \text{d}^{-1}$
- $D_{Ne,i}$ nitrogen demand for existing biomass per plant component $\text{kg ha}^{-1} \text{d}^{-1}$
- $D_{Ng,i}$ nitrogen demand of current growth per plant component $\text{kg ha}^{-1} \text{d}^{-1}$
- $D_r(l)$ root length density per soil compartment m m^{-3}
- $D_{r,c}$ root length density in the first soil compartment containing tree roots m m^{-3}
- D_T direct throughfall threshold value -
- $D_{W,i}$ biomass decrease rate per plant component $\text{kg ha}^{-1} \text{d}^{-1}$

- D_x cumulative relative root length per soil compartment -
- D_z total cumulative relative root length -
- E_0 initial light use efficiency kg J^{-1}
- $E_{A(n)}$ evaporative demand of the atmosphere mm d^{-1}
- E_I daily light use efficiency with ample soil water supply kg J^{-1}
- $E_{I,a}$ average light use efficiency during vegetative growth of the herbaceous species under optimal conditions kg J^{-1}
- $E_{I,m}$ maximum light use efficiency as function of total wood and root biomass kg J^{-1}
- $E_p(n)$ potential soil evaporation rate mm d^{-1}
- $E_s(n)$ actual soil evaporation rate mm d^{-1}
- E_w water use efficiency for dry matter production $\text{kg ha}^{-1} \text{mm}^{-1}$
- $E_{w,c}$ water use efficiency of a closed tree canopy $\text{kg ha}^{-1} \text{mm}^{-1}$
- $E_{w,s}$ water use efficiency of a solitary tree $\text{kg ha}^{-1} \text{mm}^{-1}$
- e_j microbial growth efficiency g g^{-1}
- F_{sh} cumulative fraction of intercepted PAR by a solitary tree as function of relative distance x_r from the tree -
- $F_{w(n,l)}$ water infiltration into soil compartment l mm d^{-1}
- $F_{w,2(n,l)}$ water infiltration into soil compartment l which comes from soil compartment $l-2$ mm d^{-1}
- f_a fraction absorbed PAR -
- f_c critical fraction of PAR with respect to leaf death -
- f_d effect of daylength on development rate during the vegetative phase of the herbaceous species -
- f_i fraction intercepted rain, applied to precipitation minus direct throughfall -
- $f_{i,m}$ minimum fraction intercepted rain -
- f_l effect of latitude on development rate during the vegetative phase of the herbaceous species -
- f_{Pr} fraction intercepted rain subtracted from potential transpiration -
- f_p effect of production stress due to belowground resources on the shoot biomass partitioning factor -
- $f_{r,lV}$ fraction of reserves in the leaves that can be translocated -
- $f_{r,st}$ fraction of reserves in the stem -

- f_s effect of stress on development rate during the vegetative phase of the herbaceous species -
- $f_{sh}(n)$ fraction of the intercepted radiation by the tree population with respect to each subarea -
- f_{shd} effect of shading on the shoot biomass partitioning factor -
- f_{st} fraction of tree stem flow, applied to precipitation minus direct throughfall and interception -
- $f_{t,g}$ effect of average daily temperature on development rate during the reproductive phase of the herbaceous species -
- $f_{t,v}$ effect of average daily temperature on development rate during the vegetative phase of the herbaceous species -
- $f_{w,i}$ nitrogen translocation fraction per plant component -
- f_{wd} fraction of woody tree root litter -
- G_{br} growth rate of branch biomass $\text{kg ha}^{-1} \text{d}^{-1}$
- $G_{c_{lv}}$ leaf growth rate realized from current biomass production $\text{kg ha}^{-1} \text{d}^{-1}$
- $G_{e_{lv}}$ exponential leaf growth rate $\text{kg ha}^{-1} \text{d}^{-1}$
- G_L rate of increase in leaf area index $\text{m}^2 \text{m}^{-2} \text{d}^{-1}$
- G_{lv} actual leaf biomass growth rate $\text{kg ha}^{-1} \text{d}^{-1}$
- G_{rs} rate of increase in reserves $\text{kg ha}^{-1} \text{d}^{-1}$
- G_{st} growth rate of stem biomass $\text{kg ha}^{-1} \text{d}^{-1}$
- $G_{W,i}$ biomass growth rate per plant component $\text{kg ha}^{-1} \text{d}^{-1}$
- g psychrometric constant mbar K^{-1}
- I_0 daily shortwave radiation $\text{J m}^{-2} \text{d}^{-1}$
- I_a daily absorbed PAR by a tree population $\text{J ha}^{-1} \text{d}^{-1}$
- $I_a(n)$ daily absorbed PAR by the herbaceous vegetation $\text{J ha}^{-1} \text{d}^{-1}$
- $I_{a,0}$ absorbed shortwave radiation by a closed tree canopy $\text{J m}^{-2} \text{d}^{-1}$
- $I_{a,L}$ daily absorbed PAR by the foliage of a tree population $\text{J ha}^{-1} \text{d}^{-1}$
- I_m amount of PAR, available for absorption (equal to absorbed PAR, if $f_a = 1$) $\text{J ha}^{-1} \text{d}^{-1}$
- $I_{m,a}$ average I_m during the vegetative period for which E_a has been determined $\text{J ha}^{-1} \text{d}^{-1}$
- I_p daily photosynthetically active radiation $\text{J ha}^{-1} \text{d}^{-1}$
- I_r daily reflected PAR by a tree population $\text{J ha}^{-1} \text{d}^{-1}$

- $I_{r,0}$ reflected shortwave radiation by a closed tree canopy $J m^{-2} d^{-1}$
- $I_s(n)$ daily transmitted shortwave radiation towards the herbaceous vegetation $J m^{-2} d^{-1}$
- $I_t(n)$ daily transmitted PAR towards the herbaceous vegetation $J ha^{-1} d^{-1}$
- i plant component indication number
- j soil organic matter pool indication number
- K_L extinction coefficient of leaves for I_p $m^2 m^{-2}$
- K_W extinction coefficient of branches for I_p $m^2 m^{-2}$
- k_j decomposition constant d^{-1}
- L leaf area index of a tree $m^2 m^{-2}$
- $L(n)$ leaf area index of the herbaceous vegetation $m^2 m^{-2}$
- L_0 herbaceous leaf area index at initialization $m^2 m^{-2}$
- $L_c(n)$ critical leaf area index per subarea with respect to leaf death $m^2 m^{-2}$
- L_e threshold LAI for exponential leaf area growth of the herbaceous species $m^2 m^{-2}$
- $L_{N,i}$ nitrogen loss rate per plant component $kg ha^{-1} d^{-1}$
- L_r leaf area index threshold value with respect to runoff $m^2 m^{-2}$
- L_T total dead and living leaf area index of the trees $m^2 m^{-2}$
- $L_T(n)$ total dead and living leaf area index of the herbaceous vegetation per subarea $m^2 m^{-2}$
- l soil compartment indication number
- l_e leaching efficiency -
- $M_{N,j}(n)$ nitrogen mineralization rate $kg ha^{-1} d^{-1}$
- N actual tree population density tree ha^{-1}
- N_c tree population density of a closed tree canopy tree ha^{-1}
- $N_{i,0}$ initial nitrogen content per plant component $kg (plant)^{-1}$
- $N_j(n)$ amount of nitrogen in soil organic matter pool j $kg ha^{-1}$
- $N_{j,0}$ initial amount of nitrogen in soil organic matter pool j $kg ha^{-1}$
- $N_{m,0}$ initial amount of mineral nitrogen per unit soil thickness $kg ha^{-1} m^{-1}$
- $N_{rs,s}$ tree nitrogen reserves located in the stems $kg ha^{-1}$
- N_s threshold tree population density for intertree shading tree ha^{-1}
- N_{st} stem nitrogen content $kg ha^{-1}$
- n subarea indication number
- n_{sl} number of soil compartments for determining emergence of the herbaceous species -

- P net rate of herbaceous biomass increase $\text{kg ha}^{-1} \text{d}^{-1}$
- P_1, P_2 precipitation threshold values for calculating f_i mm d^{-1}
- P_a actual rate of dry matter production $\text{kg ha}^{-1} \text{d}^{-1}$
- P_{dt} rate of direct throughfall mm d^{-1}
- P_m theoretical rate of maximum production $\text{kg ha}^{-1} \text{d}^{-1}$
- P_p potential rate of dry matter production, as function of absorbed radiation $\text{kg ha}^{-1} \text{d}^{-1}$
- P_r daily rainfall mm d^{-1}
- P_{t1} rainfall threshold value for starting tree leaf flush mm d^{-1}
- p_e evaporation proportionality factor m^{-1}
- p_h lateral root distribution parameter -
- p_i biomass partitioning factors -
- $p_{nw,j}$ partitioning coefficient of non-woody litter to organic matter pool j -
- p_{OM} soil organic matter distribution parameter -
- p_{rt} root biomass partitioning factor -
- p_{sh} actual shoot biomass partitioning factor -
- $p_{sh,0}$ shoot biomass partitioning factor as function of stem biomass (tree species) or as function of DVS (herbaceous species) -
- p_v vertical root distribution parameter -
- $p_{wd,j}$ partitioning coefficient of woody litter to organic matter pool j -
- Q_A assimilate requirement for dry matter production kg kg^{-1}
- Q_b maximum infiltration rate of bare soil mm d^{-1}
- $Q_m(n)$ actual maximum infiltration rate per subarea mm d^{-1}
- Q_s maximum infiltration rate of surrounding fields mm d^{-1}
- Q_v maximum infiltration rate of a soil with an herbaceous leaf area index of L_r or higher mm d^{-1}
- q_a ratio of area of surrounding fields and field that receives runoff -
- $q_i(n)$ ratio of intercepted PAR in a subarea and intercepted PAR by a closed tree canopy -
- q_K ratio between extinction coefficient for shortwave radiation and photosynthetically active radiation -
- q_{PN} minimum nitrogen-phosphorus ratio g g^{-1}

q_{ps} ratio between PAR (I_p) and daily shortwave radiation -

q_{sc} ratio between absorbed PAR of a solitary tree and an individual tree in a closed tree canopy -

Rd_2 reduction factor for potential biomass production due to ageing at $DVS = 2$ of the herbaceous species -

Rd_B reduction factor for potential biomass production, caused by nitrogen deficiency or due to ageing of the herbaceous species -

Rd_m reduction factor for soil organic matter decomposition due to low soil water content -

Rd_U nitrogen uptake reduction factor -

Rd_w water uptake reduction factor -

R_{el} rooted depth elongation rate $m\ d^{-1}$

R_{gd} development rate during the reproductive phase of the herbaceous species d^{-1}

$R_{gd,0}$ reference development rate during the reproductive phase of the herbaceous species d^{-1}

$R_L(n,l)$ root length per soil compartment in each subarea m

$R_N(n)$ net absorbed radiation term $mm\ d^{-1}$

$R_s(n)$ radius of a subarea with respect to the tree base m

R_{vd} development rate during the vegetative phase of the herbaceous species d^{-1}

$R_{vd,0}$ reference development rate during the vegetative phase of the herbaceous species d^{-1}

$R_{w,st}$ stem reserve mobilization rate during reproductive phase $kg\ ha^{-1}\ d^{-1}$

R_{ws} rate of change in accumulated water stress days d^{-1}

$r_{0,s}$ reflection coefficient for I_0 of a soil surface (albedo) -

$r_{0,v}$ reflection coefficient for I_0 at 100% absorption of a vegetation (albedo) -

$r_{br,y}$ annual relative death rate of tree branches yr^{-1}

r_c reflection coefficient for I_0 of a forest -

$r_{i,d}$ mean daily relative death rate of tree roots or branches d^{-1}

r_{glv} maximum relative tree leaf growth rate during leaf flush d^{-1}

r_L relative death rate of leaf biomass d^{-1}

$r_{L,d}$ relative rate of leaf death as function of development stage (herbaceous species)

or as function of time (tree species) d^{-1}

$r_{L,s}(n)$ relative rate of leaf death per subarea as function of radiation level d^{-1}

$r_{L,ws}$ relative rate of leaf death as function of water stress d^{-1}

r_{LAI} maximum relative rate of increase in leaf area index of the herbaceous species d^{-1}

r_{LC} reference relative rate of leaf death as function of radiation level d^{-1}

r_p reflection coefficient for I_p -

$r_{rt,y}$ annual relative death rate of tree roots yr^{-1}

S_L specific leaf area $ha\ kg^{-1}$

S_r specific root length $m\ g^{-1}$

S_W specific wood area $ha\ kg^{-1}$

T_a actual transpiration rate of the tree population $mm\ d^{-1}$

T_c characteristic transpiration rate $mm\ d^{-1}$

$T_d(n)$ drying power term of potential transpiration $mm\ d^{-1}$

T_h transpiration ratio threshold value -

T_m potential transpiration rate of a closed vegetation $mm\ d^{-1}$

T_p potential transpiration rate of the tree population $mm\ d^{-1}$

$T_p(n)$ potential transpiration rate of the herbaceous vegetation $mm\ d^{-1}$

$T_r(n)$ radiation term of potential transpiration $mm\ d^{-1}$

t_1 number of first possible day of growth calculations of the herbaceous species or number of first day of tree leaf flush -

t_{12} maximum period of reserve mobilization for tree leaf growth d

t_3 number of latest possible day of beginning leaf fall period -

t_{ei} number of days between emergence and initialization of the herbaceous species d

t_r number of days without significant infiltration counted from the last day with significant infiltration d

$U_{N,df}(l)$ nitrogen uptake rate by diffusion $kg\ ha^{-1}\ d^{-1}$

$U_{N,mf}(l)$ nitrogen uptake rate by mass flow $kg\ ha^{-1}\ d^{-1}$

$U_{N,x}$ maximum rate of nitrogen uptake by diffusion per unit root length $g\ m^{-1}\ d^{-1}$

$U_w(l)$ water uptake rate by a species per soil compartment ($U_{w,T}(n,l)$ or $U_{w,H}(n,l)$) $mm\ d^{-1}$

$U_{w,H}(n,l)$ water uptake rate per soil compartment in each subarea by the herbaceous vegetation $mm\ d^{-1}$

$U_{w,T}(n,l)$ water uptake rate per soil compartment in each subarea by the tree population $mm\ d^{-1}$

- $U_{w,x}$ maximum rate of water uptake per unit root length $\text{kg m}^{-1} \text{d}^{-1}$
- W wood area index of a tree $\text{m}^2 \text{m}^{-2}$
- Wc_1 threshold water content in a soil compartment for decomposition $\text{cm}^3 \text{cm}^{-3}$
- Wc_2 critical water content in a soil compartment for decomposition $\text{cm}^3 \text{cm}^{-3}$
- Wc_a actual water content in a soil compartment $\text{cm}^3 \text{cm}^{-3}$
- Wc_d water content at air dry $\text{cm}^3 \text{cm}^{-3}$
- Wc_f water content at field capacity $\text{cm}^3 \text{cm}^{-3}$
- Wc_r reduced water content per soil compartment in each subarea -
- Wc_T reduced water content threshold value for nitrogen uptake by diffusion -
- Wc_w water content at wilting point $\text{cm}^3 \text{cm}^{-3}$
- W_{dm} demand for reserves for leaf growth $\text{kg ha}^{-1} \text{d}^{-1}$
- W_i biomass per plant component kg ha^{-1}
- $W_{i,0}$ biomass per plant component at initialization kg ha^{-1}
- W_{lv} leaf biomass kg ha^{-1}
- $W_{lv,x}$ maximum tree leaf biomass as function of branch biomass kg (plant)^{-1}
- W_N total nitrogen translocation rate $\text{kg ha}^{-1} \text{d}^{-1}$
- $W_{N,i}$ nitrogen translocation rate per plant component $\text{kg ha}^{-1} \text{d}^{-1}$
- W_{rs} total amount of reserves kg ha^{-1}
- W_{st} stem biomass kg ha^{-1}
- W_t water availability threshold value for determining emergence mm
- $X(l)$ lateral tree root extension per soil compartment m
- X_c lateral root extension in the first soil compartment containing tree roots m
- $X_{c,0}$ initial value of lateral root extension in the first soil compartment containing tree roots m
- $x(l)$ relative lateral tree root extension -
- x_r relative distance from the tree base with respect to crown cover radius -
- Z soil depth m
- Z_0 initial rooted depth of the herbaceous species m
- Z_c soil depth at which the first tree roots are found m
- Z_1 thickness per soil compartment m
- Z_m maximum root depth m

Z_{OM} maximum depth of soil organic matter distribution m

Z_r rooted depth of a tree at the tree base m

$Z_r(n)$ rooted depth of the herbaceous species m

Z_w virtual water column m

z relative soil depth -

II. User manual

4. Model input requirements

4.1. Introduction

This chapter contains an overview of the files needed to run RECAFS and elaborates briefly on the effects of the input data on the model calculations. It may help in selecting input data for a sensitivity analysis, because not all input data are equally important and some have similar or even identical effects. A small number of parameters in the model are not derived from input files (Appendix C.1). They are not available for sensitivity analysis without changing the model source code. In Table 4.1 the input files needed for running RECAFS are listed.

Table 4.1. The input files of RECAFS

CONTROL.DAT	(Appendix C.2)
RERUNS.DAT	(Appendix C.3)
TIMER.DAT	(Appendix C.4)
MLI61.973	(Appendix C.5)
TREE.DAT	(Appendix C.6)
GRASS.DAT	(Appendix C.7)
LISAG.DAT	(Appendix C.8)

The tables or functions that are read from the input files as pairs of numbers can be presented graphically by plotting each pair as an X, Y point. Between each point a straight line should be drawn to find the Y-value for intermediate X- values.

The model has been developed in the simulation language FORTRAN 77 and uses the FORTRAN Simulation Environment (FSE) . The main program (van Kraalingen, 1991), the weather system (van

Kraalingen *et al.*, 1991) and the utility library (Rappoldt & Van Kraalingen, 1990) of FSE are not described in this report.

4.2. CONTROL.DAT

The file CONTROL.DAT contains the file names of the various input and output files used by RECAFS, except the weather data file whose name is given in TIMER.DAT. During initialization of each simulation run the model reads each file name from CONTROL.DAT so that these files can be identified. The input files should be present in the directory containing the executable file of the model (RECAFS.EXE). Only the weather input file may be stored in another directory, which must be specified in TIMER.DAT. All names in CONTROL.DAT can be changed if the input data have been stored in other files.

4.3. RERUNS.DAT

The rerun facility of FSE offers an opportunity for a quick view of the results of multiple runs into one graph, e.g. when performing sensitivity analysis. The file RERUNS.DAT contains the variable name(s) and the various value(s) of this (these) variable(s). An example is given in [Appendix C.3](#). The file RERUNS.DAT is only necessary if this rerun facility of FSE is used.

4.4. TIMER.DAT

The file TIMER.DAT contains 4 types of input data: weather, time, control and output. More information can be found in the documentation of FSE (van Kraalingen, 1991). Two production control variables, used by RECAFS, have been added to the original timer file of FSE. The first one, ISC, identifies the species combination and offers the possibility to simulate only grass growth, only tree growth or their combination in one run. The second one, IPS, identifies the production situation with the following options: potential production, water- limited or water- and nitrogen-limited production. Both variables affect the calculations by selecting the appropriate modules and skipping the modules, not needed during the simulation run.

The time variable ISPY offers the possibility for multi-annual runs of the model while using the same weather file for each year. This option is activated if the value of ISPY exceeds one. In that case FINTIM should exceed 366 to avoid a run stop due to the condition of finish time ([Appendix C.4.2](#)). If PRDEL also exceeds 366, the results from the calculations are printed to the output file only at the beginning of each year. An alternative for simulating a multi-annual period needs successive weather files for the whole period and FINTIM should equal the total number of days in that period ([Appendix C.4.1](#)).

The time step of integration (DELTA) is one day and should not be changed, because the weather input modules can not handle other time steps.

4.5. MLI61.973

The following weather data should be available on a daily basis: short-wave radiation, minimum and maximum temperature, early morning vapour pressure, mean wind speed and precipitation. MLI61.973 is an example from Segou in Mali.

4.6. TREE.DAT

The file TREE.DAT contains a biomass, a water and a nitrogen part with the necessary input data for the various production situations. If e.g. the potential production situation is selected ($IPS = 0$), the input data of the water and nitrogen part are not used in the model, because the corresponding modules are not selected. On the other hand, a simulation of water- or nitrogen-limited growth always uses the biomass part of the input file.

4.6.1. Biomass

TRDENS

The minimum number of trees per hectare equals one, but the model specifies no maximum. Total tree cover is calculated in the model by multiplying tree population density with individual tree crown cover. An agroforestry system with many small trees can thus be compared to a system containing a few large trees, while both have the same total tree cover.

WLVI_T

The present version of RECAFS (version 1.0) refers to a deciduous tree species, i.e. the initial leaf biomass should equal zero, if the model calculations start before the first possible day of leaf flush (*ISTART_T*) during the leafless stage. The suffix '_T' distinguishes between this input and its equivalent for the grass species, which is necessary if a sensitivity analysis is performed using the rerun facility of FSE.

WSDI

Seed biomass at the start of simulation.

WSTI_T

Stem or trunk biomass is used in the model to calculate crown cover per tree. Any variation in initial stem biomass may have a direct effect on tree crown cover, depending on the function that is used for this relation. This variation also affects the biomass partitioning factors which have been defined as a function of stem biomass. Light use efficiency, used in the model to convert absorbed radiation into biomass production, is also defined as a function of stem biomass in combination with branch and root biomass.

WBRI

Growth of tree leaves has been correlated to branch biomass by using a positive relation between branch biomass and maximum leaf biomass during the leaf flush period. This implies that variations in initial branch biomass, e.g. due to pruning, may result in a change in maximum leaf biomass at the end of the leaf flush period. Furthermore, branch biomass may also influence light use efficiency in combination with stem and root biomass.

WRTI_T

The maximum amount of water or nitrogen that can be taken up by the root system is positively correlated to root biomass. At high water or nitrogen demands, low initial root biomass can limit uptake of these resources and therefore cause a reduction in production. The sum of root biomass and total aboveground wood biomass is also used to characterize total tree size to determine light use efficiency.

WRSI

Reserves may be used to accelerate leaf growth during early development. If the available reserves cannot meet the demand, tree leaf growth is retarded with consequences for tree production, shading conditions, water and nutrient uptake. Reserves are assumed to be stored in the branches and the trunk of the tree and the sum of *wst* and *wbr* includes these reserves.

XRTI

At initialization the ratio of *xrti* and crown cover radius is calculated and this ratio is used during simulation to find the average length of the lateral roots, *XRT*, as a function of crown cover radius. The average length of the lateral roots determines the area from which water and nutrients can effectively be taken up from the upper soil layer by a solitary tree. Soil resources beyond this area are not available for this tree, but may be available for its neighbour at higher tree densities, if the whole area is rooted by the entire tree population. The average length *XRT(i)* is also used at low tree densities to determine the outer boundary of the second subarea around each tree and is therefore part of the biomass input data.

IDVSTR

The phenological stage of the tree should be zero at the onset of the simulation, if the simulation of a deciduous tree species starts before its leaf flush at the leafless period (see also *WLVI_T*).

ISTART_T

This parameter determines the start of the leaf flush of a deciduous tree species. Changing this parameter affects the length of the growth period of the tree species and possibly also the interaction with the herbaceous species, especially if the start of grass growth is close to the first day of tree leaf flush.

IDOY3

First day of the leaf fall period in the absence of severe water stress. The maximum length of the leaf fall period is set by the function describing the relative rate of decrease in leaf weight (*RDLVTB*).

KL, KW

The PAR extinction coefficients of leaves and branches are used in the description of a number of

processes in the model. Changing these parameters affects the interception of photosynthetically active radiation of both tree and grass species. Also the interception of short-wave radiation changes with possible consequences for potential evapotranspiration of the grass species. Finally, rainfall redistribution by the tree crowns is influenced by these parameters. Biomass production, water use and rainfall infiltration are thus all affected. The leaf extinction coefficient is only operational if the tree has leaves.

SLA

The effect of relative variations in the specific leaf area is similar to that of relative variations in the leaf extinction coefficient.

RAPFST

The effect of varying the absorption ratio is similar to that of varying the extinction coefficients with the exception that rainfall interception remains unaffected. The effect is maximal for solitary trees and decreases with increasing tree population density, because the absorption of radiation is then gradually approaching the situation of a forest with a closed tree canopy.

TRDNSI

An increase in the tree population density, at which the transition occurs from solitary trees to the situation of intertree shading, results in higher absorption of radiation and lower water use efficiency of the tree population at lower tree densities. For a closed tree canopy it has no effect.

FWBUD

A higher leaf bud biomass fraction accelerates potential leaf growth, because it leads to higher initial leaf biomass at the onset of the exponential growth during leaf flush. Leaf growth is only affected until the maximum leaf biomass as a function of branch biomass is reached. The number of days needed to reach the maximum leaf biomass may therefore decrease. Actual acceleration of leaf growth also depends on availability of reserves (WRSI) and daily growing conditions.

RGRWLV

The effect of variations in relative growth rate of leaves is similar to that of variations in the leaf bud biomass fraction. It is only used during the reserve mobilization period ($IDVSTR = 1$) to calculate potential leaf growth.

PRDRM

An increase in the value of PRDRM extends the maximum number of days during which leaf growth can be supported by reserves. It is only effective until maximum leaf biomass is reached. The sensitivity of the model to PRDRM depends also on FWBUD, RGRWLV, WRSI and actual growing conditions, because they determine the actual number of days needed to reach the maximum leaf biomass.

FWWLV_T

Only during the leaf fall period, reserves can be withdrawn from leaves before abscission to contribute

to the increase in tree biomass, while decreasing leaf litter production. At a value of one a complete withdrawal of all leaf biomass is assumed and consequently leaf litter will be zero. A value of zero implies that finally leaf litter production equals leaf biomass production.

FAWRS

The rate of increase in reserves is positively correlated to the maximum reserve partitioning factor until the maximum reserve level in the tree is reached. A low value for *fawrs* can result in insufficient replenishment of the reserves which may cause limitations in the growth of leaves during the next leaf flush. It has only consequences for tree production if the time period of simulation exceeds one year.

CRESMX

The rate of reserve storage is related to the difference between actual and maximum reserve level. Therefore, any variation in *CRESMX* does not only change the potential level, but also the rate of change in reserves during the reserve storage period, i.e. phenological stage 2 and 3 of a deciduous tree.

RDRBRY

Variations in the relative rate of decrease in branch biomass affects branch biomass of the tree (see also *WBRI*) and organic matter input from dead branches.

RDRRTY

Variations in the relative rate of decrease in root biomass affects the root biomass of the tree (see also *WRTI*) and organic matter input from dead roots.

RDLVTB

This function gives leaf death as a function of the phenological stage of a deciduous tree. Time is expressed in number of days from *IDOY3*. Leaf death induced by water stress is modelled separately and is added to leaf death calculated with this function. Variations in *RDLVTB* may be introduced in the distribution of leaf death within the leaf fall period or in the length of the leaf fall period. The last value of this table should always be one, because it corresponds to the last day of the leaf fall period and only at a relative decrease rate of one all leaves will fall from the tree.

RSDSTB

Field data of the simulated tree species should be used for the relation of seed or fruit fall in time.

FWSHTB_T

The shoot biomass partitioning factor is calculated as a function of trunk biomass. In the course of the life cycle of a tree biomass partitioning varies and this could be incorporated in the model by relating it to trunk biomass. Because of lack of data a constant partitioning factor is used. The root biomass partitioning factor equals one minus the shoot biomass partitioning factor. Changing the shoot biomass partitioning factor (possible values between 0 and 1) therefore also affects root growth.

FWSTTB_T

Trunk biomass growth equals the product of the trunk biomass partitioning factor and shoot biomass growth.

FWBRTB

Branch biomass growth equals the product of the branch biomass partitioning factor and shoot biomass growth.

FWLVTB_T

Leaf biomass growth equals the product of the leaf biomass partitioning factor and shoot biomass growth augmented by translocation of reserves during the leaf flush period. The seed or fruit partitioning factor equals one minus the sum of the partitioning factors for trunk, branches and leaves. Variations in any of these partitioning factors also affects seed or fruit growth.

LUETB

Light use efficiency is defined as a function of total wood and root biomass. In general, light use efficiency decreases at higher tree biomass, because of higher maintenance requirements. On a daily basis tree production is linearly related to light use efficiency, but on a seasonal basis water and nutrient availability may be limiting. The effect of variations in light use efficiency also depends on the supply of other resources and the competitive interactions with the herbaceous species.

CRCVTB

Crown cover is defined as a function of trunk biomass. If severe cutting of branches as a management tool is practised, this relation can not be used. It should then be replaced, e.g. by a function that relates crown cover to branch biomass. Lopping a few branches does not affect crown cover, but results in a lower leaf area index in the model because of the relation of maximum leaf biomass to branch biomass.

WLMXTB

In the model maximum leaf biomass during the leaf flush period is calculated as a function of branch biomass at the first day of the leaf flush. Maximum leaf biomass only affects tree production and shading conditions if growing conditions or availability of reserves are favourable enough to attain this leaf biomass at the end of the leaf flush period.

SSATB

A negative correlation between branch biomass and specific branch area has been incorporated in the model to describe the decreasing ratio between biomass and area in the course of the life cycle of the tree. Variations in this function affects branch area index and thus the light and rain interception capacity of the tree crown.

SHADE

The shade function describes the distribution of intercepted radiation around a solitary tree for calculation of the irradiance at the level of the herbaceous vegetation. The X-value of each pair, multiplied by the crown cover radius represents the distance from the tree, and the Y-value represents

the fraction of intercepted radiation within that distance. Two types of distribution may be selected: shade concentrated near the tree by increasing the Y-value of the second pair or shade spread over a larger area by decreasing the Y-value of the second pair and increasing the X value of the third pair. The values of the first pair (0,0) and the last pair (10000,1) should not be changed and the Y-value of the one but last pair should equal 1 to ensure that all intercepted radiation is distributed.

4.6.2. Water

ZRTI_T

The length of the taproot determines the maximum soil depth from which the trees can extract water and nutrients under their crown. Any water or nutrients leached beyond this depth can not be taken up. The rooted depth outside the tree crown in subarea 2 is correlated to the relative vertical distribution of tree roots, using PRLIV, and XRTI, and is generally less than ZRTI_T. Increasing rooting depth can be advantageous in case of water stress if water is still available in deeper soil layers. However, an extended rooting depth in combination with a constant root biomass results in lower root densities in the upper soil layers. If nitrogen, rather than water limits production an extended rooting depth may not be advantageous, because less water will be taken up from the upper soil layers, where in general most nitrogen is available.

ZRT0

If a soil compartment boundary coincides with the value of ZRT0, water and nutrients in the layer above ZRT0 are only available for uptake by the herbaceous species. Increasing ZRT0 favours therefore the herbaceous species because in general the availability of soil resources in the upper compartments is high. Variability in this parameter may result from soil management practices, such as ploughing.

RAINTH

The rainfall threshold value can be used to determine the onset of the leaf flush period for water-limited situations. Daily rainfall exceeding the value of rainth triggers leaf flush if day number has passed ISTART_T. Before ISTART_T leaf flush is not possible and if a value of zero is used for rainth, leaf flush occurs always 3 days after ISTART_T. Variations in the threshold value of daily rainfall may cause a change in the first day of leaf flush. In a sensitivity analysis with different weather files this change will not be constant, because it also depends on the actual weather conditions of the selected year.

TRDWS_T

A high transpiration threshold value indicates that the tree leaves are stressed by water shortage already at low levels of water shortage, defined by the ratio of actual and potential transpiration. Accumulation of water stress days for leaves is accelerated at higher values of this parameter under suboptimal water supply. This means that leaf fall due to water stress may start earlier.

PRLIV

A high value of the vertical root distribution parameter results in most roots being located in the upper parts of the soil, whereas with a low value more roots are distributed to deeper layers.

PRLIH

A high value of the horizontal root distribution parameter results in most roots being located under the tree crown, whereas at a low value more roots are located in the second subarea around the tree.

SRL_T

This characteristic determines the capacity of the root system for water and nitrogen uptake in combination with total root mass and the maximum uptake of water or nitrogen per unit root length. Low values may result in restricted water or nitrogen uptake rates if the demand for these resources is relatively high.

FWRMX-T

Variations in the maximum uptake rate of water by the roots can affect actual water uptake under high demand and low root length densities. It also influences nitrogen uptake through its effect on mass flow.

TRANSC_T

The characteristic transpiration rate affects the capacity of the tree root system to take up water at low soil water contents. A low value implies that the deviation between actual and potential transpiration starts at relatively high soil water contents. The consequences are that water stress may accumulate relatively early and that also the competitiveness for soil water is lower relative to that of the herbaceous species. Evidently, these effects only occur in case of water shortage and are aggravated under low water availability.

WUE1

Variations in the average seasonal water use efficiency of solitary trees affects the water uptake by the tree population. This effect will decrease with increasing tree population density if WUE2 is not changed simultaneously.

WUE2

Higher average seasonal water use efficiency of trees in a closed tree canopy improves water use efficiency of the tree population at higher tree densities if actual tree population density exceeds that marking the onset of intertree shading (TRDNS1).

VPCMX

A value of zero for this parameter implies that the vapour pressure of the air is unaffected by the presence of trees and that the water use efficiency of the grass vegetation under a tree crown canopy is lower than that of a grass monoculture. Increasing the value of this parameter improves the water use efficiency of the herbaceous vegetation to a level that can exceed that of the monoculture. It has no direct effect on tree growth in the model. An indirect effect exists through the competition for soil water due to modification of the water demand and uptake of the herbaceous species.

TMCMX

Variations in the maximum relative decrease in temperature affects average temperatures near the trees

with consequences for water use efficiency of the herbaceous vegetation, its development rate and relative growth rate of the leaf area index during early development of the herbaceous species.

WNCMX

Variations in the maximum relative decrease in wind speed has similar effects as variations in *VPCMX*.

DIRTHR

A higher direct throughfall threshold value causes a larger part of the rainfall to directly infiltrate homogeneously. Consequently, interception of rainfall by the tree crowns and tree stem flow will be lower. It favours shallow-rooting species (see also *STFTHR*).

RNTH1

The fraction of rainfall interception by the tree crowns is positively correlated to the value of this rainfall threshold. Only the trees can profit from increased interception, whereas for the herbaceous species less water infiltrates in the soil under the tree. However, tree stem flow is lower at higher interception and if the storage of water at greater depths through tree stem flow is important for the tree, an increase in *RNTH1* might have negative effects on tree growth or tree survival.

RNTH2

See *RNTH1*.

FIRMIN

A higher minimum fraction of intercepted rain has a similar effect as increasing the rainfall threshold values.

STFTHR

The range in this parameter is from 0 and 1. A value of zero implies no stem flow and all rainfall minus interception, i.e. total throughfall, infiltrates homogeneously. A value of one implies no indirect throughfall and all rainfall minus direct throughfall and intercepted rain infiltrates as stem flow. Infiltration of stem flow water will in general be deeper and thus result in a higher soil water availability for a deep-rooting tree species and in lower water supply for a shallow-rooting herbaceous species, which grows under the tree crown. These calculations only refer to the precipitation of the area covered by the crowns of the tree population.

STFINF

The depth of infiltration of stem flow is negatively related to the infiltration factor, representing the ratio of the area of infiltration of the tree stem flow and the crown cover area. Possible values for this parameter fall between 0 and 1. If the value of *STFINF* equals 1, tree stem flow infiltrates homogeneously over the whole crown cover area identical to the direct and indirect throughfall. A value of zero is not possible.

RDRWTB_T

This function describes the effect of water stress on the additional leaf death calculated by the model. The standard function shows that after 5 days of water stress leaves start falling and that after 30 days total leaf biomass has died. Trees that can withstand long periods of water stress can be discriminated from more sensitive species by changing the first and/or the last day to higher values.

FBRSTB_T

This function relates the shoot biomass partitioning factor to the level of stress, due to insufficient uptake of belowground resources. Increasing stress causes a reduction in the shoot biomass partitioning factor and thus a higher root biomass partitioning factor. Hence, root growth is favoured at the expense of shoot growth, which eventually may lead to a relief of the stress situation. The second and third number in the table can be changed. By decreasing the second or increasing the third a stronger effect is simulated. No effect on root-shoot partitioning is simulated if the second number equals one. Neither of the numbers should exceed one or become negative.

4.6.3. Nitrogen

NLVI_T

Initial leaf nitrogen content should equal zero, if the model calculations start before the first possible day of leaf flush (see also *WLVI_T*).

NSDI_T

Seed or fruit nitrogen content at the start of simulation.

NSTI_T

Initial stem nitrogen content partly determines the amount of nitrogen reserves and has therefore an effect on leaf growth in case of nitrogen shortage during the reserve mobilization period. A low value may retard the leaf flush.

NBRI

The effect of varying the amount of nitrogen in the branches is similar to that of nitrogen in the stems. Furthermore, the amount of nitrogen in living branches also influences nitrogen mineralization, because the input of nitrogen in the soil through litterfall of the branches is related to the nitrogen concentration of living branches. A higher value of NBRI has a positive effect on mineralization of nitrogen from soil organic matter.

NRTI_T

The amount of root nitrogen has no direct effect on tree production. The effect on nitrogen mineralization is similar to that of the branches.

FWNLV_T

A high value for the leaf nitrogen translocation fraction decreases the demand for nitrogen from the soil during leaf death, but also decreases nitrogen input in the soil. It favours the tree species at the expense

of the grass species under low soil nitrogen availability during the leaf fall period.

FWNBR, FWNRT_T

The effect of the nitrogen translocation fractions of branches and roots is comparable to that of the leaves. The translocation fraction of the branches also determines the amount of nitrogen reserves in the stems and branches, which can have an effect on early leaf growth under nitrogen shortage.

CNLVMX, CNSDMX, CNBRMX, CNSTMX, CNRTMX

Maximum nitrogen concentrations affect the nitrogen demand and therefore nitrogen uptake from the soil. A higher value increases nitrogen uptake and may accelerate depletion of available nitrogen in the soil with possible negative consequences for the other species. The nitrogen demand of each plant component is also used in calculating their nitrogen partitioning coefficients. Changing only one of the maximum nitrogen concentrations therefore modifies the nitrogen partitioning within the tree.

CPLV, CPSD, CPBR, CPST, CPRT

Field data for the phosphorus concentrations during the whole year should be used. At low phosphorus concentrations the maximum concentrations of nitrogen in the plant components decrease, which influences nitrogen demand, nitrogen uptake and soil nitrogen depletion rate. This may lead to higher nitrogen availability for the grass species. Low phosphorus concentrations in the leaves also have negative effects on biomass production through the associated low nitrogen concentration in the leaves.

PNLVMN_T, PNSDMN_T, PNBRMN_T, PNSTMN_T, PNRTMN_T

At low phosphorus concentrations, variations in the minimum slope of the relation between nitrogen and phosphorus has an identical effect as varying the actual phosphorus concentrations. This parameter is not effective at higher phosphorus concentrations.

CNLVMN_T

At a lower value for the minimum leaf nitrogen concentration, biomass production is less reduced at low leaf nitrogen concentrations.

CNBRMN, CNSTMN

At low nitrogen concentrations in the stems and branches, the minimum nitrogen concentrations of these plant components determine the amount of reserve nitrogen available for early leaf growth. High values are associated with low nitrogen reserves and can affect leaf growth during the leaf flush period.

RCNOX_T

The product of RCNOX_T and CNLVMX represents the optimum leaf nitrogen concentration for unlimited biomass production with respect to nitrogen. At a lower value for this parameter, biomass production is less reduced at intermediate nitrogen concentrations.

RNURLX_T

Variations in the maximum uptake rate of nitrogen by the roots can affect actual nitrogen uptake under

high nitrogen demands and low root length densities.

4.7. GRASS.DAT

4.7.1. Biomass

PLDENS

Variations in plant population density affects initial biomass of roots, stems and leaves, leaf area index and total root length of the grass vegetation at initialization. In general, higher values for *pldens* accelerate biomass growth through increased capacity to absorb resources.

WLVI_G

Initial leaf biomass of the vegetation is given by the product of plant population density and *WLVI_G*. At initialization, leaf area index is not correlated to this state variable.

WSTI_G

Initial stem biomass of the vegetation is given by the product of plant population density and *WSTI_G*.

WRTI_G

Initial root biomass of the vegetation is given by the product of plant population density and *WRTI_G*. Root length index is linearly related to root biomass. If at initialization root length index limits water uptake of the grass vegetation, an increase in *WRTI_G* can increase biomass production of the herbaceous vegetation.

LA0

Initial leaf area index is given by the product of plant population density and *LA0*. Early leaf area development is described by an exponential function (see *RGRLAI*) and is thus proportional to initial leaf area index. Higher *LA0* accelerates leaf area development, which in general stimulates grass production possibilities.

DVSI

At emergence development stage equals zero.

ISTART_G

The parameter *ISTART_G* defines the first possible day of emergence (compare *ISTART_T*).

DVSE

Varying the development stage at which harvest takes place, determines the length of the growth cycle of grass. In *RECAFS*, *DVSE* equals the first day at which leaf growth stops as a function of development stage (see *FWLVTB_G*).

INDEME

This parameter defines the number of days needed for emergence. At the end of this period the model starts with grass growth calculations and during this period competition with the tree species is not simulated. Variations in this parameter affects the length of the period in which water and nitrogen uptake by the tree population and soil evaporation take place without interference of the grass vegetation. Higher values for INDEME favours tree growth at the expense of grass growth at water- or nitrogen-limiting situations.

DVRVEG

The number of growing days in the vegetative stage is inversely proportional to DVRVEG. A lower value increases herbaceous production if water or nitrogen availability can sustain this higher production.

DVRGEN

The number of growing days in the reproductive stage is inversely proportional to dvrgen. The effect on production is less compared to DVRVEG, because of lower leaf and root growth during the reproductive phase.

LUE

Higher values for the light use efficiency, measured at average radiation levels (RDDLUE), increase the production per unit absorbed radiation when water or nitrogen are available for the crop. This effect is reduced at lower radiation levels due to the relation between light use efficiency and radiation level. It influences therefore the ratio in grass production from different subareas, particularly in case of ample supply of water and nitrogen.

RDDLUE

The effect of changing RDDLUE is similar to that of LUE, but with a smaller impact on grass production.

LUEINI

Higher values for the light use efficiency at zero radiation increase light use efficiency of the vegetation at lower radiation levels. This effect ceases as radiation level approaches RDDLUE. It influences the ratio in grass production from different subareas, especially at high water and nitrogen availability.

RDVS2

The reduction in biomass production during the reproductive phase due to ageing is negatively correlated to RDVS2. A value of one implies no reduction and the minimum value for DVS2 with maximum reduction equals zero. Its effect decreases with increasing nitrogen stress.

FWWLV_G

As leaves die, reserves can be withdrawn before abscission to contribute to the increase in biomass of the herbaceous vegetation, while decreasing leaf litter production. A value of one implies complete withdrawal of all leaf biomass and consequently leaf litter will be zero. A value of zero implies leaf litter production to equal leaf biomass.

FWWST

During the reproductive phase, reserves in the stem are mobilized and added to the pool of assimilates for partitioning to the various plant components. One effect of a higher value for FWWST is a higher proportion of translocatable reserves in the stem and thus lower stem biomass at harvest. But, depending on the partitioning factors during this development phase, leaf and root biomass may profit from the increased availability of assimilates, which can have a positive effect on stem biomass through increased production. The effect on stem biomass is therefore difficult to predict, but leaf and root biomass generally increase, whereas the effect is strongest on seed biomass.

LAITHR

A low value for the leaf area index threshold value has a negative effect on production, because it shortens the period of exponential, i.e. maximum, leaf area growth.

RGRLAI

A high value for RGRLAI accelerates leaf area development until the threshold value is reached (LAITHR). In general the grass vegetation responds with a higher leaf area index and increased production, unless water or nitrogen are severely limiting.

PARCR

Higher critical PAR levels result in increased leaf death and eventually root death if PAR drops below this critical level. The light conditions in the lower part of the grass canopy is influenced by the leaf area index of the herbaceous species, but also by the presence of the trees.

TRDWS_G

Similar to TRDWS_T.

DVRVTT, DVRGTT, DVRVDT, DVRVLT, DVRVST

Variations in one of these functions, that describe the correlation between temperature, daylength, latitude and stress level and development rate, affects phenological development in the vegetative or reproductive phase with implications for the growth period of the grass species (see also DVRVEG and DVRGEN).

RDRTB

This function describe relative leaf death in relation to development stage. Leaf death due to water stress or low radiation levels is calculated separately. Variations in this function affect leaf biomass, but may also influence root death, because relative root death is set equal to relative leaf death when leaf area index drops below a preset fraction of the maximum leaf area index during the growth period.

RDRWTB_G

Similar to RDRWTB_T.

FWSHTB_G, FWLVTB_G, FWSTTB_G

In general, the biomass partitioning factors have a strong effect on biomass production and water and nitrogen uptake of the vegetation.

FBRSTB_G

Similar to FBRSTB_T.

FSRSTB

This function relates the level of shading to the shoot biomass partitioning factor. Increasing shade results in a higher shoot partitioning factor at the expense of the root partitioning factor. This effect is intensified by increasing the 4th or the 6th number or by decreasing the 3rd number of the table.

SLATB

A higher specific leaf area, defined as a function of development stage, increases leaf area growth per unit leaf biomass growth after the exponential leaf growth period. If conditions with respect to water and nitrogen are favourable, a higher leaf area results in increased production.

KLTB

The extinction coefficient has been defined as a function of leaf area index to simulate the effects of incomplete ground cover and self-shading at low leaf area indices. This option can be activated by decreasing the second number in the table, which equals the extinction coefficient at initialization.

4.7.2. Water*ZRTI_G*

Higher values for the initial rooted depth decrease the risk of crop failure due to water stress. Crop failure leads to a delay in the grass growth period, which generally has negative consequences for production due to a shorter vegetative phase and continuing depletion of resources by the tree species.

IFINAL

The parameter IFINAL defines the last possible day of emergence. A lower value for IFINAL reduces the period in which crop failure due to water stress can be followed by a new emergence flush.

ILREF_G

The number of soil layers which are used in determining emergence of the grass species as a function of water availability, should correspond with the soil depth where the grass seeds are found.

WATHR_G

Higher values for the water content threshold for emergence delay the start of the grass species, but decrease the risk of crop failure. Depending on the occurrence of a situation of prolonged water stress after the start of grass growth a higher value can be favourable or unfavourable for the production possibilities of the grass. The water content threshold should not exceed the amount of water, that can be

stored above wilting point in the upper soil layers used for determining the start of grass growth.

ZRTMC

The grass species may attain its maximum rooted depth under favourable soil water conditions. Higher values for ZRTMC increases water and nitrogen availability for the plants when root extension is not limited by other causes. At equal root biomass, a larger rooted depth also decreases the root density in the upper soil layers, which may be disadvantageous with respect to nitrogen uptake, because nitrogen availability is highest in the upper soil layers (see also ZRTI_T).

EZRTC

Higher values for the daily root extension rate accelerate the rate of soil depth penetration, which can have beneficial effects in case of water shortage in the upper soil layers, but also adverse effects if only nitrogen limits the production (see also ZRTMC).

PRLI

Similar to PRLIV of the tree species.

TRANSC_G, SRL_G, FWMRX_G

Similar to TRANSC_T, SRL_T and FWRMX_T.

RDRWTB_G

This function describes the effect of water stress on the additional leaf death calculated by the model. The standard function shows that after 2 days of water stress leaves start dying and that after 10 days total leaf biomass has died (see also RDRWTB_T).

FBRSTB_G

Similar to FBRSTB_G.

4.7.3. Nitrogen

NLVI_G

If a low value for NLVI_G is selected relative to WLVI_G, biomass production at the start of the grass growth calculations is reduced due to low leaf nitrogen concentrations. This situation may change quickly within one timestep depending on the availability of mineral nitrogen in the soil and the nitrogen uptake capacity of the grass vegetation.

NSTI_G, NRTI_G

The effect of the initial values for the nitrogen content in stems and roots on grass production is absent. The values for NLVI_G, NSTI_G and NRTI_G should be selected such that the concentrations do not exceed the maximum concentrations.

FWNLV_G, FWNRT_G

Similar to FWNLV_T and FWNRT_T.

PNSDMN_G, PNBRMN_G, PNSTMN_G, PNRTMN_G

Similar to their counterparts for the tree species.

CNLVMN_G, RCNOX_G, RNURLX_G

Similar to CNLVMN_T, RCNOX_T, RNURLX_T.

CNLVXT, CNSTXT, CNSDXT, CNRTXT

Similar to their counterparts for the tree species.

CPLVTB, CPSTTB, CPSDTB, CPRTTB

Similar to their counterparts for the tree species.

4.8. LISAG.DAT

DSLRL

The number of days since last rain at initialization can be derived from the weather data file of the year before the selected year. One hundred days is an estimate of the length of the dry season until the first of January and is used in the model because the calculations start at the beginning of the year. A lower value for this parameter may increase soil water loss through evaporation, if water is available in the soil above air dry.

WCLQTM

Actual water contents should be given for each soil compartment. Higher water contents at initialization can increase water uptake by plants and/or soil evaporation. Also deep percolation of water may increase. Initial soil water contents should be between air dry and field capacity (WCAD, WCFC).

NL

The maximum number of soil compartments is 10.

EES

The evaporation proportionality factor determines the distribution of water loss among the various soil compartments by evaporation. A higher value results in a higher proportion of the evaporation to be extracted from the upper soil compartments.

RONOFF

This parameter is a switch with predefined values: -1 corresponds to runoff and 1 indicates run-on. Any other value results in a situation where precipitation minus interception equals infiltration.

INFMXB, INFMXC

Daily rainfall exceeding the maximum infiltration rate runs off. A bare soil corresponds with a situation

where the leaf area index of the herbaceous vegetation equals zero. It has been assumed that the maximum infiltration rate of a soil with a vegetation is higher than that of a bare soil. INFMXC should therefore never be smaller than INFMXB. For a leaf area index of 5 or more the maximum infiltration rate is given by INFMXC. Higher values for these two parameters reduce the amount of runoff, depending on the number of rainfall events exceeding the original values for INFMXB and INFMXC.

INFMXS

The difference between daily rainfall and maximum infiltration rate of the surrounding area runs off towards the field for which the calculations are performed. The amount of run-on for this field is negatively correlated to the value of INFMXS.

RSAF

Runoff from the surrounding areas occurs in case of a positive difference between precipitation and maximum infiltration rate of these areas. The amount of water received also depends on the ratio between the total area of the surrounding fields and the area of the field of interest. A higher ratio implies that water from a larger area flows towards this field and thus increases the amount of run-on.

TKL

Low values for the thickness of the soil compartments imply lower infiltration depths. Another effect is that water uptake of a shallow-rooting species is stimulated because the water content of the deepest soil compartment containing infiltrated water is closer to field capacity after a shower. The sum of all compartment thicknesses should at least equal the rooted depth of the tree species, otherwise an error will occur.

WCST

The water content at saturation has no effect on the calculations, because it is not used in the present version of the model, that assumes free-draining soils.

WCFC

Lower values for WCFC cause deeper infiltration in the soil profile. It also increases the ability of the plants to take up water from the soil, because actual transpiration rate is related to the reduced water content, which is negatively correlated to WCFC.

WCWP

Variations in the water content at wilting point affects the ability of the plants to take up water from the soil through the reduced water content. Higher values result in increased water stress if water availability in combination with demand is limiting water uptake.

WCAD

Each soil compartment contains at least an amount of water equal to the water content at air dry, also during the dry season. Water stored between wilting point and air dry is not available for plant uptake, but may be lost by soil evaporation. If the water content at air dry is increased, the amount of water

needed for attaining wilting point and field capacity will be less, resulting in deeper infiltration and higher water availabilities. In the soil input file water content at air dry is equal to the water content at wilting point divided by three. If both are changed simultaneously without changing this ratio, the total effect on model results is difficult to predict because separately, they have opposite effects.

NMINM

Mineral soil nitrogen content at initialization determines initial availability of soil nitrogen for either immobilization processes in soil organic matter or for uptake by plants.

CSOM1I, CSOM2I, CSOM3I, CSOM4I

Increasing soil organic carbon without a similar change in soil organic nitrogen results in lower nitrogen concentrations in the organic matter. In the short term nitrogen mineralization is then reduced and may even become negative. In the long term it has no effect on the availability of soil nitrogen.

NSOM1I, NSOM2I, NSOM3I, NSOM4I

Increasing soil organic nitrogen without a similar change in soil organic carbon results in higher nitrogen mineralization rates. After some time this effect disappears. Nitrogen from the first two pools is released rapidly, but the effect quickly disappears, whereas changes in the other two pools are slower, but last longer, due to the differences in their decomposition constants.

ZMXSCN

A lower value for the maximum depth of organic matter and mineralization is an advantage for the shallow-rooting species, because a higher proportion of the total mineralized nitrogen is released in the upper soil compartments. If ZMXSCN exceeds the maximum rooting depth of one of the species in a subarea, the nitrogen released between this depth and ZMXSCN can not be taken up by that species.

PDSCNS

An increase in the distribution parameter for nitrogen mineralization has a beneficial effect on the shallow-rooting species, because a higher proportion of the total mineralized nitrogen is released in the upper soil compartments.

WCTCN1, WCTCN2

The water content threshold values represent the sensitivity of the decomposition process to low soil water contents. At high values for these two parameters total decomposition and mineralization of soil organic matter is reduced. If this leads to a lower growth rate and therefore to a lower water uptake by the vegetation, the depletion rate of soil water is reduced as well, which partly compensates the reduction in decomposition and mineralization.

CNRAIN

A higher nitrogen concentration in the precipitation increases nitrogen input into the ecosystem.

FNEFF

This parameter has a value between 0 and 1. A value of zero means that water flow from one soil compartment to the next does not result in vertical redistribution of mineral soil nitrogen, i.e. mineral nitrogen remains in the soil compartment where it is released until it is taken up by the plant roots. Nitrogen input into the ecosystem is then only available in the top soil compartment. A value of one implies that the soil has no adsorption capacity for mineral nitrogen and that mineral nitrogen is transported freely through the soil with the water flow.

ILITD

A value of zero results in homogeneous spatial distribution of the aboveground tree litter, whereas a value of one implies that all aboveground tree litter falls under the tree crown. In the long term a value of one may lead to increased nutrient availability under the tree compared to the area outside the tree.

FWDRT

A higher fraction of wood in the tree roots causes slower decomposition of dead tree roots and hence lower mineralization of nitrogen. In general, soil organic carbon in subareas 1 and 2 levels increase as a result of a higher FWDRT .

FCNW3, FCNW4

These parameters represent the proportion of carbon in fresh litter that decomposes relatively slowly in the organic matter pools CSOM3 and CSOM4. Decomposition of fresh litter and the associated mineralization of nitrogen is negatively correlated to the values of the carbon distribution factors,

FCWD3, FCWD4

See FCNW3, FCNW4. The parameters FCWD3 and FCWD4 should be higher than their counterparts of non-wood litter FCNW3 and FCNW4, because in general decomposition of woody litter is slower than that of non-woody litter.

K1, K2, K3, K4

Higher values for the decomposition constants of the organic matter pools indicate a higher turnover rate of carbon and nitrogen. Nitrogen in the soil organic matter is then released earlier for uptake by plants or vertical redistribution in the soil.

CRNC1, CRNC2, CRNC3, CRNC4

An increase in the critical carbon-nitrogen ratios of the soil organic matter pools reduces nitrogen mineralization at first, because more nitrogen is immobilized by the decomposers. In the long term this nitrogen becomes available again. These characteristics have no effect on organic matter decomposition, unless the amount of nitrogen needed for immobilization can not be supplied by the soil. In that case organic matter decomposition is also slowed down.

EFF1, EFF2, EFF3, EFF4

Microbial growth efficiency has a value between 0 and 1. A value of one is not possible. The mineralization rate is positively correlated to this efficiency. In general it does not affect the organic

matter decomposition unless the nitrogen needed for immobilization can not be supplied by the soil.

NGIFTB

This table represents the amount of fertilizer nitrogen applied as function of day of year. Together with the deposition of nitrogen (see CNRAIN) it forms the input of nitrogen into the ecosystem.

5. Model run checks

5.1. Introduction

Some calculations performed by the model are checked during simulation. All checks result in a message on the computer screen to inform the user. Balance and range checks result in a fatal error after which simulation is halted. Warnings indicate unusual situations and if necessary the model performs a correction and continues its calculations. Checks made by the FSE-main program and by the weather system are not described in this report. Their meaning has been documented in van Kraalingen (1991) and van Kraalingen *et al.* (1991).

5.2. Balance checks

Balance checks are used to determine whether any significant error has occurred in the calculations of dry matter, carbon or nitrogen. The sum of the amounts of dry matter, carbon and nitrogen of each compartment of a part of the ecosystem is calculated and compared with that of the previous time step. The absolute value of the difference of both sums may not deviate from the net change in this part of the ecosystem by a very small number ($1 \cdot 10^{-5}$). Also the distribution of PAR, roots and water uptake is checked in a similar way (Table 5.1). Definitions of acronyms can be found in [Appendix B](#).

Table 5.1. Balance checks in RECAFS

Acronym of variable	Description	Module
CHKRAD	distribution of radiation among transmission, reflection and absorption of both species	DISRAD
CHKWUP	distribution of actual transpiration of both species among the water uptake from various soil compartments	WATUPT
CHECK	distribution of net increase of soil water among the water content of various soil compartments	DRSAH1,-2,-3
CHKPBB	distribution of net increase in dry matter among the compartments of the tree population and the grass vegetation	TREEDM, GRASDM

CHKRTD	distribution of roots of the tree population and the grass vegetation among the soil compartments	ROOTR, ROOTG
CHKPNB	distribution of the rate of nitrogen uptake among the compartments of the tree population and the grass vegetation	TREENI, GRASNI
CHKNMS	distribution of net change in mineral soil nitrogen among the soil compartments	NITBAL
CHKNTS	distribution of net mineralization of nitrogen among the soil organic matter pools	NITBAL
CHKNSS	distribution of net change in the amount of nitrogen in the agroforestry system among soil and plant compartments	NITBAL
CHKCSS	distribution of net change in the amount of carbon in the agroforestry system among soil and plant compartments	NITBAL

5.3. Range checks

Range checks are used to verify whether calculated values of some variables range between reasonable minimum and maximum values (Table 5.2).

Table 5.2. Range checks in RECAFS

Condition for fatal error	Module
TRDNS1 > TRDNS2	DISRAD
FSHADE <> [0,1]	DISRAD
FIPAR <> [0,1]	DISRAD
PARABS <> [0, PAR]	DISRAD
PROD1 <> [0, 1000]	DMPROD
TRANSP <> [0, 20]	ETPOT
EVP <> [0, 20]	ETPOT
ATMTR <> [0,1]	PENMAN
TMIN > TMAX	PENMAN
WIND < 0	PENMAN
AVRAD < 0	PENMAN
IC > INLAY or IC > INAREA * INLAY	WATUPT
TRANSA > TRANSP	WATUPT

TRANSA < 0	WATUPT
INAREA > 3	WATBAL
WCLQT <> [WCAD, WCFC]	DRSAH1,-2,-3
IDOY > ISTART_T	TREEDM
IDOY > ISTART_G	GRASDM
ZRT > [Sigma] TKLX	ROOTR
CNLVOP < CNLVMN	TREENI
CNLVOP < CNLVMN	GRASNI
NLV > NLVMX, NSD > NSDMX, NST > NSTMX, NRT > NRTMX, NBR > NBRMX	TREENI
NLV > NLVMX, NSD > NSDMX, NST > NSTMX, NRT > NRTMX	GRASNI
RNUL > NMIN	NITUPT
RNU > NDEM	NITUPT
FLUXS =/ FLXLS	NITBAL
REDMM <> [0,1]	NITBAL
NMIN < 0	NITBAL

5.4. Warnings

Warnings provide some information for the user on the computer screen about the occurrence of a number of unusual situations (Table 5.3). Most warnings are associated with range checks but differ from those in 5.3, because they are corrected by the model and do not lead to a fatal error.

Table 5.3. Warnings in RECAFS

Situation	Correction	Module
ATMT > 1	ATMT = 1	ETPOT
VP > SVP	VP = SVP	ETPOT
RNSC < 0	RNSC = 0	ETPOT
TRANSM < TRANSP	TRANSM = TRANSP	ETPOT
WCLQT < WCAD ¹	WCLQT = WCAD	DRSAH1,-2,-3
WCLQT > WCFC ¹	WCLQT = WCFC	DRSAH1,-2,-3
EVSC ² > 0	EVSC = 0	DRSAH1,-2,-3
THRF < 0	THRF = 0	DRSAH1,-2,-3

TRWL ² > 0	TRWL = 0	DRSAH1,-2,-3
TRWL < -AVAIL	TRWL = -AVAIL	DRSAH1,-2,-3
DEMWLV < 0	SURPL = - DEMWLV and DEMWLV = 0	TREEDM
CRES > 1.5 * CRESMX	no correction	TREEDM
crop failure due to water stress	no correction	GRASM

1. These situations are only corrected during initialization, otherwise a fatal error will occur.
2. In the modules DRSAH1, -2, -3, water loss from the soil is assumed to have a negative value.

References

Anonymous, 1992. Production Soudano-Sahélienne (PSS). Exploitation optimale des éléments nutritifs en élevage. Projet de coopération scientifique. Brochure CABO-DLO, Wageningen.

Azam-Ali, S.N., P.J. Gregory & J.L. Monteith, 1984. Effect of planting density on water use and productivity of pearl millet (*Pennisetum typhoides*) grown on stored water. I Growth of roots and shoots. *Expl. Agric* 20, 203-214.

Azam-Ali, S.N., P.J. Gregory & J.L. Monteith, 1984. Effects of planting density on water use and productivity of pearl millet (*Pennisetum typhoides*) grown on stored water. II Water use, light interception and dry matter production. *Expl. Agric.* 20, 215-224.

Begue, A., J.F. Desprat, J. Imbernon & F. Baret, 1991. Radiation use efficiency of pearl millet in the Sahelian zone. *Agric. For. Meteorol.* 56, 93-110.

Belsky A.J., R.G. Amundson, J.M. Duxbury, S.J. Riha, A.R. Ali & S.M. Mwonga, 1989. The effects of trees on their physical, chemical, and biological environments in a semi-arid savanna in Kenya. *J Appl Ecol* 26:1005-1024.

Berendse, F., B. Berg, & E. Bosatta, 1987. The effect of lignin and nitrogen on the decomposition of litter in nutrient- poor ecosystems: a theoretical approach. *Can. J. Bot.* 65, 1116-1120.

Berendse, F., R. Robbink & G. Rouwenhorst, 1989. A comparative study on nutrient cycling in wet heathland ecosystems. II. Litter decomposition and nutrient mineralization. *Oecologia* 78, 338-348.

Breman, H. & J.-J. Kessler, 1995. [Woody plants in agro-ecosystems of semi-arid regions, with an emphasis on the Sahelian countries](#). Advances Series in Agricultural Sciences, vol. 23, Springer-Verlag, Berlin. 340 pp.

Breman, H. & N. de Ridder (Eds.), 1991. [Manuel sur les pâturages des pays sahéliens](#). Karthala, Paris.

485 pp.

- Conijn, J.G., 1989. Effect of nitrogen availability on the competition between plant species. A simulation study. CABO-verslag nr. 111, 45 pp. + App.
- Denmead, O.T. & R.H. Shaw, 1962. Availability of soil water to plants as affected by soil moisture content and meteorological conditions. *Agron. J.* 54, 385-389.
- Diepen, C.A. van, C. Rappoldt, J. Wolf & H. van Keulen, 1988. CWFS Crop growth simulation model WOFOST, Documentation version 4.1. CWFS, A'dam, Wageningen.
- Erenstein, O., 1990. Simulation of water-limited yields of sorghum, millet and cowpea for the 5th region of Mali in the framework of quantitative land evaluation. Student report TPE, LUW, 60 pp. (a) + Annexes (b).
- Goudriaan, J. & H. van Keulen, 1979. The direct and indirect effects of nitrogen shortage on photosynthesis and transpiration in maize and sunflower. *Neth. J. agric. Sci.* 27, 227-234.
- Jansen, D., 1984. SAHEL-5, een model voor ondergrondse concurrentie. Theoretische Teeltkunde, LUW, Wageningen.
- Jansen, D.M. & P. Gosseye, 1986. Simulation of growth of millet (*Pennisetum americanum*) as influenced by water stress. *Sim. Rep. CABO-TT no. 10*, 108 pp.
- Jongh, J. de, 1992. Soil moisture in dryland agroforestry. The influence of woody species on the soil moisture availability for herbaceous species in agroforestry systems in (semi-)arid and mediterranean areas. Dept Agroforestry, Agricultural University Wageningen.
- Kater, L.J.M., S. Kante & A. Budelman, 1992. Karité (*Vitellaria paradoxa*) and néré (*Parkia biglobosa*) associated with crops in South Mali. *Agroforestry Systems* 18:89-105.
- Kessler, J.J., 1992. The influence of karité (*Vitellaria paradoxa*) and néré (*Parkia biglobosa*) trees on sorghum production in Burkina Faso. *Agroforestry Systems* 17, 97-118.
- Keulen, H. van, 1975. Simulation of water use and herbage growth in arid regions. *Simulation Monographs*, Pudoc, Wageningen, 176 pp.
- Keulen, H. van & H. Breman, 1990. Agricultural development in the West African Sahelian region: a cure against land hunger? *Agriculture, Ecosystems and Environment*, 32, 177-197.
- Keulen, H. van, & J. Wolf (Eds), 1986. *Modelling of agricultural production: weather, soils and crops*

Simulation Monograph, Pudoc, Wageningen, 479 pp

Keulen, H. van, H. Breman, J.J. van der Lek, J.W. Menke, J. Stroosnijder & P.W.J. Uithol, 1986. Prediction of actual primary production under nitrogen limitation In: Modelling of extensive livestock production systems, 42-79. Eds N. de Ridder et al. Proc. of ILCA-ARO-CABO workshop held at ARO, Bet Dagan, Israel, 1985. International Livestock Centre for Africa, Addis Ababha, Ethiopia, 349 pp

Knevel, M.K., 1993. Solitary trees: light interception and shade patterns. Student report Dep. of Theor. Prod. Ecology, Agric. Univ. Wageningen, Wageningen. 92 pp.

Kraalingen, D.W.G. van, 1991. The FSE system for crop simulation. Simulation Report CABO-TT, no. 23, 77 pp.

Kraalingen, D.W.G. van, W. Stol, P.W.J. Uithol & M.G.M. Verbeek, 1991. User manual of CABO/TPE Weather System. CABO-DLO/TPE-WAU, Wageningen, 28 pp.

Kropff, M.J. & H.H. van Laar (Eds), 1993. Modelling crop-weed interactions. CAB International, Wallingford, UK, 304 pp.

Laar, H.H. van, J. Goudriaan & H. van Keulen (Eds.), 1992. Simulation of crop growth for potential and water-limited production situations (as applied to spring wheat). Simulation Reports CABO/TT 27, 72 pp.

Lövenstein, H.M., P.R. Berliner & H. van Keulen, 1991. Run-off agroforestry in arid lands. Forest Ecology and Management 45: 59-70

Lövenstein, H., E.A. Lantinga, R. Rabbinge & H. van Keulen, 1992. Principles of Theoretical Production Ecology. F300-001, Dept. of Theor. Prod. Ecol., WAU, 117 pp.

Penman, H.L., 1956. Evaporation: an introductory survey. Netherlands Journal of Agricultural Science 4, 9-29.

Penning de Vries, F.W.T. & M.A. Djitèye (eds.), 1982. [La productivité des pâturages sahéliens. Une étude des sols, des végétations et de l'exploitation de cette ressource naturelle.](#) Agric. Res. Rep. 918. Pudoc, Wageningen. 525 pp.

Penning de Vries, F.W.T., D.M. Jansen, H.F.M. ten Berge & A. Bakema, 1989. Simulation in ecophysiological processes of growth of several annual crops Simulation Monographs 29, Pudoc, Wageningen, 271 pp.

PIRT, 1983. Les ressources terrestres au Mali. Mali land and water resources. PIRT. Tams, New York.

Pressland, A.J., 1973. Rainfall partitioning by an arid woodland (*Acacia aneura* F. Muell) in south-west Queensland. *Aust. J. Bot.* 21:235-245.

Radersma, S., 1994. The influence of parkland trees on the soil and the herbaceous layer in the southern Sahel (with special attention to phosphorus). *Projet Production Soudano-Sahélienne (PSS)*, Niono / Wageningen. MSc thesis. Dep. Tropical Crop Science, Agricultural University, Wageningen, 108 pp.

Rappoldt, C. & D.W.G. van Kraalingen, 1990. Reference manual of the FORTRAN utility library TTUTIL with applications. *Simulation Report CABO-TT no. 20*, 122 pp.

Ridder, N. de, 1979. Fotoperiodiciteit in de Sahel. PPS report, CABO/TPE, Wageningen. 27 pp.

Singh, B. & G. Sceicz, 1979. The effect of intercepted rainfall on the water balance of a hardwood forest. *Water Resources Research* 15, 131-138.

Slatyer, R.O., 1965. Measurements of precipitation interception by an arid zone plant community (*Acacia aneura* F. Muell.). *Arid Zone Res.* 25:181-192

Soumaré, A., J.J.R. Groot, D. Koné & S. Radersma, 1994. [Structure spatiale du système racinaire de deux arbres du Sahel: *Acacia seyal* et *Sclerocarya birrea*](#). Rappports PSS no. 5. IER, Bamako/AB-DLO, Wageningen & Haren/DAN-UAW, Wageningen, 36 pp.

Spitters, C.J.T., 1989. Weeds: population dynamics, germination and competition. In: Rabbinge, R., S.E. Ward & H.H. van Laar (Eds). *Simulation and systems management in crop protection*. Simulation Monograph 32, Pudoc, Wageningen, 182-216, 332-346, 379-392

Stroosnijder, L. & D. Koné, 1982. Le bilan d'eau du sol. In: [Penning de Vries, F.W.T. & M.A. Djitèye \(eds.\)](#), *La productivité des pâturages sahéliens. Une étude des sols, des végétations et de l'exploitation de cette ressource naturelle*. Agric. Res. Rep. 918. Pudoc, Wageningen. p. 133-165.

Verberne, E.L.J., J. Hassink, P. de Willigen, J.J.R. Groot & J.A. van Veen, 1990. Modelling organic matter dynamics in different soils. *Neth. J. Agric. Sci.* 38: 221-238.

[Appendix A: Program listing](#)

[Appendix B: List of acronyms](#)

[Appendix C: Input data](#)

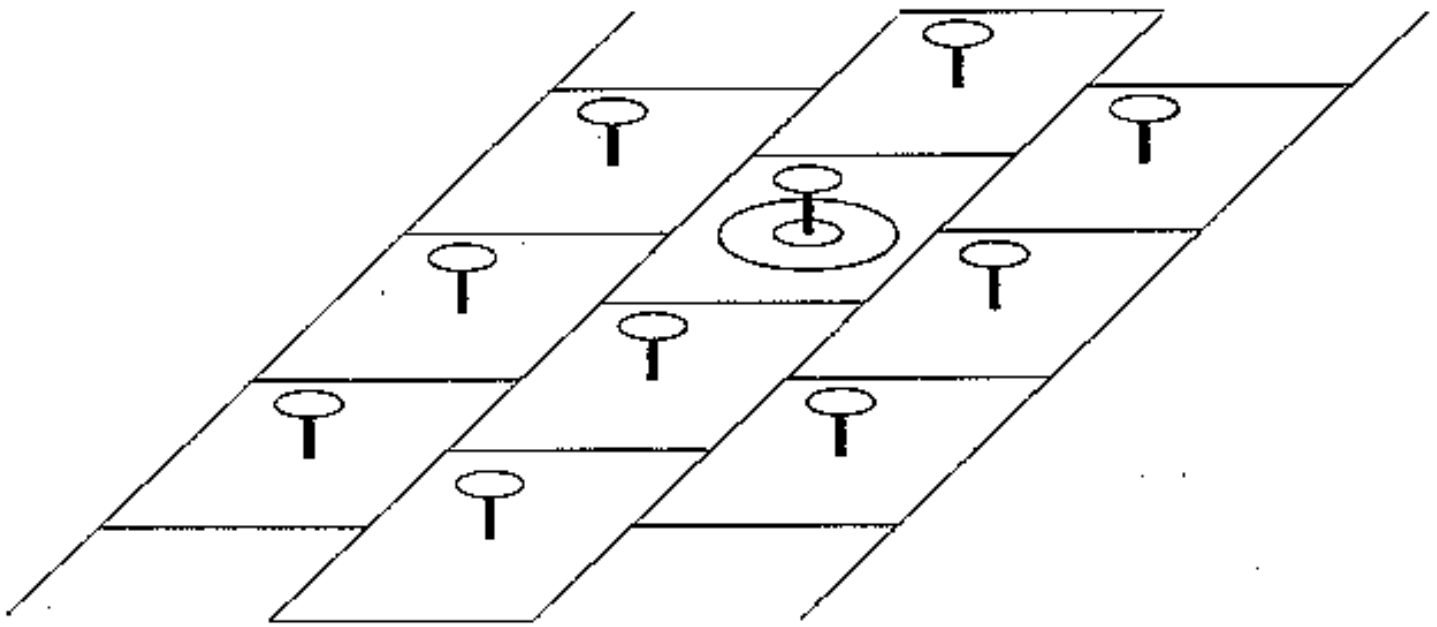


Figure 3.1. A field of 1 ha with 9 tree-grass units and 3 subareas per tree-grass unit.

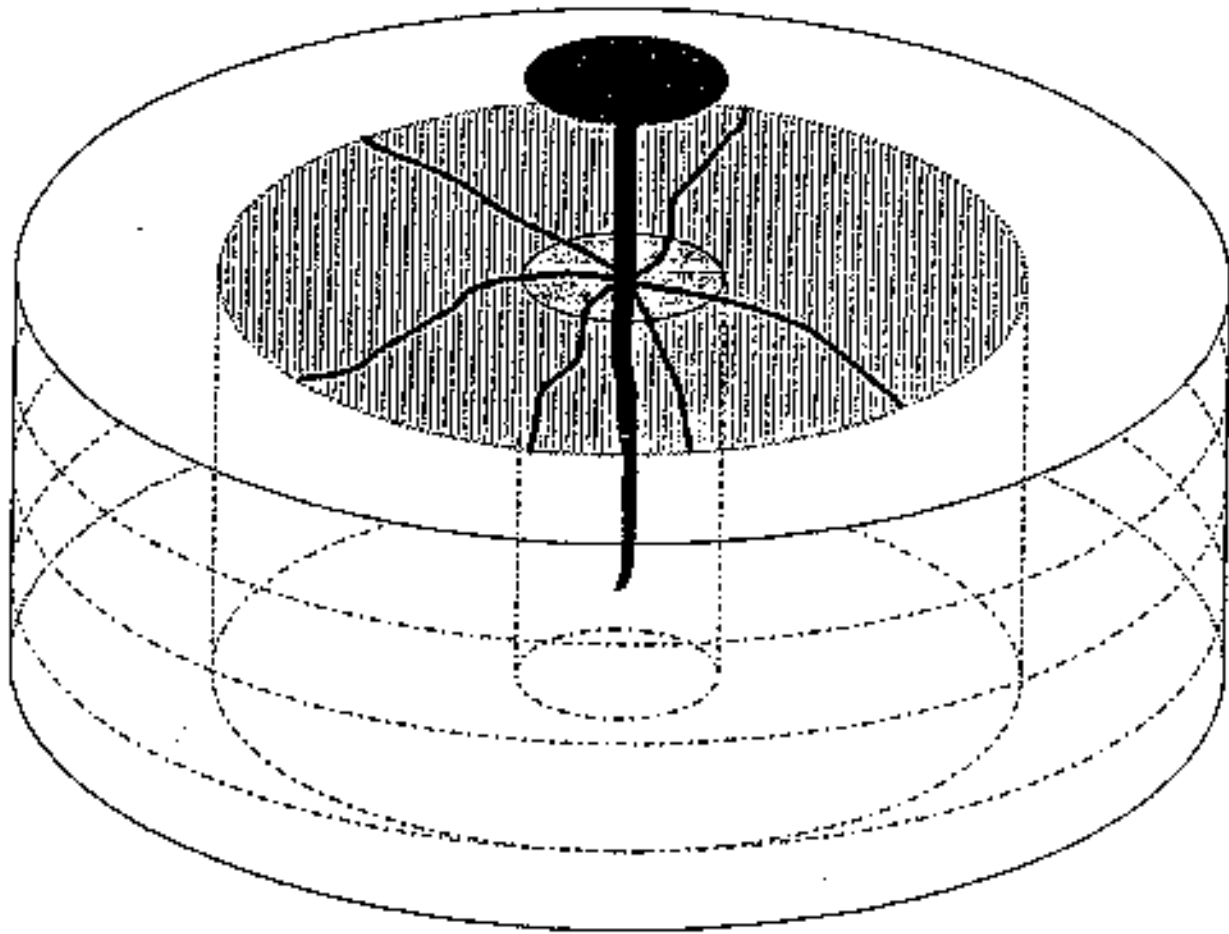


Figure 3.2. A tree-grass unit with 3 subareas and 4 soil compartments in each subarea.

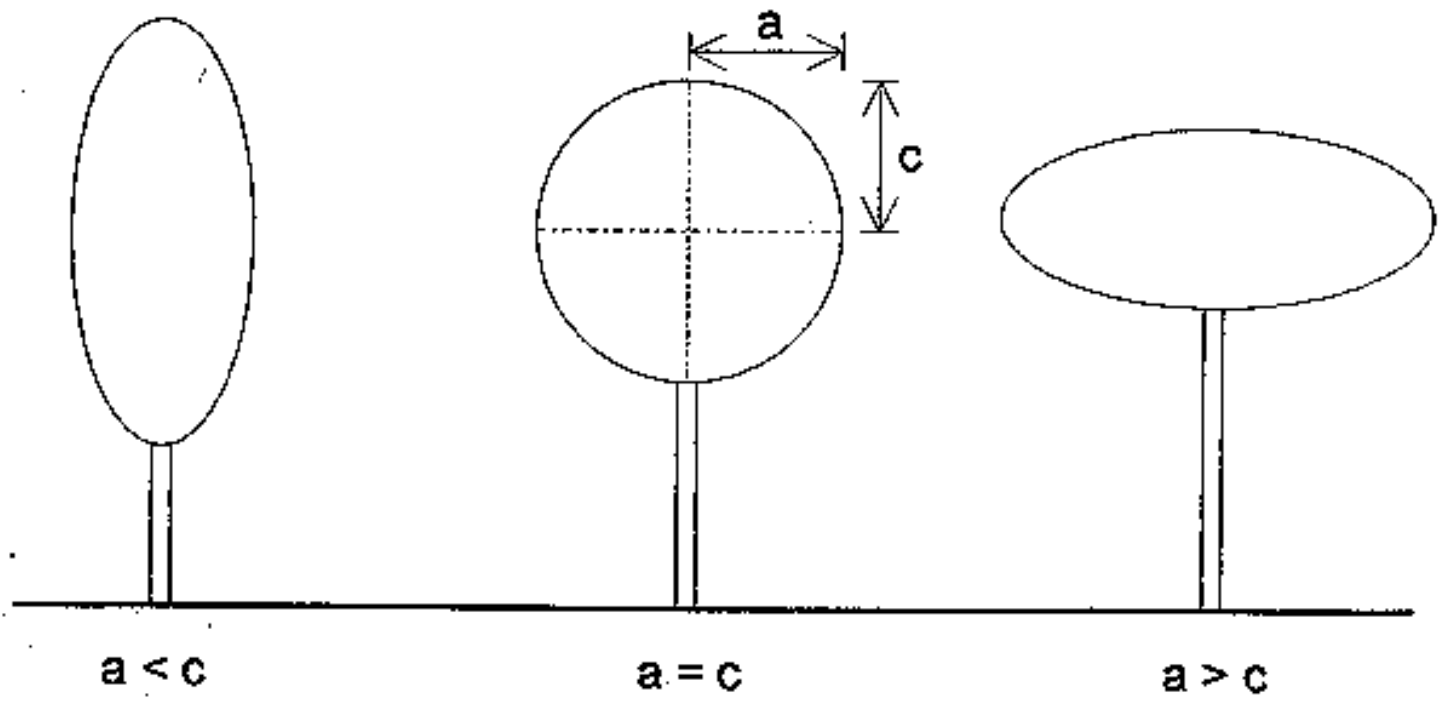


Figure 3.3. Possible tree crown ellipsoids.

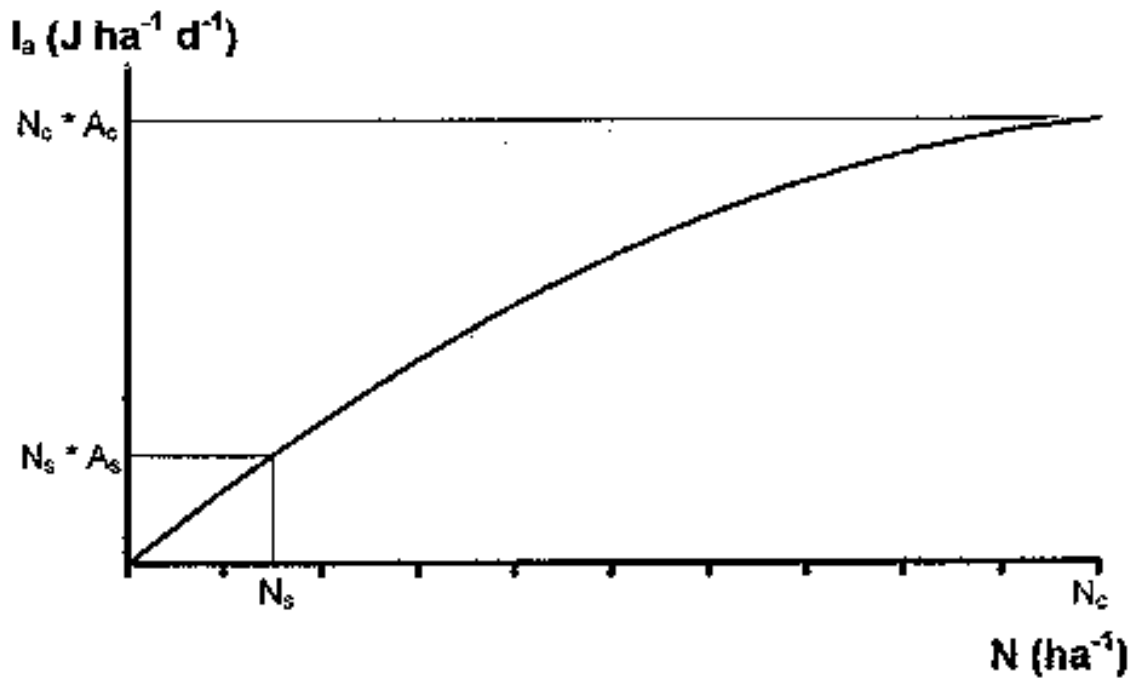


Figure 3.4. Relation between tree population density and daily absorbed PAR of a tree population.

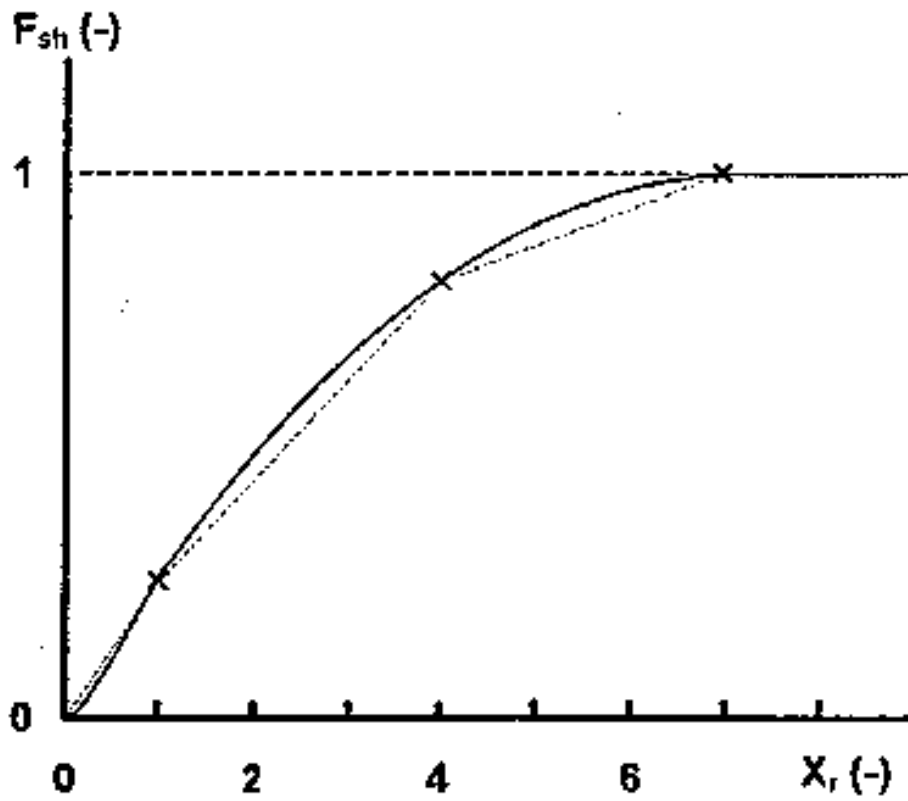


Figure 3.5. Relation between the relative distance from the tree with respect to crown cover radius, x_r , and the cumulative shade fraction, F_{sth} .

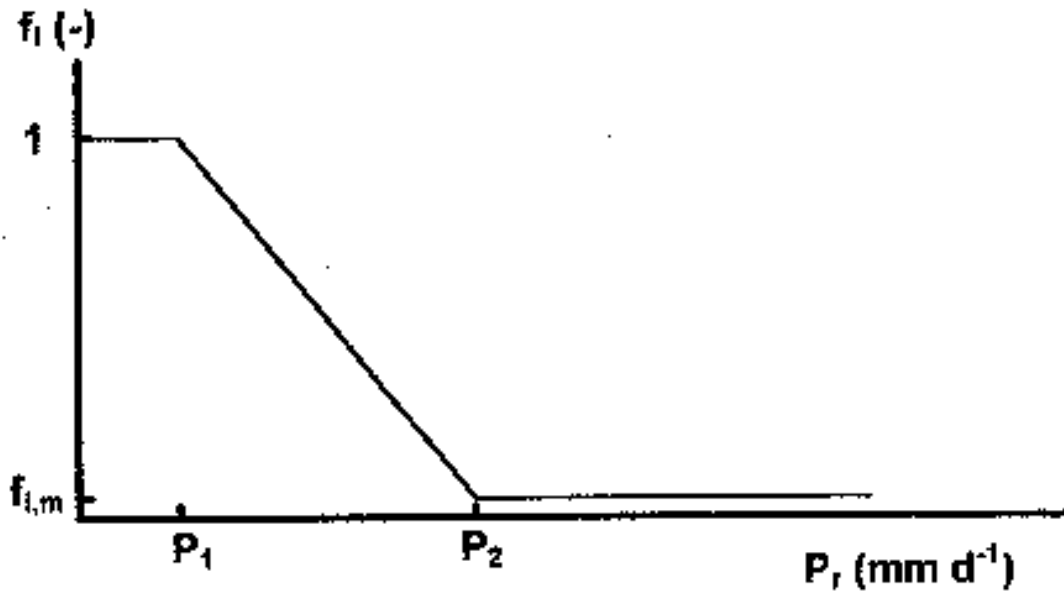


Figure 3.6. Relation between daily precipitation and the fraction intercepted rain by the tree canopies.

- f_i fraction intercepted rain, applied to precipitation minus direct throughfall (-);
- $f_{i,m}$ minimum fraction intercepted rain (-);
- P_1, P_2 precipitation threshold values for calculating f_i (mm d^{-1}).

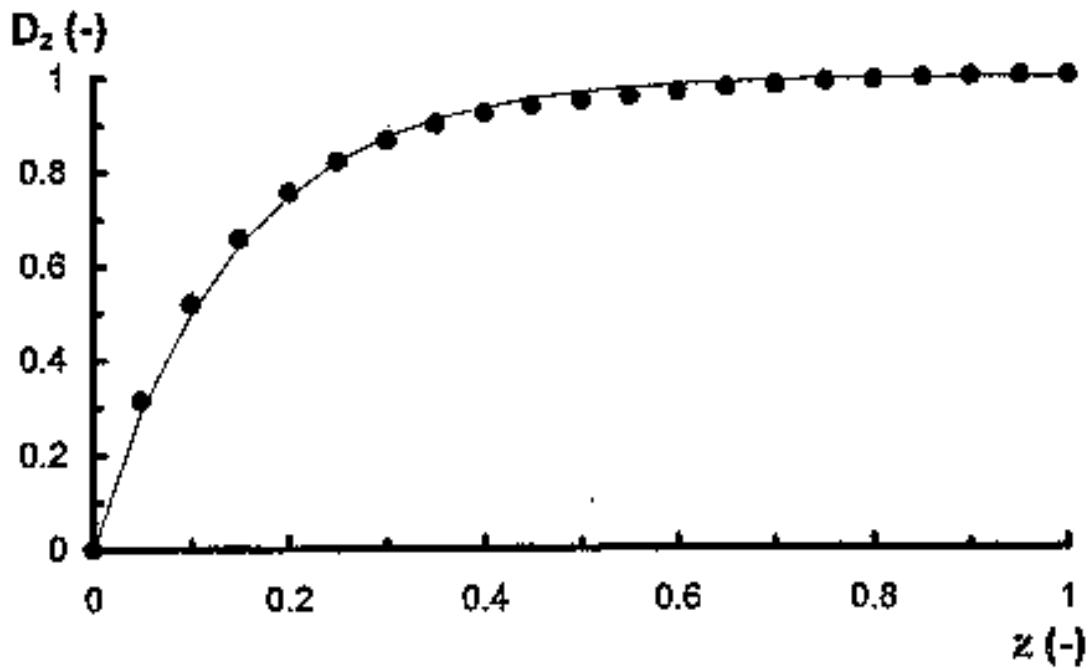


Figure 3.7. The relation between the total cumulative relative root length and relative soil depth: data and fitted curve.

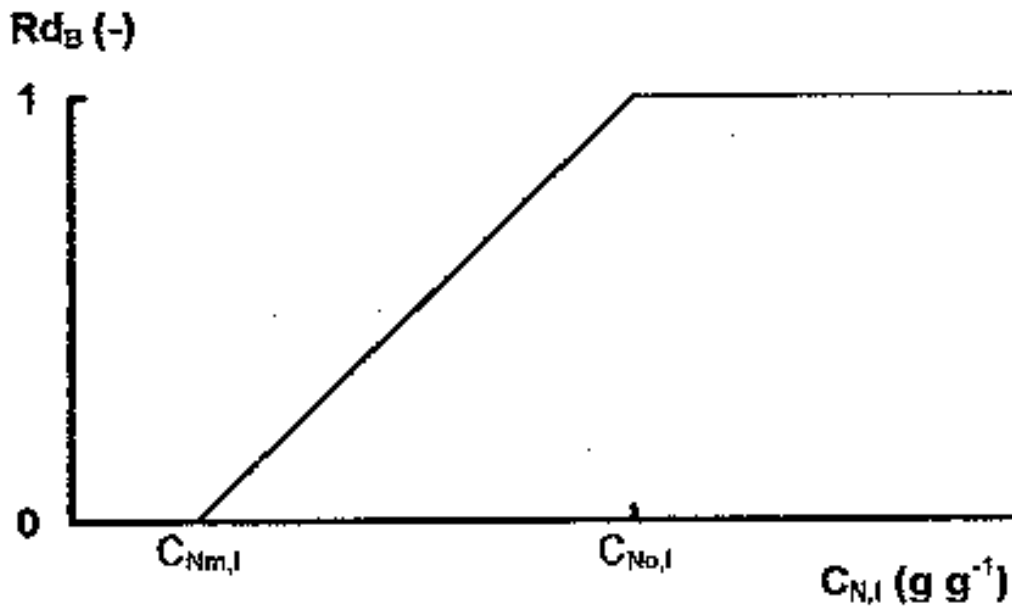


Figure 3.8. The relation between leaf nitrogen concentration and the reduction factor for dry matter production (see text for explanation).

R_{dB}	reduction factor for potential biomass production, caused by nitrogen deficiency	(-)
$C_{N,l}$	actual leaf nitrogen concentration	($g\ g^{-1}$)
$C_{Nm,l}$	minimum leaf nitrogen concentration	($g\ g^{-1}$)
$C_{No,l}$	optimum leaf nitrogen concentration	($g\ g^{-1}$)

P / f_{α} ($\text{kg ha}^{-1} \text{d}^{-1}$)

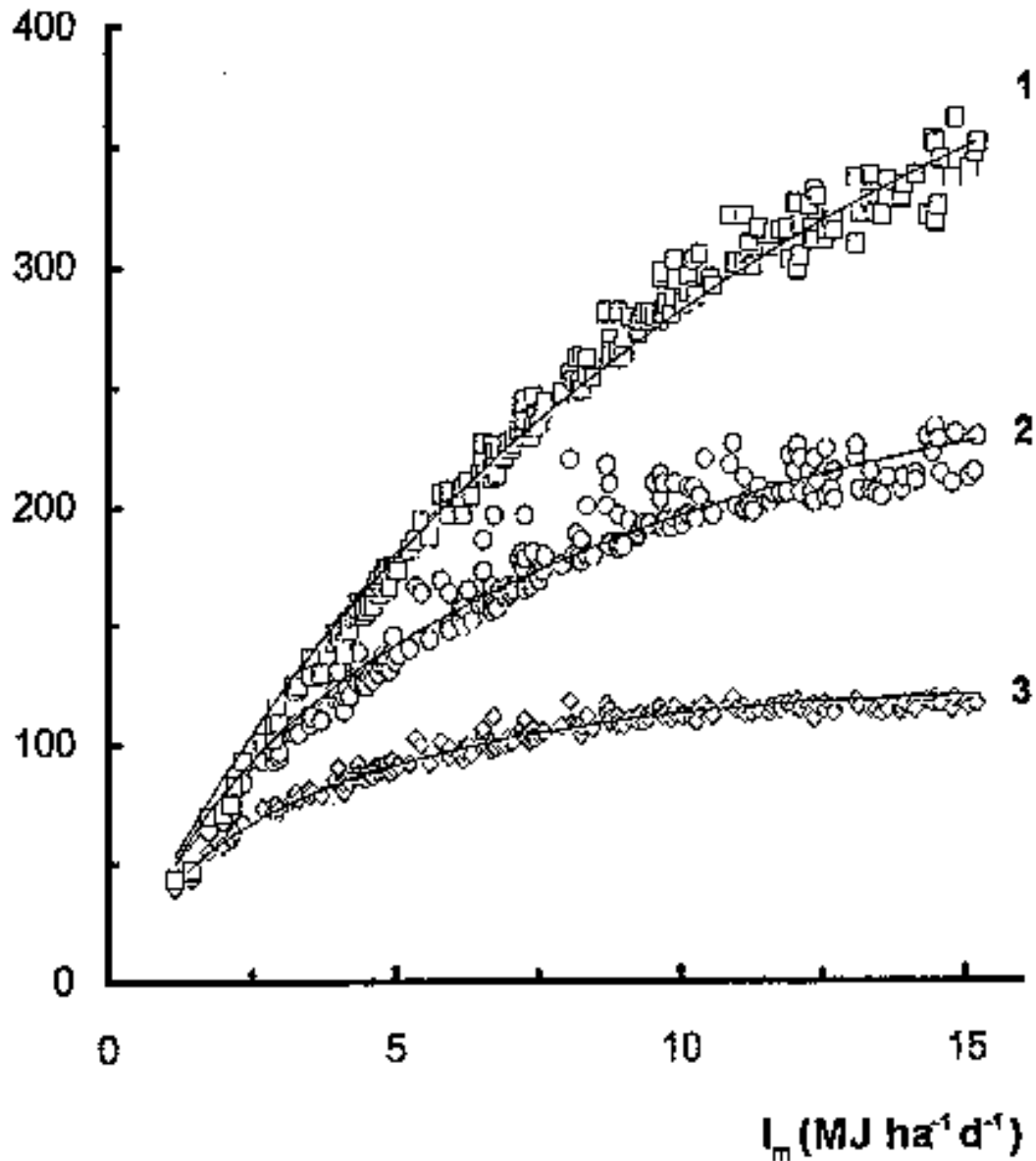


Figure 3.9a. Relation between daily total PAR, available for absorption, and ratio of net biomass production P and fraction absorbed PAR, f_{α} . Simulated data and fitted curves; see text for explanation.

E_i (g MJ⁻¹)

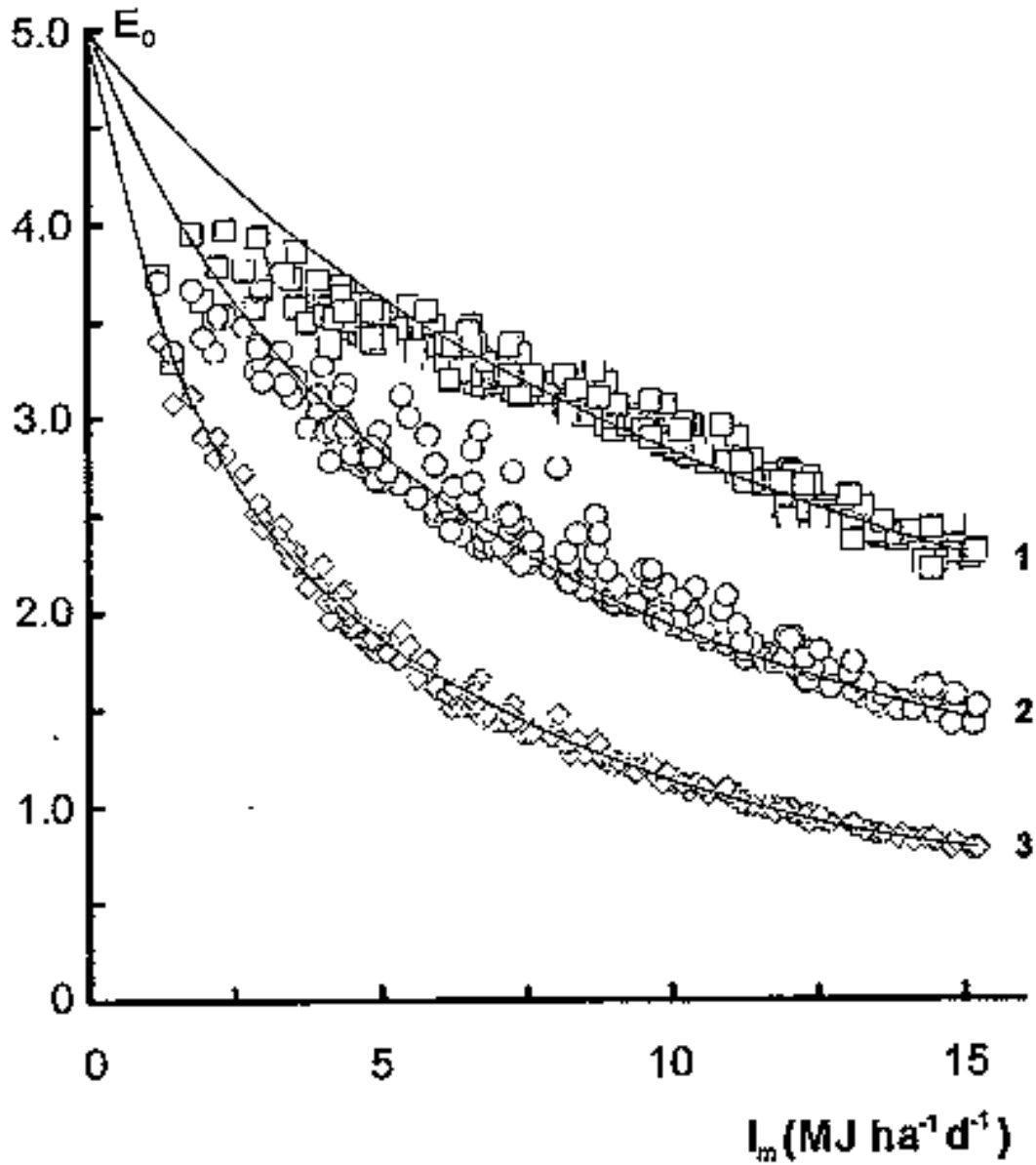


Figure 3.9b. Relation between daily total PAR, available for absorption, and daily light use efficiency. Simulated data and fitted curves; see text for explanation.

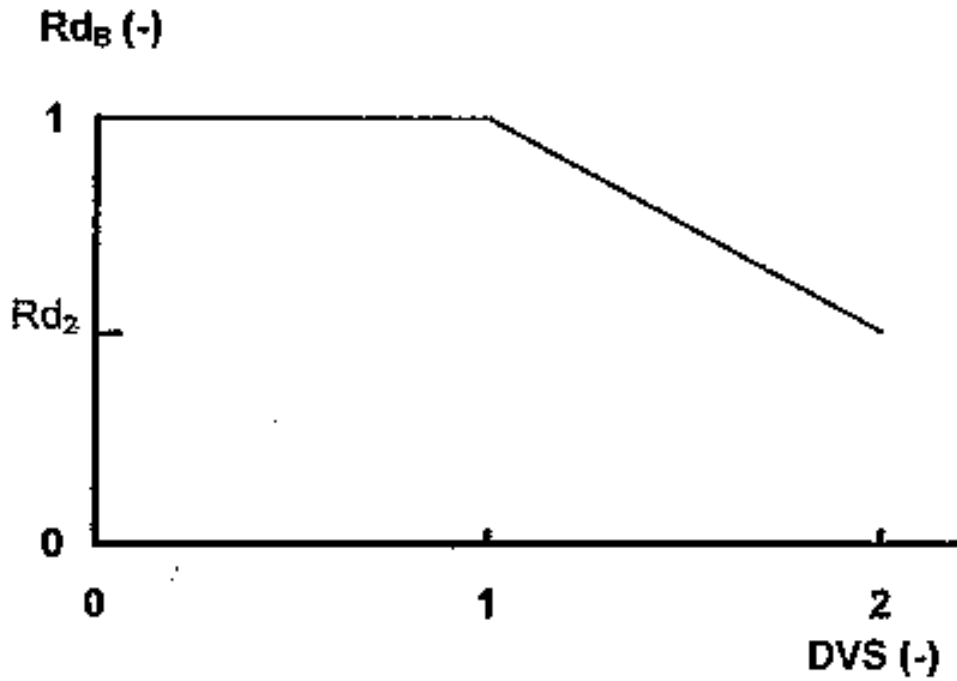


Figure 3.10. Relation between development stage (DVS) and the reduction factor for light use efficiency.

Rd_2 reduction factor for potential biomass production due to ageing at $DVS = 2$ of the herbaceous species (-).

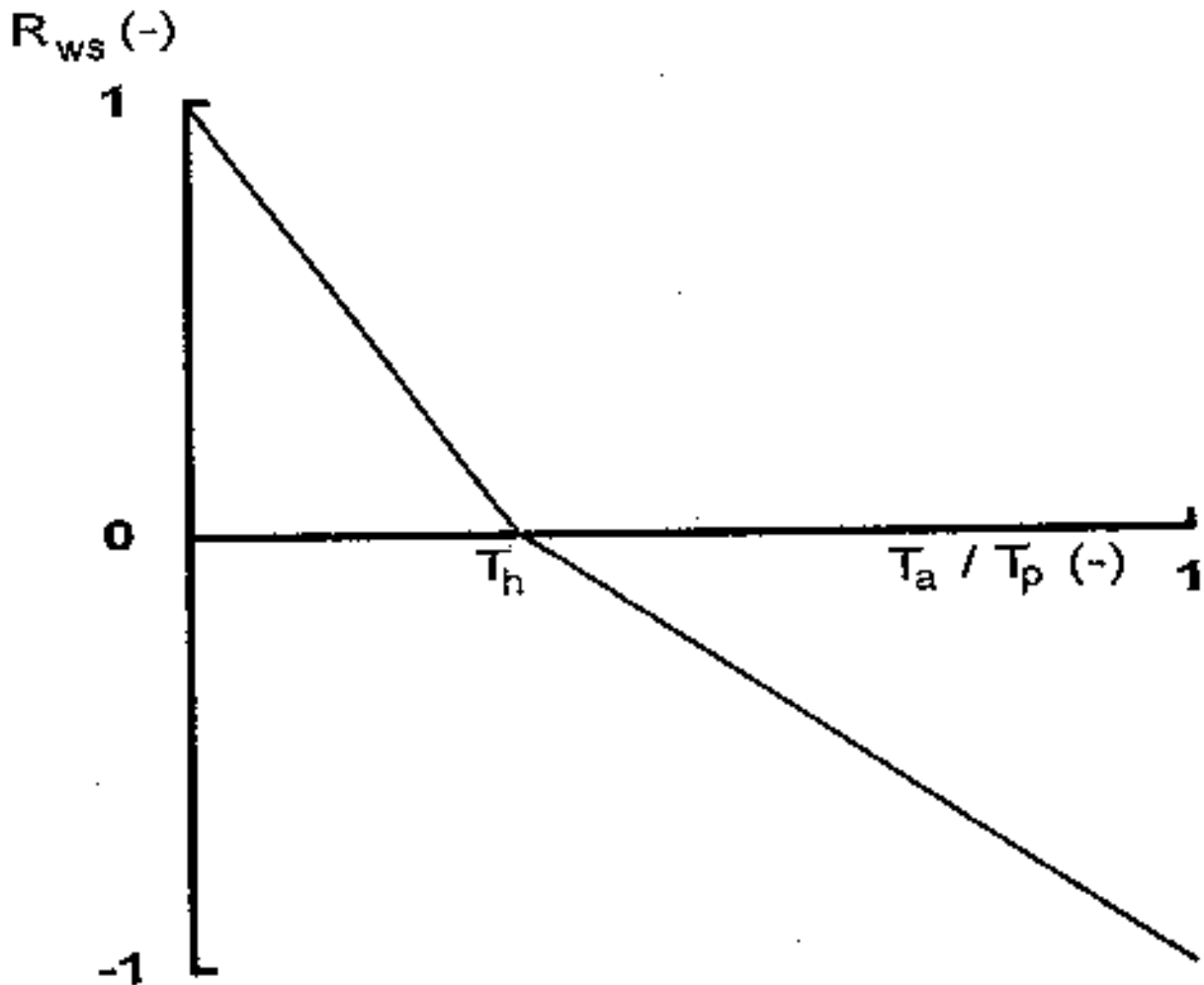


Figure 3.11. The relation between the transpiration ratio and the change in the accumulated amount of water stress days for leaves.

- R_{ws} rate of change in accumulated water stress days (d^{-1});
- T_h transpiration ratio threshold value (-);
- T_a actual transpiration rate of the tree population ($mm\ d^{-1}$);
- T_p potential transpiration rate of the tree population ($mm\ d^{-1}$).

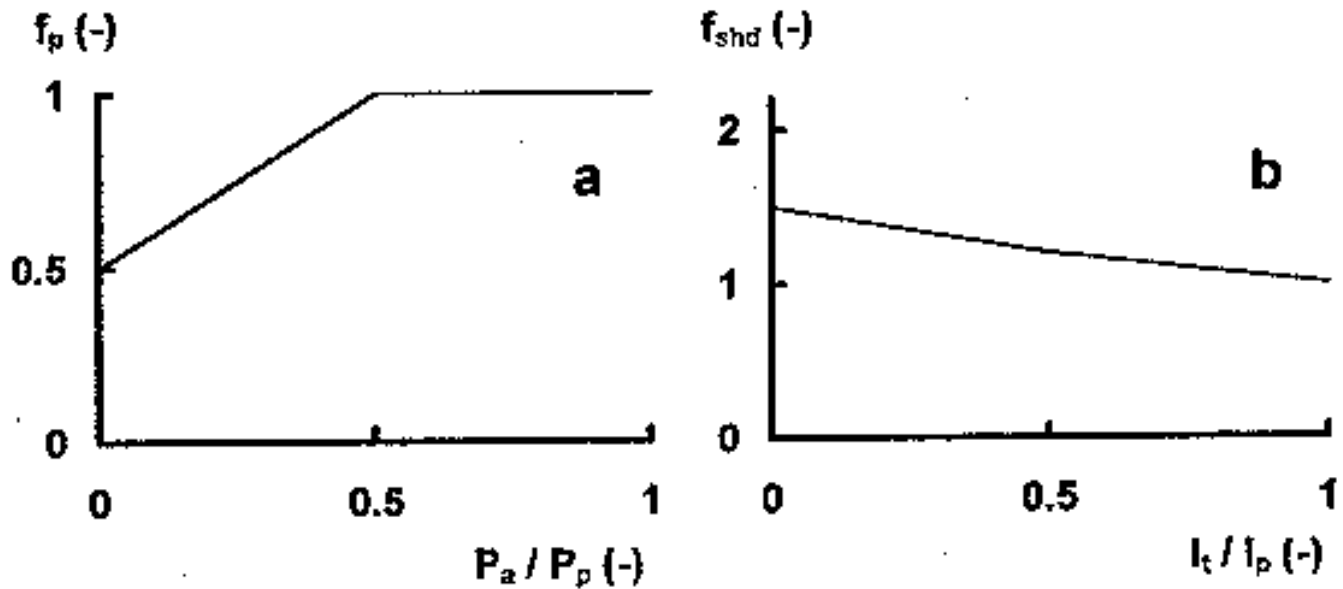


Figure 3.12. The relation between the production ratio and the relative reduction in shoot biomass partitioning factor (a) and the relation between the light availability ratio and the relative increase in shoot biomass partitioning factor (b).

f_p	effect of production stress due to belowground resources on the shoot biomass partitioning factor	(-)
f_{shd}	effect of shading on the shoot biomass partitioning factor	(-)
P_a	actual rate of dry matter production	(kg ha ⁻¹ d ⁻¹)
P_p	potential rate of dry matter production, as function of absorbed radiation	(kg ha ⁻¹ d ⁻¹)
I_p	daily photosynthetically active radiation	(J ha ⁻¹ d ⁻¹)
I_t (n)	daily transmitted PAR towards the herbaceous vegetation	(J ha ⁻¹ d ⁻¹)

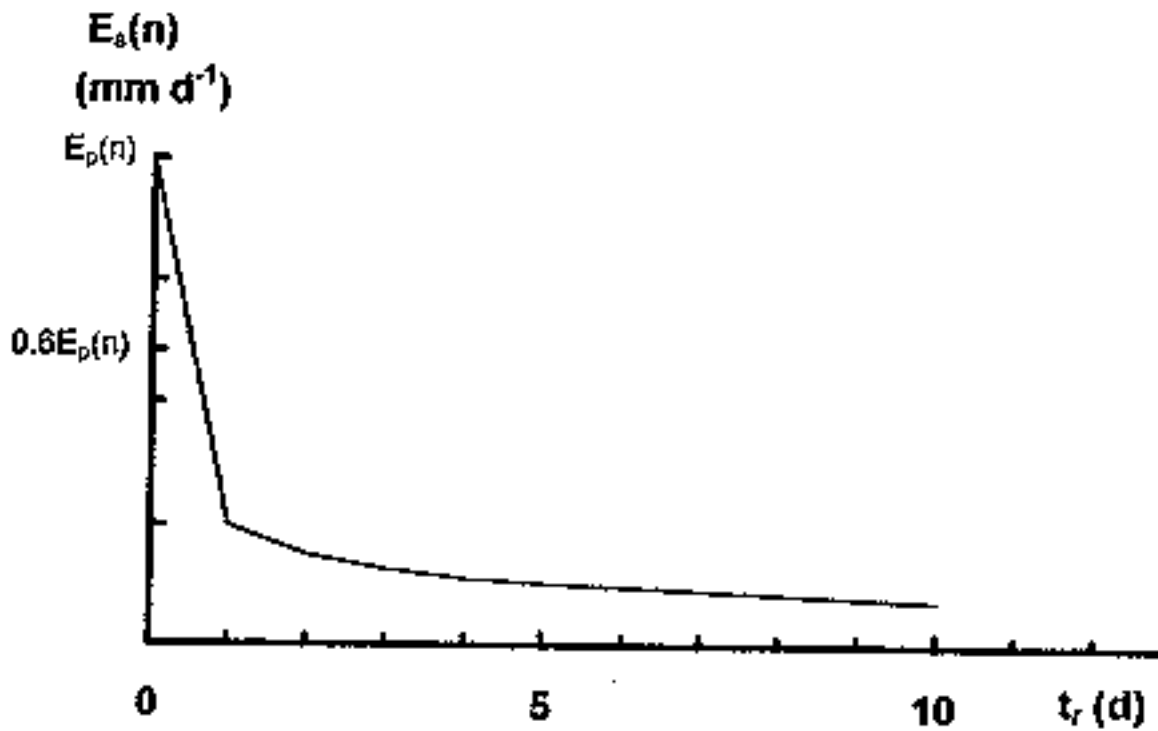


Figure 3.13. Graphical presentation of Eqn. 3.32b, assuming that
(i) $E_s(n) = E_p(n)$ at $t_r = 0$ with $F_w(n, 1) > 0.5$,
(ii) $F_w(n, 1) = 0$ at the following days ($t_r > 0$) and
(iii) a constant $E_p(n)$ during 10 days.

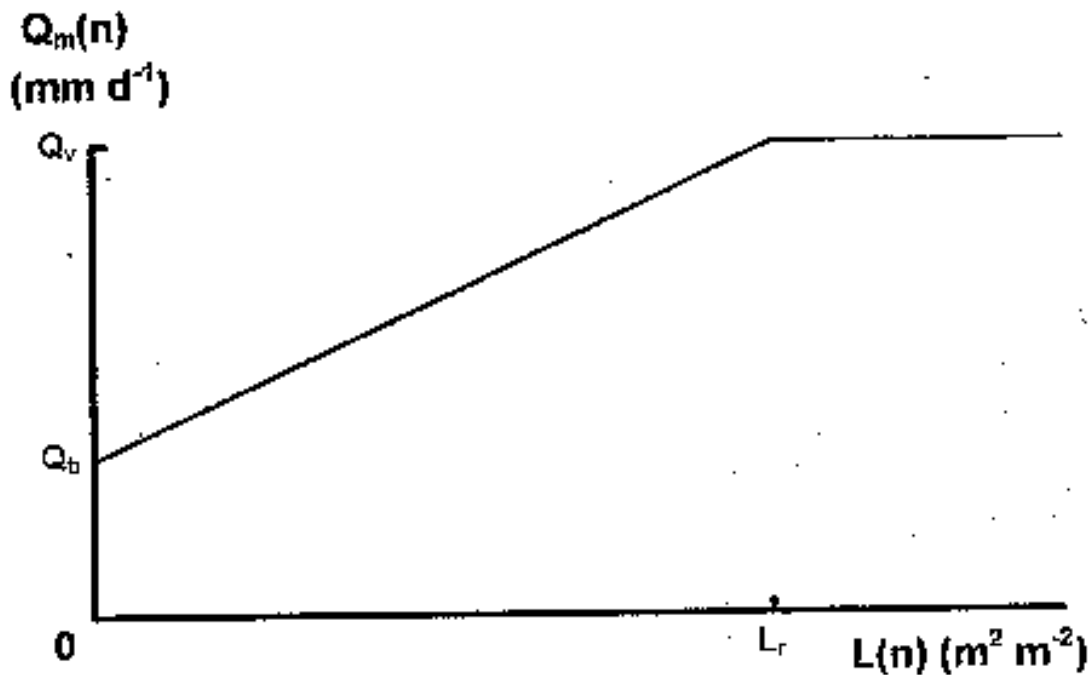


Figure 3.14. The relation between herbaceous leaf area index and the maximum infiltration rate.

$L(n)$	leaf area index of the herbaceous vegetation	$(\text{m}^2 \text{m}^{-2})$
L_r	leaf area index threshold value with respect to runoff	$(\text{m}^2 \text{m}^{-2})$
$Q_m(n)$	actual maximum infiltration rate per subarea	(mm d^{-1})
Q_b	maximum infiltration rate of bare soil	(mm d^{-1})
Q_v	maximum infiltration rate of a soil with an herbaceous leaf area index of L_r or higher	(mm d^{-1})

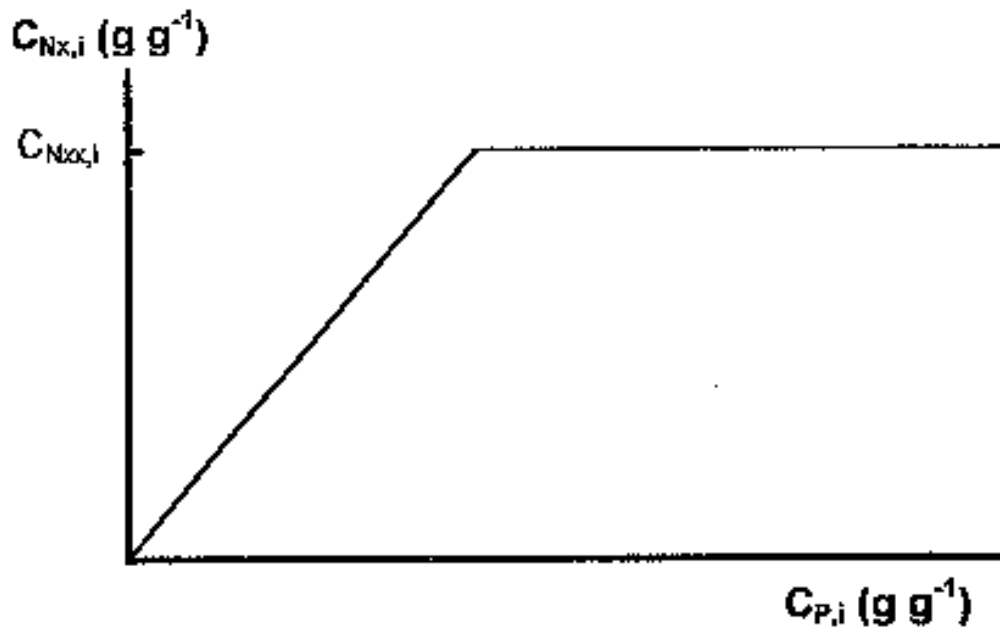


Figure 3.15. Relation between actual phosphorus concentration and maximum nitrogen concentration.

$C_{N_{x,i}}$	maximum nitrogen concentration at high phosphorus concentrations	(g g^{-1})
$C_{P,i}$	actual phosphorus concentration per plant component	(g g^{-1})

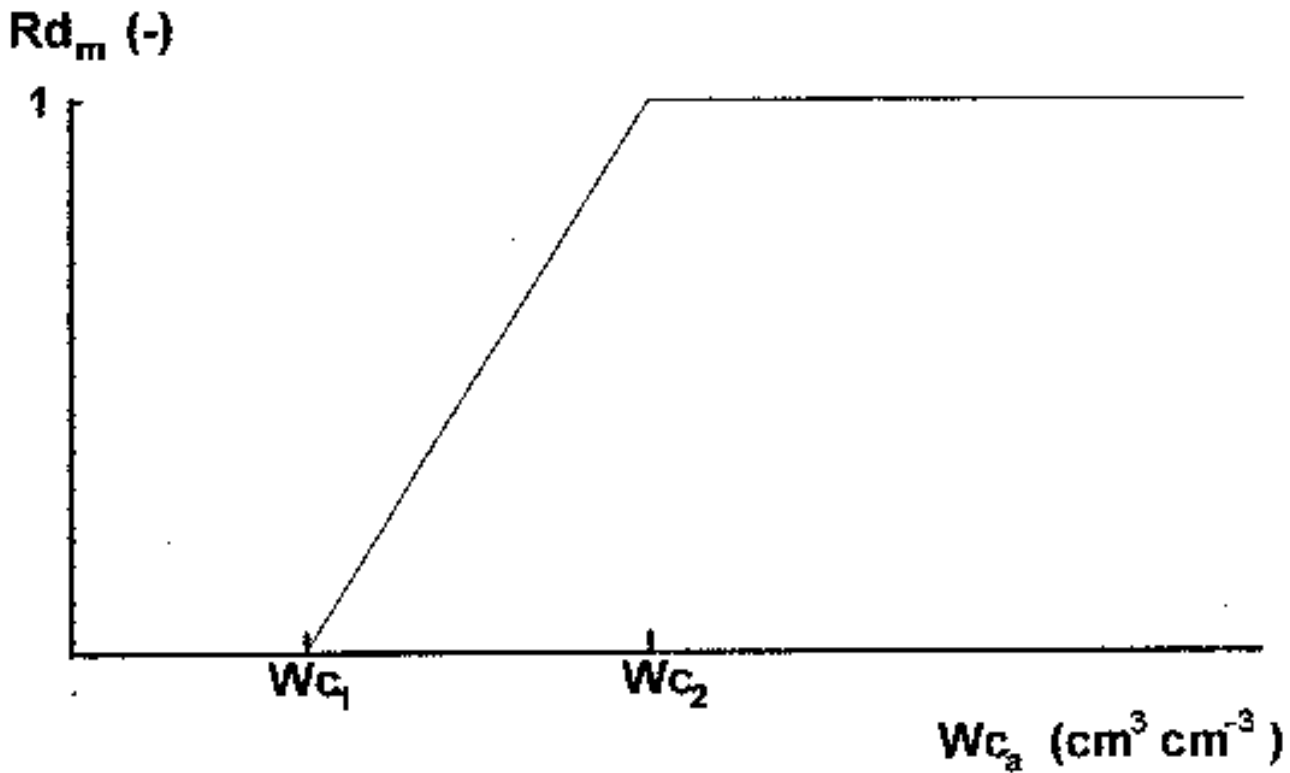


Figure 3.16. The relation between soil water content and the reduction factor for organic matter decomposition and mineralization.

Rd_m	reduction factor for soil organic matter decomposition due to low soil water content	(-)
Wc_a	actual water content in a soil compartment	($\text{cm}^3 \text{cm}^{-3}$)
Wc_1	threshold water content in a soil compartment for decomposition	($\text{cm}^3 \text{cm}^{-3}$)
Wc_2	critical water content in a soil compartment for decomposition	($\text{cm}^3 \text{cm}^{-3}$)

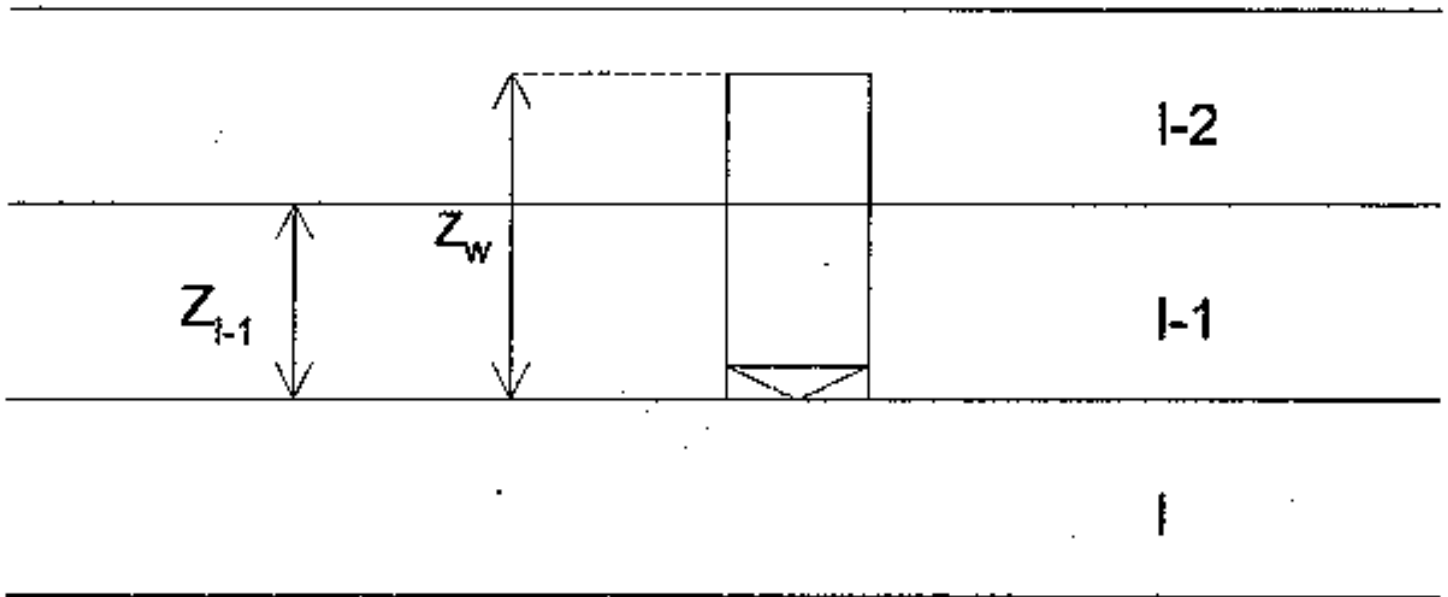


Figure 3.17. This picture gives an illustration of the calculation of nitrogen flows through the soil. For explanation see text.